UNIVERSITÀ DEGLI STUDI DI MILANO

PhD in Pharmacological Biomolecular Sciences, Experimental and Clinical

XXXIV cycle

Department of Pharmacological and Biomolecular Sciences (DiSFeB)

PhD thesis:

"Molecular mechanisms of renal disease in carriers of LCAT gene mutations"

BIO/14

PhD candidate:

ARIANNA STRAZZELLA

R12219

Supervisor: Prof. Laura Calabresi

Coordinator: Prof. Giuseppe Danilo Norata

A.A 2020/2021

INDEX

ABSTRACT (ENGLISH)

BACKGROUND: Familial LCAT deficiency (FLD) is a rare genetic disease characterized by the complete inactivity of LCAT, the only human enzyme able to esterify cholesterol in plasma; as a consequence, carriers' lipid and lipoprotein profile presents low HDL-C concentration, the accumulation of small and discoidal preβ-HDL particles and LpX. Renal disease is the major cause of morbidity and mortality in FLD carriers but the molecular mechanisms of kidney failure are poorly understood. Currently, there are no effective therapies available for these patients and the use of synthetic HDL is under investigation. Furthermore, a condition of acquired LCAT deficiency can characterize common pathologies, such as chronic kidney disease.
AIM: Aim of this project was to analyze the unknown aspects of renal disease in LCAT deficiency, including the molecular mechanisms behind the onset of renal damage and the characterization of the lipid alterations responsible for this condition, the study of potential effective therapeutic strategies and the evaluation of the impact of non-genetic LCAT reduction on renal disease development in general population,
RESULTS: The characterization of LCAT deficient carriers' HDL by lipidomics analyses identified alterations in phospholipids and sphingolipids classes, including an accumulation of phosphatidylethanolamine, dihydroceramides and ceramides, as well as a depletion in phosphatidylethanolamine plasmalogen. Moreover, carriers' HDL were enriched in short and saturated fatty acids and depleted in long chain polyunsaturated fatty acids. These alterations could potentially trigger some nephrotoxic mechanisms identified through the in vitro studies in podocytes and tubular cells, such as the increased oxidative stress and apoptosis induced by FLD carriers' lipoprotein alterations.
The metabolism and effect of a synthetic HDL, CER-001, was evaluated in murine model of LCAT deficiency; results collected in this part showed an amelioration of lipid profile after CER-001 treatment, with an increase of HDL-C and a reduction of triglycerides. Even more important, the molecule ameliorated renal function, reducing the albuminuria and restoring nestin and nephrin expression, by removing cholesterol accumulated in the kidney. The results set the basis to test the molecule in one FLD carrier, in which an analogous mechanism was identified by in vitro studies.
The results collected in the last part of the work highlighted the predictive values of non-genetic reduction in LCAT concentration on the renal disease progression in general population. The development of renal damage could be partially explained by the pro-oxidant effect mediated by the sera from subjects with low LCAT in renal cells; the involvement of the enzyme was demonstrated through the restoration of the antioxidant propriety induced by in vitro incubation of serum with rhLCAT.
CONCLUSION: Results collected within this project provided a deeper knowledge of the alterations in HDL lipid composition and the consequent nephrotoxic mechanisms in LCAT deficiency. Moreover, treatment with CER-001 demonstrated a beneficial

effect on the kidney disease in LCAT deficient mice, supporting the testing of the formulation in FLD carriers. Finally, the evaluation of the relationship between low LCAT levels and progression of renal disease revealed that LCAT concentration can predict renal kidney injury in general population.

ABSTRACT (ITALIAN)

BACKGROUND: Il deficit familiare di LCAT (FLD) è una malattia genetica rara causata da mutazioni nel gene *LCAT*, che codifica per l'unico enzima umano in grado di esterificare il colesterolo nel plasma; conseguentemente, il profilo lipidico e lipoproteico dei portatori è caratterizzato da concentrazioni ridotte di HDL-C, accumulo di LpX e di HDL piccole e discoidali, chiamate preβ-HDL. La malattia renale è la principale causa di morbilità e mortalità nei portatori, ma i meccanismi alla base dell'insorgenza del danno renale sono ancora sconosciuti. Opzioni terapeutiche risolutive per questi pazienti non sono attualmente disponibili e tra gli approcci in fase di sviluppo vi sono le HDL sintetiche. Infine, condizioni di deficit acquisito di LCAT sono riscontrabili in patologie più diffuse, quali l'insufficienza renale cronica.
SCOPO: Lo scopo del progetto è stato analizzare gli aspetti ancora non chiariti della malattia renale nell'FLD, che includono i meccanismi molecolari alla base del danno renale e la caratterizzazione delle alterazioni lipidiche responsabili di tale condizione, la valutazione di potenziali strategie terapeutiche e lo studio dell'impatto della riduzione delle concentrazioni di LCAT nello sviluppo della patologia renale nella popolazione generale.
RISULTATI: La caratterizzazione tramite lipidomica delle lipoproteine di portatori di FLD ha identificato alterazioni nelle componenti fosfolipidiche e sfingolipidiche, tra le quali l'accumulo di fosfatidiletanolammina, diidroceramidi e ceramidi, in parallelo ad una riduzione di fosfatidiletanolammina plasminogeno. Inoltre, le HDL dei portatori sono arricchite di acidi grassi saturi a catena corta e presentano ridotti livelli di acidi grassi poli-insaturi a lunga catena. Tali alterazioni potrebbero potenzialmente innescare alcuni dei meccanismi nefrotossici identificati tramite gli studi in vitro condotti su podociti e cellule tubulari, che hanno mostrato un incrementato stress ossidativo e apoptosi indotti dalle anomalie lipoproteiche nei soggetti affetti da FLD.
Il metabolismo e l'effetto di una formulazione di HDL sintetiche, CER-001, sono stati valutati in un modello murino di patologia renale associata a deficit di LCAT; in seguito al trattamento con tale formulazione il profilo lipidico degli animali ha mostrato un miglioramento, con aumento di HDL e riduzione di trigliceridi. Inoltre, la molecola ha esercitato un effetto migliorativo sulla funzionalità renale nell'animale, riducendo l'albuminuria e ripristinando l'espressione di nefrina e nestina, fondamentali per la funzionalità glomerulare, attraverso la rimozione dell'accumulo di colesterolo nel rene. Tali dati hanno consentito di testare CER-001 in un portatore di FLD, nel quale la molecola ha evidenziato un analogo meccanismo d'azione in vitro.

I risultati ottenuti nell'ultima parte del lavoro hanno dimostrato l'esistenza di una correlazione tra ridotta concentrazione di LCAT e progressione di malattia renale nella popolazione generale. Lo sviluppo del danno renale potrebbe essere parzialmente spiegato dall'effetto pro-ossidante indotto dal siero di soggetti sani ma con ridotte concentrazioni di LCAT nelle cellule renali; il ruolo dell'enzima è stato confermato dal ripristino dell'attività anti-ossidante delle HDL in seguito ad incubazione del plasma con enzima ricombinante (rhLCAT) in vitro.

CONCLUSIONE: I risultati ottenuti in questo lavoro hanno fornito un'approfondita caratterizzazione delle alterazioni nella composizione lipidica delle HDL e nei conseguenti meccanismi nefrotossici nel deficit di LCAT. Inoltre, il trattamento con CER-001 ha migliorato il danno renale in un modello murino di deficit di LCAT, supportando il test di tale formulazione nei portatori di FLD. Infine, la valutazione della relazione tra riduzione non-genetica dei livelli plasmatici di LCAT e sviluppo di malattia renale ha rivelato che la concentrazione dell'enzima può predire la progressione del danno renale nella popolazione generale.

INTRODUCTION

1. Lecithin:cholesterol acyltransferase (LCAT)

LCAT is a glycoprotein composed of 416 amino acids with a molecular weight of 67 kDa, that presents an extra mass (20% greater than prediction) due to N-linked and O-linked glycosylation (*Calabresi et al. 2012*). LCAT is the only human enzyme able to esterify cholesterol in plasma and biological fluids; it plays a crucial role in the maturation of high-density lipoproteins (HDL) and in the reverse cholesterol transport (RCT) (*Calabresi et al., 2012; Jonas, 2000*).

1.1. Gene and protein structure

1.1.1 LCAT gene

LCAT gene (4.5 kb) is localized in the region q21-22 of chromosome 16; it contains six exons and five introns, with a coding sequence of about 1.5 kb (*Calabresi et al., 2012; Jonas, 2000*).

The catalytic region of the enzyme and the one involved in the link with the substrates are codified in exons 5 and 6 (*McLean et al., 1986*).

The human gene is mainly expressed at hepatic level but it can be detected also in testicles and brain, even if in fewer percentage (*Warden et al., 1989*). The biological importance of hepatic LCAT production and it subsequent plasma secretion is well known; in plasma, LCAT concentration is around 5 mg/L, depending on age, gender, smoke and other factors (*Albers et al., 1982*).

On the other side, the role of the enzyme in brain is still debated; according to several studies, the protein has a lower concentration compared to plasma, and it is secreted by astrocytes; in cerebrospinal fluid, LCAT should esterify cholesterol in apoE-containing lipoproteins secreted by glia cells (*Hirsch-Reinshagen et al., 2009; Albers et al., 1992*).

LCAT gene expression can be modulated by several molecules, such as IL-6, which activates STAT-3, and seems to act on a specific level of gene promotor, increasing

the enzyme expression (*Feister et al., 2002*). On the contrary, many factors can reduce the amount of LCAT mRNA and activity, like TGF-β factor, as demonstrated by in vitro studies in HepG2 (*Skretting et al., 1995*). Taking advantage of the same model, it has been subsequently demonstrated that also arachidonic, eicosapentaenoic and docosahexaenoic acids affect the amount of LCAT mRNA; a similar reduction is induced also by C18 fatty acids. On the contrary, C16 fatty acids, characterized by a short and saturated chain, induce an increase in LCAT synthesis (*Kuang et al., 2012*).

Finally, it is important to underline that the hypolipidemic drugs do not influence the *LCAT* expression, except for the fibrates, which reduce enzyme activity, as well as torcetrapib and atorvastatin, that increase LCAT levels on HDL (*Rousset et al., 2009*).

1.1.2 Protein structure

Before being secreted, the neo-synthetized protein undergoes to two post-transcriptional modifications: glycosylation and disulfur bridges formation (*Jonas, 2000*).

Primary structure presents six cystein residues, two of them with a free sulfhidric group, Cys-31 and Cys-184, not directly involved in the catalytic reaction (*Francone et al., 1991*). Other cysteine residues form two sulfridic bridges (Cys50-Cys74 and Cys313-Cys356) (*Yang et al., 1987*). In solution, the bridge Cys50-Cys74 is fundamental for the bond between LCAT and the lipoprotein surfaces, as it permits the access at the catalytic site of the enzyme for the catalytic reaction (*Adimoolam et al., 1997*).

During its maturation, LCAT undergoes to other post-trascriptional modifications, O-glycosilation on Thr407 and Ser409, and N-glycosilation on the amino acids Asn20, Asn84, Asn272 and Asn384; N-glycosylated aspargine residues are responsible for the enzyme specificity for the substrates HDL and LDL (*Karmin et al., 1995*).

LCAT glycan chains are probably involved in the solubility of the protein in plasma, in the prevention of non-specific binding to cell membranes and in the removal mechanism for old plasma desialylated enzyme through the asialoglycoprotein receptor of liver cells (*Jonas, 2000*). The secondary structure of the enzyme LCAT is

characterized by an elevated amount of β-sheet and a reduced content of α-helix. However, two amphipathic α-helices from residues 151-174 and 56-68 are involved in the bond with phospholipid substrates and lipoprotein surfaces (*Jonas, 2000*).
The tertiary LCAT structure has been studied using a three-dimensional model based on a structural and functional homology with lipases, in particular the ones belonging to the α/β hydrolase-fold family. LCAT is a globular protein with a scaffold of seven parallel β-strands linked by four α-helices and loops (*Jonas, 2000*). The model highlights the position of the three amino acids in catalytic triad (Ser181, Asp345 and His377) (*Adimoolam et al., 1997*), and in 2015 Piper et al. described for the first time the high resolution crystal structure of the enzyme LCAT, showing the position of the catalytic triad (*Piper et al., 2015*).

.

1.2 Role of LCAT in HDL metabolism

1.2.1 LCAT substrates

The enzyme LCAT exerts two activities, “α-LCAT” e “β-LCAT”. The first one is characterized by an activity of the enzyme on the cholesterol carried on HDL, and the co-factor is the apolipoprotein A-I. β-activity involves the cholesterol on LDL, using apolipoprotein E as a co-factor (*Calabresi et al., 2012; Jonas, 2000*).
The main substrate of LCAT is HDL and in physiological level of lipoproteins, about 70–80% of LCAT activity is confined to the HDL fraction, while the remainder involves the LDL fraction. (*Rajaram et al., 1985*)

1.2.1.1 HDL

HDL is a very heterogeneous class of lipoproteins, as in plasma these particles undergo to a high number of modifications, which explain their both structural and functional variety.
The HDL density is between 1.063-1.21 g/mL, and their diameter range is from 70 to 130 Å, with a mean size of 8–10 nm. These lipoproteins are formed by 50% protein

and 50% lipid; the density of the particles is inversely related to their size, because of the relative contents of non-polar low-density core lipid and high density surface proteins (*Kontush et al., 2012*).

It is possible to classify HDL by density, charge, shape and size.

The separation by density can be performed by ultracentrifugation, a technique that allows to discriminate between HDL3 (δ = 1.125-1.21 g/mL), smaller and more dense, and HDL2, which are bigger and less dense (*Kontush et al., 2012*).

Five subclasses of HDL have been identified by non-denaturing polyacrylamide gradient gel electrophoresis, that separates particles according to their size: HDL3c, 7.2-7.8 nm; HDL3b, 7.8-8.2 nm; HDL3a, 8.2-8.8nm; HDL2a, 8.8.-9.7 nm; HDL2b, 9.7-12.0 nm (*Nichols et al., 1986*).

The majority of plasma HDL have a globular shape and migrate in α position on agarose gel; however, a small percentage of nascent HDL present a discoidal shape, with preβ electrophoretic migration, as these particles are deprived of hydrophobic lipids (esterified cholesterol and triglycerides).

The separation by charge in α- and pre-β-migrating HDL on the agarose gel can be combined with size, identifying different subclasses of apoA-I-containing HDL particles: pre-β (pre-β1 and pre- β 2), α (α 1, α 2 and α 3) and pre- α (pre- α 1, pre- α 2 and pre- α 3).

Finally, HDL main protein component is apoA-I, but these particles can also contain apoA-II; depending on the apolipoprotein content, it is possible to distinguish HDL containing only apoA-I (LpA-I) or containg also apoA-II (LpA-I: A-II) (*Franceschini et al., 2007*).

Density (ultracentrifugation)
HDL2 (1.063–1.125 g/mL)
HDL3 (1.125–1.21 g/mL)
Size (GGE)
HDL2b (9.7–12.0 nm)
HDL2a (8.8–9.7 nm)

HDL3a (8.2–8.8 nm)
HDL3b (7.8–8.2 nm)
HDL3c (7.2–7.8 nm)
Size (NMR)
Large HDL (8.8–13.0 nm)
Medium HDL (8.2–8.8 nm)
Small HDL (7.3–8.2 nm)
Shape and charge (agarose gel)
α-HDL (spherical)
Preβ-HDL (discoidal)
Charge and size (2D electrophoresis)
Preβ-HDL (preβ_1 and preβ_2)
α-HDL (α_1, α_2, α_3 and α_4)
Preα-HDL (preα_1, preα_2, preα_3)
Protein composition (electroimmunodiffusion)
LpA-I
LpA-I:A-II

Table 1. HDL subclasses identified by different isolation/separation techniques (Kontush et al., 2012).

HDL represent the main substrate of LCAT reaction, and about 75% of the circulating enzyme is bound to these lipoproteins (*Jonas, 2000; Kuivenhoven et al., 1997*).

1.2.1.2 VLDL and LDL

Very low density lipoproteins (VLDL) (δ = 0.930-1.006 g/mL) are synthetized at hepatic level thanks to the action of Microsomal Triglyceride Transfer Protein (MTTP), which catalyzes the reaction among apolipoprotein B-100 (apoB-100), apolipoprotein

C (apoC) and apoE with triglycerides and neo-synthetized cholesterol. VLDL are characterized by a very low level of proteins and by an enrichment in triglycerides. (*Franceschini et al., 2007; Kwiterovich, 2010*).

Circulating VLDL and triglycerides-rich lipoproteins (TGRL) undergo to the action of the lipoprotein lipase (LPL), which hydrolyzes the triglycerides and converts VLDL in IDL. IDL are then converted in LDL by the action of hepatic lipase (HL), that hydrolyzes triglycerides, apoC and apoE.

LDL (δ = 1.019-1.063 g/mL) are enriched in esterified cholesterol and their only apolipoprotein component is a molecule of apoB-100. LDL can be removed from plasma by interaction with a specific receptor (LDLR) in liver or the particles can be internalized in the peripheral cells through interaction with LDLR or scavenger receptors (*Kwiterovich, 2010*).

Despite of the LCAT high affinity for HDL, about 25% of the circulating enzyme is bound to LDL and, in small percentage, to other apoB-containing particles (*Kuivenhoven et al., 1997*).

1.2.2 HDL metabolism, Reverse Cholesterol Transport (RCT) and Reverse Remnant-Cholesterol Transport (RRT)

1.2.2.1 HDL metabolism

Nascent HDL are synthetized starting from the interaction of two molecules of apoA-I, which are mainly secreted by liver and, in a less amount, in small intestine (*Ikewaki et al., 1993*). Hepatocytes can secrete apoA-I in several forms, lipid-free or lipid-poor and lipidated (*Chisholm et al., 2002*), firstly as pro-apoA-I, that in plasma is converted into a mature form (*Edelstein et al., 1983*). Besides being synthetized, apoA-I can derive from the hydrolysis of triglyceride-rich lipoproteins through the activity of LPL, or it can be generated during the remodeling of mature HDL.

ApoA-I dimer acquires phospholipids and cholesterol interacting with the ATP binding cassette transporter A1 (ABCA1), resulting in the formation of small and discoidal nascent HDL (5.6 nm). These discoidal particles show a preβ migration on agarose

gel. The activity of ABCA1 loads phospholipids and free cholesterol on nascent HDL, turning the particles into discoidal HDL with a preβ or α4 migration (7.4 nm).

In circulation, LCAT binds the lipoproteins surface, esterifying cholesterol; the generated cholesteryl esters are more hydrophobic than free cholesterol and migrate to the particle core. This step allows the maturation of discoidal preβ HDL into spherical α-HDL (HDL3). (*Jonas, 2000*). Mature HDL can then acquire cholesterol from the macrophages of arterial wall through other mechanisms, like passive diffusion, facilitate diffusion mediated by scavenger receptor BI (SR-BI) and active transport mediated by ATP-binding cassette G1 (ABCG1) (*Yancey et al., 2003*).

HDL3 interact with Cholesteryl Ester Transfer Protein (CETP), which mediates the exchange of cholesteryl esters for triglycerides between HDL and triglyceride-rich lipoproteins. This reaction generates triglycerides-rich HDL particles, known as HDL2 (*Zechner et al., 1987*), which are subsequently hydrolyzed by HL, LPL and endothelial lipase (EL). The triglycerides and phospholipid hydrolysis lead to the formation of discoidal pre-β-HDL particles from the spherical HDL (*Clay et al., 1992*).

The protein and lipid components of HDL meet different catabolic destinies.

The protein components are catabolized at different times; in fact, apoA-II is catabolized slightly slower than apoA-I, while apoA-IV, apoCs and apoE, that are associated both with triglyceride-rich lipoproteins and HDL, are removed from the circulation faster than apoA-I (*Sun, et al. 2001; Cohn 2003*).

Liver and kidney are the main sites of catabolism of HDL particles protein components (*Sriram et al., 2011*). Clearance and re-absorption of lipid-free apolipoproteins, especially apoA-I, are mediated by the kidney (*Lee et al. 2005*). The glomerular filtration barrier filtrates apolipoproteins according to their hydrophobicity. In particular, when the re-absorption is impaired, the hydrophilic apolipoproteins apoA-I and apoA-IV can be excreted into urine, while the hydrophobic apoA-II cannot (*Graversen et al., 2008*).

Moreover, although the glomerular filtration barrier avoids the passage of mature HDL particles to the proximal tubules, filtered apolipoproteins can be re-absorbed in this site through the synergetic action of cubulin/megalin receptors (*Moestrup et al., 2005; Dugue-Pujol et al., 2007*). Megalin is a large glycoprotein belonging to LDLR family,

partly expressed in microvilli of proximal tubule epithelial cells (*Saito et al., 1994; Christensen et al., 1995*) responsible for intracellular signal transduction *(Biemesderfer et al., 2007*) and it is involved in the reabsorption of some filtered substances, such as albumin and low molecular weight proteins (*Saito et al., 2010*). Cubilin is a multi-ligand receptor expressed in the apical membrane of various absorptive epithelia, like the yolk sac and placenta, intestine and kidney (*Moestrup et al., 2000*). The protein presents a high affinity for apoA-I, mediating its endocytosis; however, cubilin is involved in the re-absorption of an elevated number of proteins in glomerular ultrafiltrate (*Kozyraki, et al. 1999*).

Anyway, it was also demonstrate that kidney is able to filtrate and re-absorb HDL particles, depending on the shape and charge of the lipoproteins; in fact, the small, discoidal and positively charged HDL are filtered faster than mature HDL (*Braschi et al., 1999*). Finally, a higher cholesteryl esters amount on HDL favorites their re-absorption (*Breznan et al., 2004*).

The balance between HDL apolipoproteins filtration and re-uptake, in particular apoA-I, can affect plasma HDL concentration, as level of apoA-I and HDL-C are inversely related to creatinine and the estimated glomerular filtration rate (eGFR) in individuals without a severe compromise of renal function (*Krikken et al., 2010*).

The lipid components of HDL, specifically cholesterol, are mainly catabolized by the liver, and secreted into bile (*Dikkers et al., 2010*).

This secretory pathway is largely mediated by hepatic SR-BI action, which depends on the mixed micelles as acceptors in bile and on the ABCB4-mediated phospholipid secretion (*Wiersma et al., 2009*). This pathway mediates the uptake of unesterified cholesterol and cholesteryl esters from HDL, without the internalization and degradation of the entire particle (*Rigotti et al., 1997*). The small lipid-poor HDL generated as a result of this process can be remodeled being incorporated into other HDL or eliminated by the kidney (*Wang et al., 1998; Webb et al., 2004*).

However, some studies suggest the existence of another pathway for the execration of cholesterol, involving the proximal small intestine in murine models (*Brown et al., 2008; Temel et al., 2010*). Lipid components of HDL can be removed by the uptake mediated by holoparticle HDL receptors. Holo-HDL particles can accumulate in

endosomes and be subsequently moved to multivescicular bodies or to lysosomes for their degradation (*Rohrl et al., 2010*).

Some molecules are involved in the action mediated by holoparticle HDL receptor, including cubilin, ectopic beta-chain of membrane-bound ATP synthase (*Martinez et al., 2003; Vantourout et al., 2010*) and hepatic CD36 (*Brundert et al., 2011*), but this process does not seem to be the main execration pathway for lipid component of HDL (figure 1).

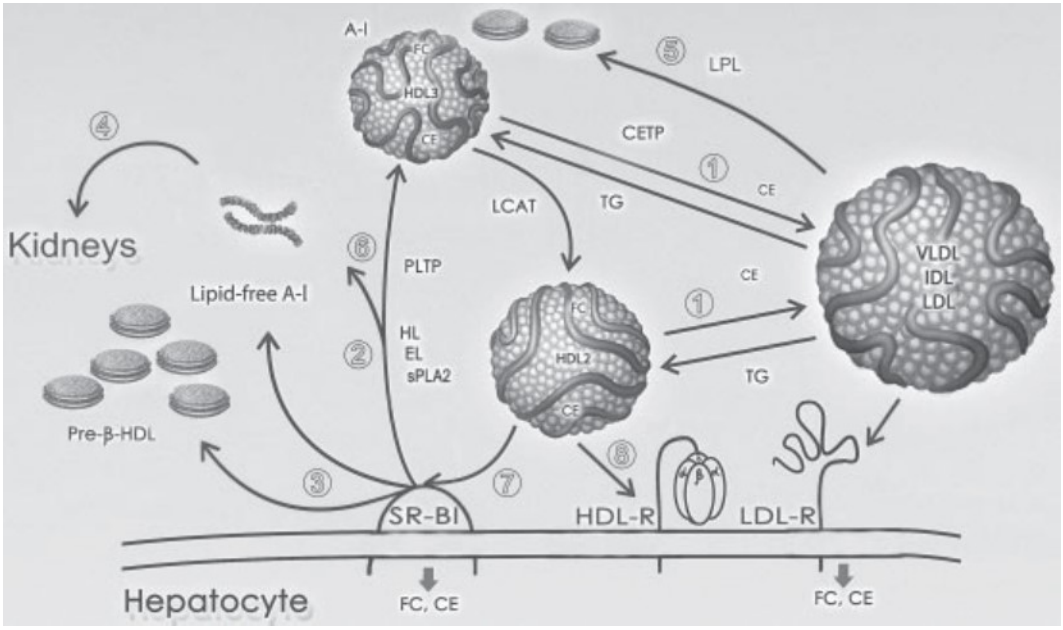

Figure 1. Major pathways involved in HDL remodeling. (1) Spherical HDL2 and HDL3 are remodeled by CETP that transfers cholesteryl esters (CE) from HDL to TGRL in exchange with triglycerides. As a result, HDL particles become enriched in triglyceride (TG). (2) HDL triglycerides can be hydrolyzed by hepatic lipase (HL), while HDL phospholipid represents a substrate for endothelial lipase (EL). (3) Uptake of HDL cholesteryl esters via SR-BI lead to the recycle of small, lipid-poor HDL subspecies and lipid-free/lipid-poor apoA-I. (4) Lipid-free apoA-I is rapidly excreted through the renal pathway mediated by cubulin and megalin receptors. (5) Hydrolysis of TGRL by LPL contributes to the plasma HDL transferring the surface constituents. (6) Hydrolysis of HDL TG and phospholipids accelerates apoA-I detachment from HDL particles. HDL are also remodeled by PLTP. (7) HDL CE are selectively taken up via hepatic SR-BI. (8) HDL can be also removed from the circulation interacting with HDL holoparticle receptor(s). FC, free cholesterol; HDL-R, holoparticle HDL receptor; LDL-R, LDL receptor (Kontush et al., 2012).

1.2.2.2 Reverse Cholesterol Transport (RCT)

The reverse cholesterol transport (RCT) is a process responsible for the removal of cholesterol from the peripheral cells, including the macrophages in the arterial walls;

in this context, the HDL exert the fundamental function of promoting the efflux of cholesterol from the macrophages and transport it to the liver for the elimination through the bile (figure 2) (*Glomset, 1968*). This process is considered anti-atherogenic, as prevents the accumulation of cholesterol in the arterial wall that could lead to a plaque destabilization and consequently to an acute cardiovascular event.

The first step of RCT is represented by the cell cholesterol efflux, and the exchange of free cholesterol from cells to extracellular acceptors can occur through several distinct pathways: aqueous diffusion, according to cholesterol gradient, or it can be mediated by different transporters (*Jessup et al., 2006*). The involved transporters are ABCA1 and ABCG1, with an ATP-dependent and unidirectional action, and SR-BI, that mediates an ATP-independent bidirectional pathway.

The expression of ABCA1 and ABCG1 is particular high in macrophages, confirming the role of these proteins in HDL-mediated cholesterol efflux. ABCA1 is involved in the formation of small discoidal preβ-HDL, as, interacting with apoA-I, it promotes the flow of phospholipids and cholesterol to these particles. The generated particles are efficient cholesterol acceptors and are able to further increase the removal process from peripheral cells. Moreover, both preβ-HDL and α-HDL particles are good cholesterol acceptors through ABCG1 pathway (*Jessup et al., 2006; Favari et al., 2019*). On the other side, the role of SR-BI in mediating macrophage cholesterol efflux in vivo is probably not quantitatively relevant, despite the in vitro results (*Wang et al., 2007*).

Free cholesterol on HDL is later on esterified through the action of LCAT enzyme; the generated cholesteryl esters are more hydrophobic than free cholesterol, and migrate to lipoprotein core, contributing to the particle enlargement. The catabolic destiny of cholesteryl esters includes the exchange for triglycerides to apoB-containing lipoproteins via CETP, to be finally catabolized with this particles in the liver. Another alternative way to catabolize cholesteryl esters is the direct removal of HDL through hepatic SR-BI (*Ji et al., 1999*).

In this context, for a long time, LCAT has been considered a key enzyme for the promotion of the process. Initially, in fact, it was believed that the reaction catalyzed by LCAT was involved in the maintenance of cell cholesterol efflux, preserving the

cholesterol gradient between the cell membrane and extracellular acceptors and facilitating cholesterol efflux by passive diffusion or transporters (*Glomset 1968; Matsuura et al., 2006*). However, some evidences contrast this concept: for example, it has been demonstrated that macrophage cholesterol efflux occurs even if LCAT is not present, both in animal models and in humans with genetic LCAT deficiency (*Tanigawa et al., 2009; Calabresi et al., 2009*); moreover, the conversion of preβ-HDL into α-HDL mediated by LCAT leads to a deprivation of the small and discoidal particles, which are ABCA1-mediated cholesterol efflux best acceptors (*Favari et al., 2004*).

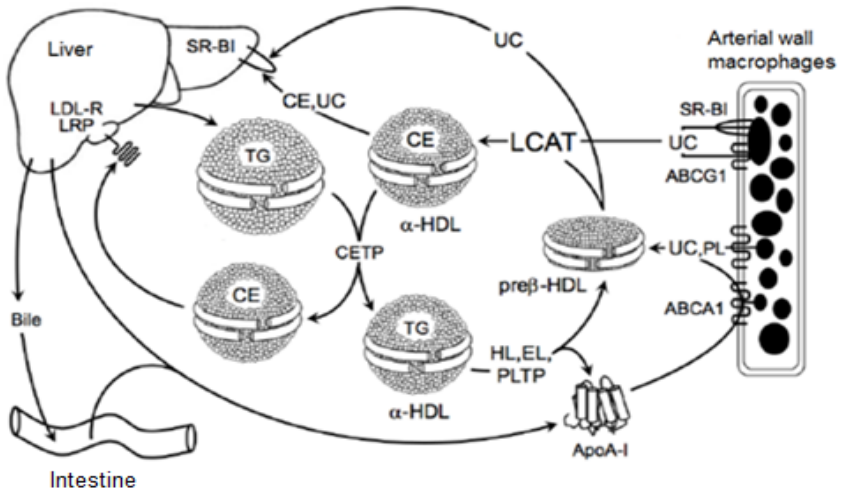

Figure 2. Schematic representation of Reverse Cholesterol Transport (RCT) (Calabresi et al., 2010)

1.2.2.3 Reverse Remnant-cholesterol Transport (RRT)

Low concentrations of HDL-C are a well-known cardiovascular risk factor, but it was also demonstrated that high concentration of HDL-C is associated with a paradoxical increase of cardiovascular and overall mortality (*Kontush et al., 2013; Ko et al., 2016; Hirata et al., 2016; Matsen et al., 2017*). Thus, it is a widespread hypothesis that HDL-C concentration is not directly associated with atheroprotection, but instead alterations in HDL cardioprotective functions could be involved in the mortality for cardiovascular events (*Rader et al., 2012*).

As previously described, the main function of HDL is to remove cholesterol from the arterial wall to the subsequent elimination, in the process of RCT. However, there are some pitfalls in this assumption, which include the absence of a relationship between RCT and HDL (*Turner et al., 2012*) and the lack of strong data documenting removal of cholesterol from human atherosclerotic intima through RCT (*Madsen et al., 2018; Kontush et al., 2020*). Moreover, if the HDL function is usually reduced at low HDL-C (*Kontush et al.,2006*), the RCT seems to not be impaired in subjects with extremely high HDL-C, as the cholesterol efflux capacity of lipoproteins of these subjects is increased (*Matsuura et al., 2006; El Khoury et al., 2014*); thus, this observation does not explain the U-shaped relation between HDL-C concentration and cardiovascular events.

Intravascular metabolism of HDL is linked to the one of triglyceride-rich lipoproteins (TGRLs), as demonstrated by the existence of a negative correlation between the levels of HDL-C and triglycerides levels (*Nordestgaard et al., 2014; Rosenson et al., 2014*).

In the circulation, HDL and TGRLs interact mainly exchanging cholesterol and triglycerides by the action of CETP, but another key pathway involves the transfer of the surface remnants generated by the TGRLs lipolysis by lipoprotein lipase (LPL) to HDL (*Nikkila et al., 1978*), in a process called reverse remnant-cholesterol transport (RRT). This process is responsible for the delivery of a large amount of free cholesterol to HDL and represents the main source of HDL-C (*Magill et al., 1982*). In the circulation, TGRLs undergo to the action of LPL, which mediates the lipolysis of free fatty acids with a consequent shrinkage of the hydrophobic core; as a consequence, small and high density TGRLs remnants are produced (*Kontush, 2020; Patsch et al., 1978*). An excess of molecules, including apolipoproteins, phospholipids and free cholesterol, is released from the surface of lipoproteins as surface remnants, which can rearrange in large-size vesicular structures or in small discoidal preβ-HDL particles (*Schaefer et al., 1982; Chung et al., 2000*). Plasma HDL can acquire remnant derived free cholesterol, for its following transport to the liver after the esterification mediated by LCAT; esterified cholesterol can subsequently be

transferred to the liver by SR-BI or by apo-B containing particles through CETP-dependent or independent pathways (*Kontush, 2020; Cedo et al., 2020)* (figure 3).

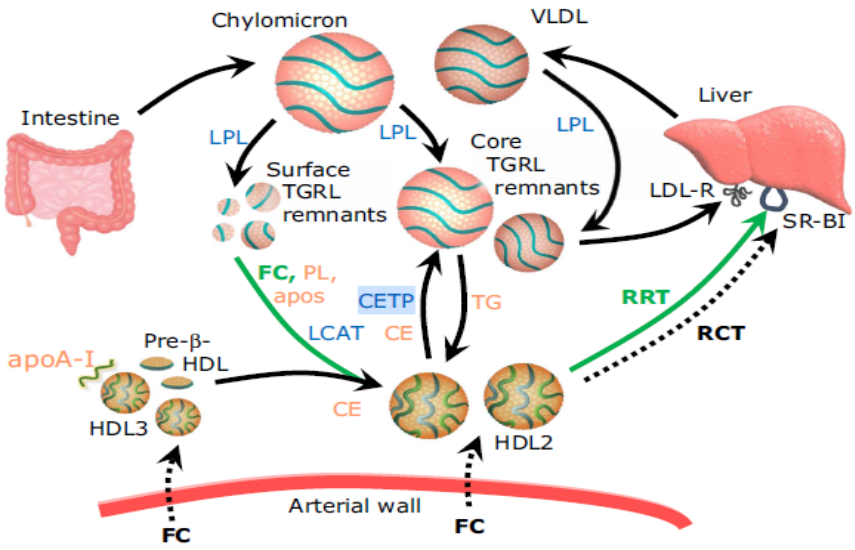

Figure 3. The Reverse Remnant-Cholesterol Transport (RRT) Pathway. Upon TG lipolysis by lipoprotein lipase (LPL), TGRL are converted into core and surface remnants. Core remnants are excreted by hepatic LDL-R. Surface remnants contain FC, phospholipid (PL), and apolipoproteins, which combine with the plasma HDL pool, resulting in FC esterification by LCAT and enlargement of HDL particles. Bound FC and CE are transferred to the liver directly via SR-BI (in green) or indirectly via apoB-containing lipoproteins. The reverse cholesterol transport (RCT) pathway from the arterial wall is shown as broken lines. Lipoprotein components are in orange, and enzymes and lipid transfer proteins are in blue (Kontush, 2020)

The RRT hypothesis suggest that in pathological conditions associated with cardiovascular outcomes, the transfer of free cholesterol from TGRLs to HDL could be impaired, as demonstrated by a recent study published by Feng et al. (*Feng et al., 2020*). In this study, it was reported that the rate of this process is decreased both at low levels and at extremely high concentrations of HDL-C, inversely reflecting the U-shape relation between HDL-C levels and cardiovascular mortality. Moreover, the inhibition of CETP or LCAT by iodoacetamide leads to an accumulation of free cholesterol in HDL, revealing a possible multi-step mechanism of transport between TGRLs and HDL which involves the uptake of free cholesterol by HDL and its subsequent esterification mediated by LCAT followed by CETP-mediated exchange of the cholesteryl ester for triglyceride present in TGRLs. However, the functionality of RRT in genetic LCAT inihibition has never been tested and it remains to be

established whether in conditions of low HDL-C the accumulation of free cholesterol on the particles due to the lack of LCAT is still observable.

On the contrary, the HDL-C ability to uptake phospholipids derived by TGRL lipolysis is directly correlated with HDL-C levels and is not associated with cardiovascular risk , in clear contrast to the U-shaped relationships observed between FC and HDL-C. The absence of the relationship between cardiovascular mortality and HDL capacity to acquire PL attests to the specificity of the relationship of the lipolytic FC transfer with cardiovascular disease (Feng 2021).

In conclusion, the impairment of the RRT could be likely due to alterations in HDL composition or in lipid transport proteins and enzymes, and this recent finding could highlight a possible link between HDL-associated cardiovascular risk and triglyceride metabolism (*Feng et al., 2020*); thus,the capacity of HDL to acquire free cholesterol upon TGRL lipolysis by LPL in vitro may represent a superior biomarker of cardiovascular risk than plasma HDL-C levels (Kontush 2020)..

1.3.1 LCAT activation mediated by bond with lipoproteins

LCAT bond with lipoproteins is a fundamental step for the activity of the enzyme and some molecules play a crucial role as LCAT activators. Among these, the main LCAT activator is represented by apoA-I and mutations of this gene are associated with poor enzyme activation; however, other apolipoproteins can activate the enzyme to a lesser degree, like for example apoE, which exerts an important LCAT activation on apoB-containing lipoproteins and in cerebrospinal fluid (*Hirsch-Reinshagen et al., 2009; Zhao et al., 2005*), apoA-IV (*Emmanuel et al., 1994*) and apoC-I (*Soutar et al., 1975*).

Some requirements for LCAT activation by apolipoproteins are lipid binding and amphipathic α-helical structures with a non-polar face of approximately 100 degrees, an opposite central region of acidic residues and a distribution of basic residues at the polar-nonpolar interface (*Jonas, 2000*). In fact, a precise conformation of α-helical structures and amino acid sequence of apoA-I are required for an efficient activation of LCAT. Three specific arginine residues in apoA-I (R149, R153, and R160) seems to be involved in LCAT binding, as they are responsible for the formation of multiple

hydrogen bonds between the arginine guanidinium group of Arg and lipid polar groups and phosphatidylcholine esters may be exposed to active center (*Cho et al., 2001*); amino acid alterations in these regions interfere with the activation of the enzyme (*Sorci-Thomas et al., 1997*). Finally, apoA-I also residues between 143 and 187 are necessary for LCAT activation; if these residues are altered by site-directed mutagenesis, the apolipoprotein is no longer able to activate LCAT (*Jonas, 2000*).

1.3.2 Mechanism of reaction

LCAT is an ATP-independent enzyme responsible for the formation of cholesteryl esters in plasma. Its plasma concentration correlates with plasma enzyme activity, as demonstrated with endogenous lipoproteins (cholesterol esterification rate) or a standardized exogenous substrate (LCAT activity) (*Calabresi 2012*). The enzyme exerts three catalytic activities: phospholipase A2, acyltransferase activity and lysolecithin acil transferase (LAT) activity. The most important activities are the first ones, that lead to the formation of a lysophospholipid and esterified cholesterol. The process can be divided into two phases:

1) phospholipase A2, that cleaves the fatty acid in sn-2 position of lecithin and transfers it onto Ser181. The result is the acylation of the enzyme and the formation of lysolecithin.

2) acyltransferase activity, that permits the fatty acid transesterification to the free 3-β-hydroxyl group of cholesterol, generating cholesteryl ester (CE) (*Jonas, 2000*). (Figure 4)

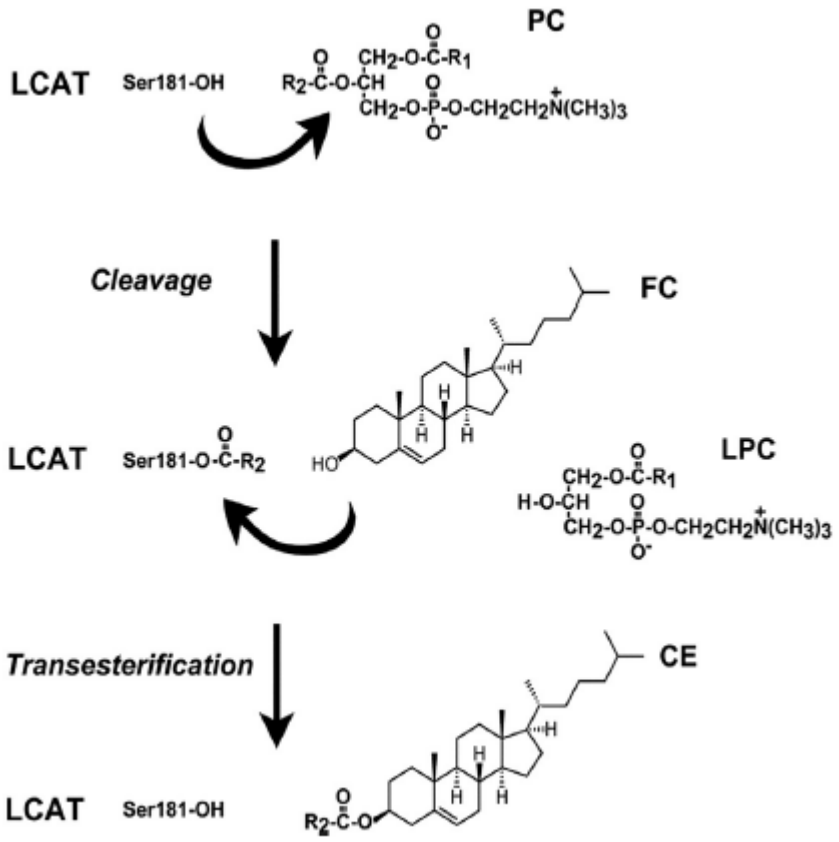

Figure 4. Representation of LCAT Reaction. Step 1: Cleavage—Phospholipase cleavage of fatty acid from sn2 position of phosphatidylcholine (PC) with formation of lysophosphatidilcholine (LPC). Step 2: Transesterification— Transfer of fatty acid bound to Ser181 of LCAT to the hydroxyl group of cholesterol or other sterol acceptor (Rousset et al., 2009).

The limiting step of the enzymatic reaction is the bond between the phospholipid and LCAT.

The main phospholipidic substrate of LCAT is phosphatidylcholine (PC), the donor of acyl group; however, it has been demonstrated that the enzyme can use also phosphatidylethanolamine, for which has a comparable affinity (*Pownall et al., 1985*; *Rousset et al., 2009*).

The length and the unsaturation rate of the sn-2 fatty acid can affect LCAT action, as the enzyme prefers polyunsaturated fatty acids with variable dimension depending on the species (*Rousset et al., 2009; Parks et al., 1997; Pownall et al., 1985*).

The bond between LCAT and PC is established through the acyl chain of PC, which acquires a variable orientation in the active site; this explains why, when the 2-sn fatty acid is very long (18:0, 18:1 (trans), 20:4), the enzyme uses the sn-1 acyl chain,

suggesting that the dimensions of the acyl-chain binding area are restricted (*Jonas, 2000*).

Besides phospholipids, the second LCAT substrate is cholesterol. The binding site is not well described, it but could be identify close to Cys31 e Cys184, as mutations on these amino acids cause alterations in the transesterification process of the enzyme, without compromising the other activities (*Bonelli et al., 1989*). Cholesterol is the main acceptor of acyl group on the enzyme, but it was demonstrated that other steroid molecules, like dehydroepiandrosterone, pregnenolone e 25-hydroxycholesterol could represent good substrates for the transesterification process (*Lavallee. et al., 1996*).

Finally, the third activity of LCAT, the LAT activity, mediates the conversion of lysophosphatidylcoline to phosphatidylcholine. This particular activity is exerted in absence of an acceptor substrate or if a part of the lysolecitihin produced by LCAT reaction is reacylated in the plasma itself presumably on the LDL surface; this reaction is stimulated by LDL and does not require apoA-I as cofactor (*Liu et al., 1993*).

As previously anticipated, the preferential lipid substrates for LCAT are the small, discoidal and preβ-migrating HDL, on which LCAT is activated by apoA-I and esterifies cholesterol via α-LCAT activity. However, LCAT has also been found on LDL particles, where it esterifies cholesterol within apoB-containing lipoproteins via β-LCAT activity using apoE as a cofactor (*Calabresi et al., 2012*), even if with a reduced efficiency compared to HDL. In conclusion, LCAT is the primary source of cholesteryl esters on HDL and also on apoB-containing lipoproteins; a small amount of cholesteryl esters on lipoproteins are derived from the liver and intestine after VLDL and chylomicrons secretion and production mediated by one of the intracellular enzymes acyl-CoA:cholesterol acyltransferase (ACAT) (*Chang et al., 2009*).

1.3.3 LCAT inhibition

While some molecules act as LCAT activators, as previously discussed, others exert an inhibition of the activity of the enzyme. Some examples of LCAT inhibitors include

sphingomyelin, apoA-II, hydroperoxides of PC and PC with trans-fatty acids and chains of 18 carbons.

Sphingomyelin is a strong inhibitor of LCAT activity through several mechanisms, like the decrease of interfacial binding, the alteration of apoA-I conformation and charge. Moreover, the sphingolipid competes with phosphatidylcholine, that is the acyl-donor in the reaction, leading to non-productive bond of sphingomyelin to the active site of enzyme (*Subbaiah et al., 1993; Subbaiah et al. 2012*).

ApoA-II inhibits LCAT activation, masking the binding sites on apoA-I and competing with apoA-I for binding sites on the phosphatidylcholine- cholesterol vesicles (*Soutar et al., 1975*). In murin models, it was also demonstrated that the transfer of cholesterol from preβ-HDL to α-HDL is slower in apoA-I/apoA-II compared to apoA-I transgenic mice, suggesting an impairment of cholesterol efflux and a consequent pro-atherogenic phenotype when apoA-II is expressed in concentrations similar to humans (*Escolà-Gil et al., 1997*).

Hydroperoxides of phosphatidylcholine generated during mild oxidation of lipoprotein lipids lead to an inhibition of LCAT activity. Plasma oxidation causes the reduction of phosphatidylcholine concentration and the inhibition of LCAT ability of transferring long-chain acyl groups to cholesterol or to lyso-PC; on the other side, the transfer capacity of the enzyme for short-chain acyl groups is not only retained, but also increased, suggesting a potential physiological role of LCAT in the metabolism of oxidized PC in plasma (*Subbaiah et al.,1996*).

Finally, also trans-fatty acids or chains of 18 carbons may exert an inhibitory effect on LCAT. In fact, trans unsaturated fatty acids not only decrease HDL through their inhibition of LCAT activity, but also influence LCAT positional specificity, leading to a major formation of saturated cholesteryl esters, which are more atherogenic. PCs containing 18:1 trans or 18:2 trans fatty acids interfere with the LCAT activity, leading to a major inhibition compared to the corresponding isomers cis. Moreover, C18:1 trans fatty acids in sn-2 exert an increased inhibition of LCAT activity compared to the fatty acids position sn-1 (*Subbaiah et al., 1998*).

1.3.4 Other functions of LCAT

Besides the already described LCAT activities, the enzyme has a key role also in other physiological processes associated with atherosclerosis, in particular in the oxidation of lipoproteins. It was in fact demonstrated through in vitro studies that the enzyme has a pro-oxidant activity on VLDL, even if the molecular mechanism of this process has not been entirely defined yet; the hypothesis is that LCAT mediates the transfer of oxidized acyl groups from HDL and other lipids to VLDL (*McPherson et al., 2007*).

At the same time, LCAT plays an anti-oxidant activity on LDL: the enzyme seems to act as a "chain-break" anti-oxidant (*Vohl et al., 1999*). Ser181 residue in the active site of LCAT gives the proton to a radical carbon generated in the first phases of oxidative process, thanks to the presence of two sulfidic groups (Cys31 e Cys184); moreover, the amino acid is restored through the intervention of histidine and aspartic acids residues (Figure 5) (*McPherson et al., 2007; Vohl et al., 1999*).

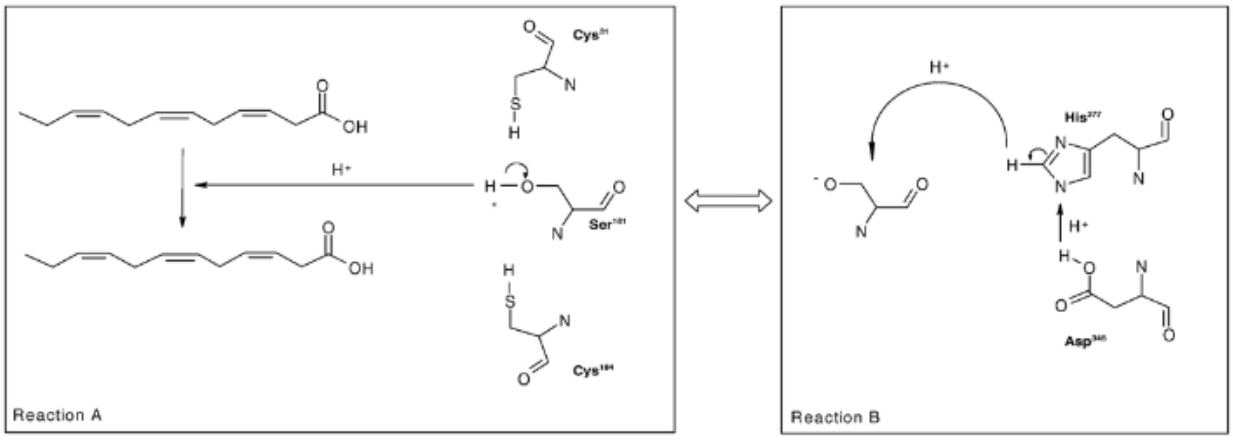

Figure 5. Theoretical mechanism for LCAT's antioxidant role in PUFA oxidation. LCAT acts as an antioxidant by donating a proton into the oxidative milieu, neutralizing the unpaired electron on the fatty acid chain and interrupting the oxidation cascade (Reaction A). The deprotonated serine residue could then be regenerated by a proton donation reaction, thanks to the proximal aspartate and histidine residues in LCAT's catalytic triad (Reaction B). *(McPherson et al., 2007)*

Supporting this hypothesis, McPherson et al. demonstrated with an in vitro study that native LDL are more resistant to oxidative stress compared to LCAT-depleted LDL,

confirming the anti-oxidant activity of the enzyme on these lipoproteins (*McPherson et al., 2007*).

A subsequent study on carriers of mutations on *APOA1, ABCA1* and *LCAT* genes demonstrated that alterations in HDL biogenesis pathway can result in particles with reduced antioxidant or anti-inflammatory ability in conjunction to impaired PON1 or PAF-AH or LCAT activity (*Daniil et al., 2011*).

Finally, LCAT is able to esterify and hydrolyze the Platelet-Activating Factor (PAF) and oxidized PC with short fatty acids chains in position sn-2 without being activated by apoA-I. (*Goyal et al., 1997*).

2. Genetic LCAT deficiency

Genetic LCAT deficiency is a rare genetic disorder inherited by a recessive autosomic mechanism, characterized by “loss-of-function” mutations on the *LCAT* gene. The pathology was first described by Norum and Gjone in 1967 in Norway, in a 33-year-old woman presenting with corneal opacities, anemia, proteinuria, mild hypoalbuminemia, and hyperlipidemia; the same abnormalities were then identified in her siblings (*Norum et al., 1967; Torsvik et al.,1968*).

Since the first case, a high number of LCAT gene mutations has been identified through the investigation of single cases, or small families in which a defect in the LCAT gene was predicted from the biochemical or clinical presentation. Up to now, 117 different molecular defects have been identified spread all along the LCAT gene in carriers. It is interesting to underline that most of the described mutations are private; among them, 77 are classified as FLD and 12 as FED, while 28 mutations have not been classified yet. Moreover, all the pathogenic LCAT mutations described cause and abolishment of α-LCAT activity, while no mutations affecting only the β-LCAT activity have been described yet. This observation suggests that the interaction between LCAT and the apoA-I-containing particles is much more sensitive to LCAT structural changes compared to the interaction between the enzyme and the apoB-containing lipoproteins (*Pavanello et al., 2020*).

The mutations can present in homozygosis, heterozygosis or compound heterozygosis; depending on the genotype, carriers of mutations in both alleles can develop two different LCAT deficiency syndromes, characterized by different biochemical and clinical manifestations: familial LCAT deficiency (FLD) and fish-eye disease (FED) (*Santamarina-Fojo et a., 2001*).

In FED, LCAT partially loses its activity, esterifying cholesterol only on LDL (enzyme retains β-LCAT activity), while FLD syndrome is characterized by the total lack of LCAT activity on both HDL and LDL, as well as a reduction in LCAT synthesis (*Santamarina-Fojo et al., 2001*).

The differential diagnosis of FLD and FED in homozygous carriers requires the measurement of the ability of plasma to esterify cholesterol incorporated into endogenous lipoproteins (α-LCAT plus β-LCAT activity) or into a synthetic HDL substrate (α-LCAT activity) (*Calabresi et al., 2005*). For heterozygous carriers, it is not possible to diagnose FLD or FED based on biochemical or clinical criteria (*Calabresi et al., 2005*). Thus, to classify the genotype of carriers of mutation on one allele, measurement of LCAT concentration and activities in cell media or transient expression of LCAT mutants in cultured cells are used (*Calabresi et al., 2009*).

2.1 Biochemical features in LCAT deficiency

2.1.1 Lipid and lipoprotein profile of LCAT deficient carriers

Homozygous carriers present a dramatic reduction of HDL-C (<10 mg/dL), paralleled by a strong increase in the amount of free cholesterol (>75%), with the consequent increase of unesterified cholesterol/total cholesterol ratio. Moreover, these subjects have variable concentrations of total cholesterol and LDL-C, and in FLD LDL are smaller and enriched in triglycerides; finally, frequently VLDL-C and triglycerides concentration is enhanced (*Santamarina-Fojo et al., 2001; Calabresi et al., 2005*). Hypertriglyceridemia is a common trait in LCAT deficient carriers; this condition could be likely explained by a reduction in LPL activity, as demonstrated in a murine model (*Ng et al., 2004*) and in some FLD subjects (*Frohlich et al., 1988*) or could be due to an increase in hepatic triglycerides synthesis (*Ng et al., 2004*).

Heterozygous carriers present an intermediate lipid profile between homozygous and healthy subjects, with HDL-C concentration in the normal range or slightly reduced, and physiological levels of LDL-C and total cholesterol (*Calabresi et al., 2005*).
In carriers of two mutant alleles, plasma LCAT concentration is reduced, and, depending on the phenotype, the enzymatic activity is null in FLD or partial in FED. In heterozygous carriers, on the contrary, plasma enzyme concentration is barely reduced, and LCAT activity is in normal range. (*Kuivenhoven et al., 1997; Calabresi et al., 2005).*
Homozygous and compound heterozygous have a significant reduction in plasma concentration of apoA-I, apoA-II e apoB (*Calabresi et al., 2005*).

2.1.2 Lipoprotein abnormalities in genetic LCAT deficiency

Mutations on LCAT gene have a strong influence on lipoprotein profile. The analysis of homozygous carriers' HDL by 2D- electrophoresis, a technique that separate HDL for surface charge and size, highlights a drastic redistribution of apoA-I-containing-particle (*Astzalos et al., 2007*) (figure 6).

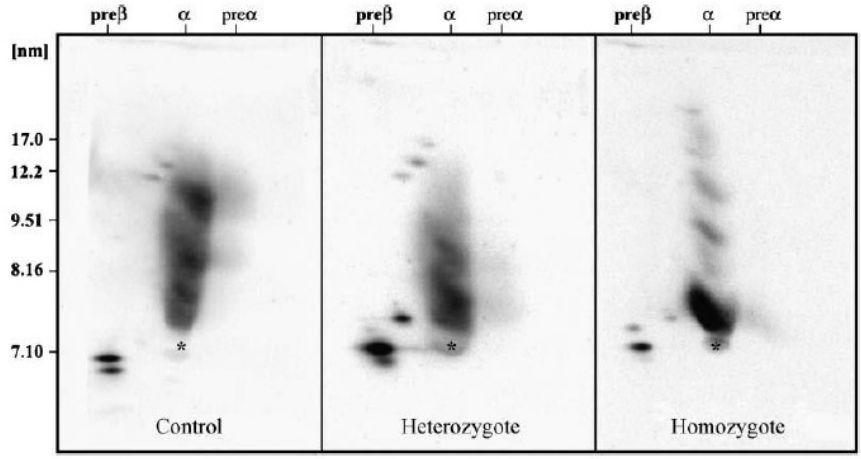

Figure 6. Apolipoprotein A-I (apoA-I)-containing HDL subpopulations of control, heterozygous, and homozygous LCAT deficient carriers separated by 2D, nondenaturing agarose-PAGE. The asterisk represents the endogenous human serum albumin marking the a-mobility front (Astzalos et al., 2007).

As demonstrated in the image, the majority of homozygotes' apoA-I is concentrated in preβ e α4 migrating HDL, which are small, discoidal and lipid-poor particle; on the contrary, the signal of apoA-I is not detectable in mature HDL. However, despite the

low plasma concentrations of apoA-I in homozygous carriers, concentrations of this apolipoprotein in these particles were comparable to those of controls (*Astzalos et al., 2007*).

Regarding heterozygotes, the 2D-electrophoresis analysis shows an intermediate profile between homozygotes and controls: apoA-I distribution in these subjects is shifted toward the smaller HDL particles, with a 2-fold increase in preβ-1 level, a 23% increase in α-4, and a 45% increase in preα-4 levels compared with controls. There is a significant decrease in the concentrations of all the other HDL particles, whereas the mean concentration of α-3, an intermediate-sized particle, is similar to controls. (*Astzalos et al., 2007*)

The genetic defect of LCAT affects also the distribution of apoA-II in HDL (figure 7):

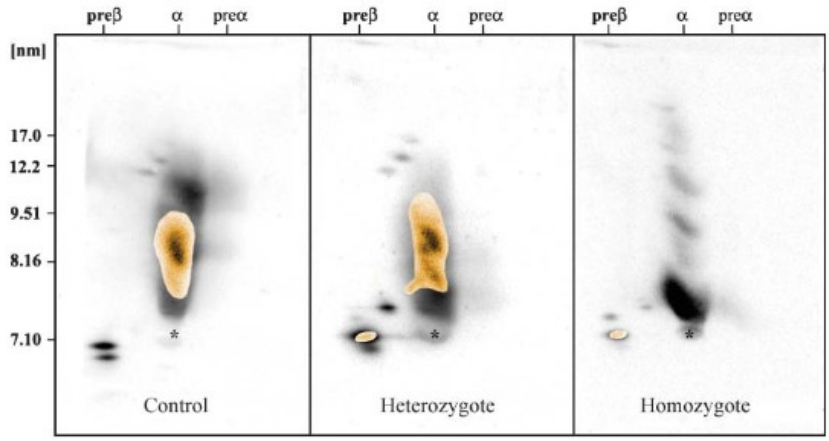

Figure 7. ApoA-II-containing HDL subpopulations of control, heterozygous and homozygous LCAT deficient carriers superimposed on the image of apoA-I-containing subpopulations. ApoA-II in LCAT deficient subjects is concentrated in small, preβ-migrating HDL particles. The asterisk represents the endogenous human serum albumin marking the α-mobility front (Astzalos et al., 2007).

The figure clearly shows that in control subjects, α-2 and α-3 HDL contain both apoA-I and apoA-II. Heterozygotes present the apoA-II signal also in preβ-1, but the majority of it is mainly focused in α-2 and α-3 subpopulations. On the other side, homozygotes have very low level of apoA-II concentrated in small and discoidal particles co-migrating with LpA-I preβ-1 HDL (*Astzalos et al., 2007*).

Despite of the alterations in HDL, in homozygous FLD carriers an abnormal lipoprotein, called LpX, is detectable (*Narayanan et al., 1984*); this particle, absent in physiological condition, is mainly composed of phospholipid and cholesterol, contains

a high content of phosphatidylcholine (60%) and unesterified cholesterol (30%) and present an intermediate density between VLDL and HDL (isolated with LDL in a density gradient of 1.019-1.063 g/ml (*Narayanan et al., 1984*). Unfortunately there are no routine clinical laboratory methods for LpX quantification, but, differently from other lipoproteins, LpX has a positive charge that allows its retro-migration through the cathode during gel agarose electrophoresis; the following staining permits its detection (*Frohlich et al., 1995*) (figure 8).

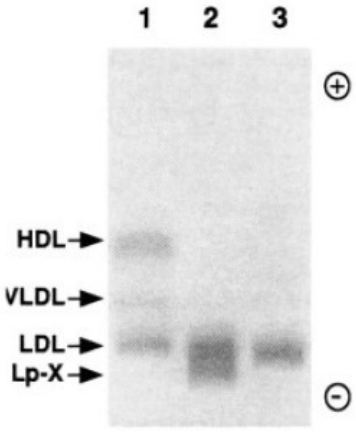

Figure 8. Lipoprotein electrophoresis. Sera from controls (lane I), pooled sera from obstructive jaundice patients (lane 2), or LDL isolated from normal serum (lane 3) loaded on a 1% agarose gel and electrophoresed for 35 min. The lipoproteins were stained with Sudan Black. The arrows indicate the position of individual lipoproteins (Frohlich et al., 1995).

Electron microscopy analysis highlights the multi-lamellar structure of LpX, composed by bi- or multi-layer of phospholipids (*Ossoli et al., 2016*) (figure 9).

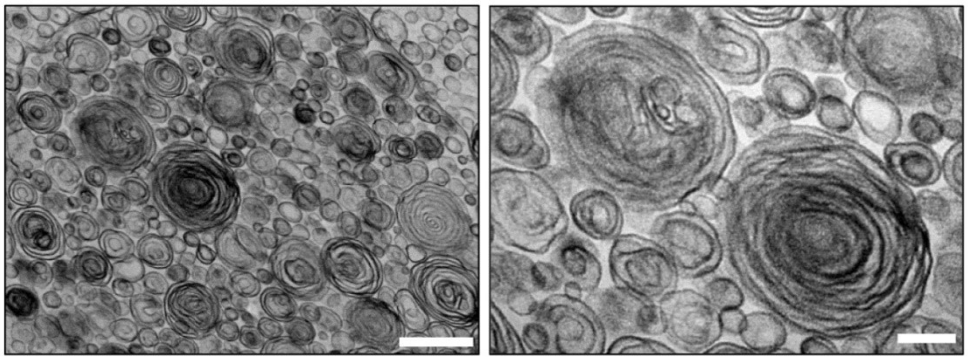

Figure 9. **TEM analysis of synthetic LpX particles.** *Left panel*: Low magnification image (Scale bar; 500 nm*). Right panel*: High magnification (Scale bar; 100 nm) (Ossoli et al., 2016)

The size of LpX variates from 30 to 70 nm. The main phospholipid of the abnormal lipoprotein is phosphatidylcholine, while sphingomyelin represent the minor fraction. LpX also contains cholesteryl ester (2%), triglycerides (2%), and a small amount of protein (6%). Proteins contained in LpX are albumin and apoCs (apoC-I, C-II and C-III). Albumin is trapped in the aqueous core of the particle, while the apoCs are present on the surface. Very small amounts of apoA-I and apoE have also be associated with LpX particles (*Narayanan et al., 1984*).

The molecular mechanisms of LpX formation are still poorly understood. The first hypothesis suggested that LpX is an intestinal lipoprotein, normally catabolized by the liver, and its accumulation is the result of liver dysfunction.

The formation of this abnormal lipoprotein in familial LCAT deficiency seems to be associated with the metabolic fate of VLDL and chylomicrons, which cannot undergo to LCAT action and the consequent catabolism; this process leads to an accumulation of these particles, that represent a source of unesterified cholesterol and phospholipids (*Boscutti et al., 2011*) .

The importance of LCAT activity in the formation of LpX has been confirmed by the inverse relationship between plasma concentration of LpX and enzymatic activity in patients with familial LCAT deficiency after blood transfusion, indicating that lack of LCAT activity is a prerequisite for LpX formation (*Norum et al., 1984*).

Another pathological condition characterized by the presence of LpX is hepatic cholestasis, probably because of the excretion of bile salt micelles rich in phospholipid into the plasma compartment (*Narayanan et al., 1984*).

Patients affected by this condition present dyslipidemias, which include hypertriglyceridemia, increased plasma phospholipids, decreased LCAT activity and hypercholesterolemia. An increase of unesterified cholesterol, principally transported in LpX, characterizes the hypercholesterolemia. Moreover, defects of hepatic lipase, lipoprotein lipase and LCAT can also occur in cholestasis (*Frohlich et al., 1995*).

2.2 Clinical features of genetic LCAT deficiency

Clinical manifestations of genetic LCAT deficiency affect only homozygous carriers and include corneal opacity, normochromic anemia and kidney disease. Renal disease is the main cause of morbidity and mortality in FLD carriers, and it will be deeply discussed in a following chapter.

2.2.1 Corneal opacity

Corneal opacity is the most common characteristic in FLD and FED patients. This condition appears since childhood and it can progress over the years. Affected subjects' cornea is cloudy, but in the majority of cases the vision is relatively normal under good lighting conditions. Ophthalmological analysis highlight the presence of diffuse haziness of the corneal stroma, with an enhanced opacity near limbus, organized in diffuse, grayish, circular bands (*Cogan et al., 1992*) (figure 10).

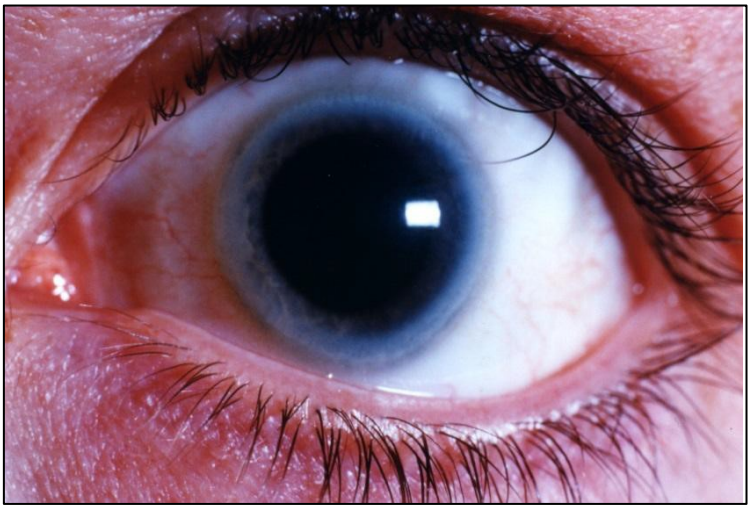

Figure 10. Typical corneal opacity in LCAT deficiency patients (Calabresi et al., 2009)

The corneal opacity is due to a high number of 5-200 nm vacuoles diffused in the stroma, which contain free cholesterol and phospholipids. In physiological conditions, LCAT, either directly or because of its effect on increasing HDL levels, removes these lipids from the corneal tissue; in case of genetic defect of the enzyme, this process is impaired, with consequent lipid accumulation (*Viestenz et al., 2002*). In addition to the

presence of vacuoles, amyloid plaques mainly concentrated close to Descemet membrane have been noticed; an hypothesis is that these structures can derive from secondary amyloidosis due to the accumulation of apolipoproteins in absence of LCAT (*Viestenz et al., 2002*) (figure 11).

Often, at first analysis, the diagnoses deduced from the histopathologic evidences are erroneously associated to other pathological conditions, like corneal dystrophy, cystinosis, and mucopolysaccharidosis; moreover, a similar corneal damage has been described in another hypoalphalipoproteinemia such as Tangier disease (*Winder et al., 1985*)

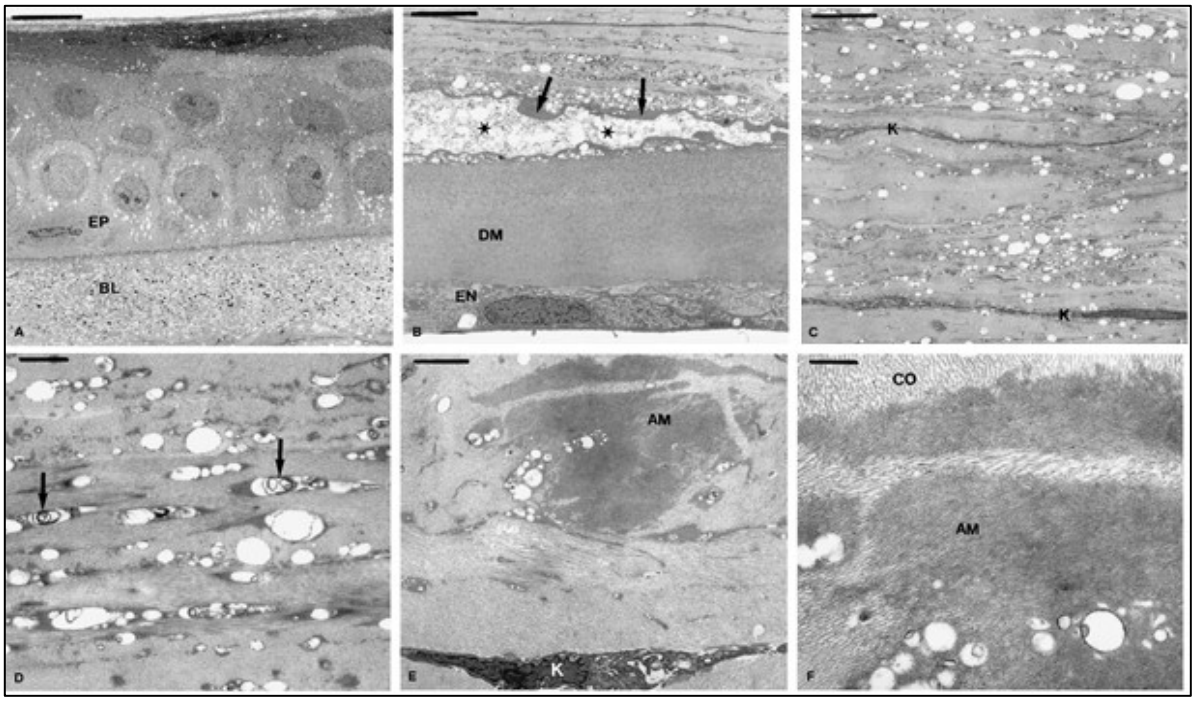

Figure 11. Transmission electron micrographs of the corneal button. A: Corneal epithelium (EP) with vacuolar inclusions in the basal cell layer and dense deposits of small vacuoles in Bowman's layer (BL) (bar = 10 µm). **B:** A broad band of electron-transparent material (asterisk) associated with amyloid (arrows) close to normal Descemet's membrane (DM) and corneal endothelium (EN) (bar = 5 µm). **C:** Corneal stroma with abundant electron-lucent extracellular vacuoles and elongated keratocytes (K) (bar = 5 µm). **D:** Higher magnification of the corneal stroma presenting extracellular vacuoles with lamellar inclusions (arrows) (bar = 1 µm). **E:** Amyloid (AM) deposits in the corneal stroma (K, keratocyte; bar = 2 µm). **F:** Higher magnification of amyloid (AM) deposits (CO, collagen; bar = 0.5 µm). (119)

2.2.2 Normochromic anemia

One of the most common clinical manifestations of FLD carriers is a mild chronic normochromic anemia associated with increased reticulocyte., which can appear between 30 and 40 years. In this condition, hemoglobin concentration is between 10 and 12 g/dL, with values that can reach 8-10 g/dL with the worsening of proteinuria (*Suda et al., 2012*).

Erythrocytes implement adaptive modifications to preserve the correct membrane fluidity despite of the alteration of plasma lipid profile and the increased circulating free cholesterol. The adaptive changes include deep alteration in the composition of the cellular membranes, which are enriched of unesterified cholesterol, phosphatidylcholine and polyunsaturated

short chain fatty acids, at the expense of the presence of phosphatidylethanolamine, sphingomyelin and long chain fatty acids. All these changes described in LCAT deficiency are associated with abnormal properties such as deformability and membrane fluidity (*Yawata et al., 1984*). Moreover, the structural changes of erythrocytes lead to a reduction of their half-life and to an increase of mean corpuscular volume of about 7%; in addition these cells present an heterogeneity in shape and about 20% of the erythrocytes in LCAT deficient carriers is represented by Target cells or Knizocytes (*Suda et al., 2012*).

In bone marrow it is possible to distinguish a reduction of erythropoiesis process and the presence of blue-colored histiocytes (detectable with Giemsa coloration) and foamy cells, that are associated with the lipid accumulation due to the defect of LCAT, responsible for their HDL-mediated removal, and to an abnormal release from LpX (*Boscutti et al., 2011*).

2.3 Acquired LCAT deficiency: not only genetics

LCAT deficiency has mainly a genetic origin, but some more common pathological conditions present an acquired defect of the enzyme. In 2012, for example, Simonelli et al. described a case of acquired LCAT deficiency due to the presence of anti-LCAT antibodies in plasma of a non-Hodgkin lymphoma patient (*Simonelli et al., 2012*).

Conditions of acquired LCAT deficiency have been frequently described in patients affected by chronic kidney disease (CKD), a pathology presenting kidney damage or the reduction of glomerular filtration rate (GFR) for more than 3 months, which can be classified into five stages based on the values of GFR (*Levey et al., 2011; Strazzella et al., 2021*). CKD is strongly associate with the onset of cardiovascular disease (CVD); the risk of cardiovascular events increases as the kidney function declines (*Foley et al., 1998*). The main CVD risk is represented by the dyslipidemia that characterized CKD patients: alterations in lipid profile of these subjects include hypertriglyceridemia and decreased HDL-C levels, while the levels of LDL-C are within or below the normal range (*Hager et al., 2017*).

Reduced HDL-C concentration is a typical trait of the CKD dyslipidemia; the HDL level is the only lipid trait considered an independent predictor of the progression of chronic kidney disease progression in CKD subjects, in terms of kidney function, increasing rate of creatinine and/or earlier entry in dialysis (*Baragetti et al., 2013*).

The reduction of HDL-C and consequently of apoA-I concentrations in CKD can be partly explained by the downregulation of apoA-I synthesis in the liver (*Lacquaniti et al., 2010*), but more importantly by the defective LCAT concentration and activity, leading to altered plasma HDL remodeling (*Calabresi et al., 2014*).

In 2014, Calabresi et al. demonstrated a strong impairment of cholesterol esterification process in patients with CKD, enhanced in subjects under hemodialysis. In the study, plasma concentration of LCAT and the enzyme activity are strongly reduced; in parallel, the maturation of HDL particles is impaired because of the delayed LCAT-dependent conversion of nascent discoidal preβ-HDL into mature spherical α-HDL (*Calabresi et al., 2014; Miida et al., 2003*) (figure 12).

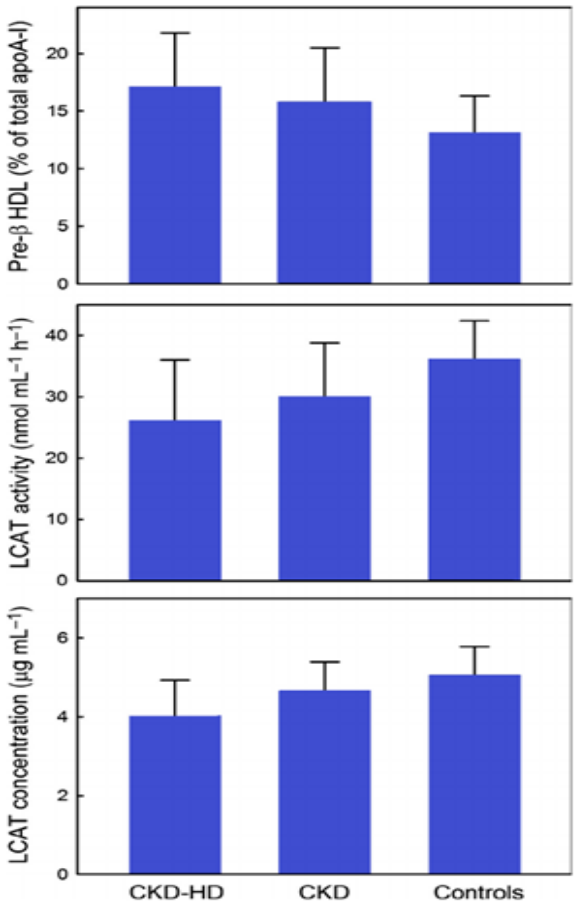

Figure 12. Plasma LCAT activity, LCAT concentration and preβ-HDL amount in patients with chronic kidney disease (CKD) undergoing hemodialysis (CKD-HD, n = 198), patients with CKD (n = 50) and healthy subjects (controls, n = 40). Data are mean ± SD (Calabresi et al., 2014).

In addition to the reduced LCAT activity, other factors are involved in the increased lipid-poor HDL particles in the plasma of CKD patients; among these, an impaired renal clearance (*Kuchta et al., 2019*) and the elevated concentration of triglyceride-rich lipoproteins, which are a source of nascent HDL (*Feng et al., 2020*).

Moreover, CKD patients' HDL are characterized by a selective reduction of LpA-I:LpA-II particles, probably explained by an enhanced catabolism of these particles when LCAT activity is decreased, as observed in genetic LCAT deficiency (*Calabresi et al., 2014; Rader et al., 1994*).

The reduction of LCAT in CKD impacts also on HDL composition (*Marsche et al., 2020*); in fact, the proteome of CKD subjects' HDL presents deep alterations, as the enrichment of serum amyloid 1 (SSA1), which is one of the major inflammatory acute-

phase proteins and an atherogenic mediator (*Malle et al., 1996*), as well as the increase of apoC-III, an inhibitor of lipoprotein lipase and a strong predictor of CVD risk (*Wyler et al., 2015*). In parallel with the enrichment in these components, a reduction in apoA-I, apoA-II, apoC-I, apoM, and paroxonase-1 (PON 1) has been described in HDL of CKD subjects (*Strazzella et al., 2021*).

All these structural modifications are associated with the impairment of fundamental HDL functions, like their ability of promoting cholesterol efflux from macrophages (*Maeba et al., 2018*) and HDL capacity to maintain correct endothelial homeostasis, because of chronic inflammation and oxidative stress (*Speer et al., 2013*). Moreover, also HDL anti-oxidant ability is impaired in patients with CKD (*Moradi et al., 2009*), because of the reduction in PON-1 and apoA-I content, two molecules known to exert antioxidant activity (*Kontush et al., 2010*), and a concomitant enrichment of acrolein-modified apoA-I (*Suematsu et al., 2019*). Finally, in patients with CKD, the enrichment in acute-phase proteins, such as SAA and in apoC-III, which are involved in the organ damage by alternative inflammasome activation and in the activation of inflammatory cell response explains in part the loss of the anti-inflammatory activity of HDL (*Zewinger et al., 2020*) (figure13).

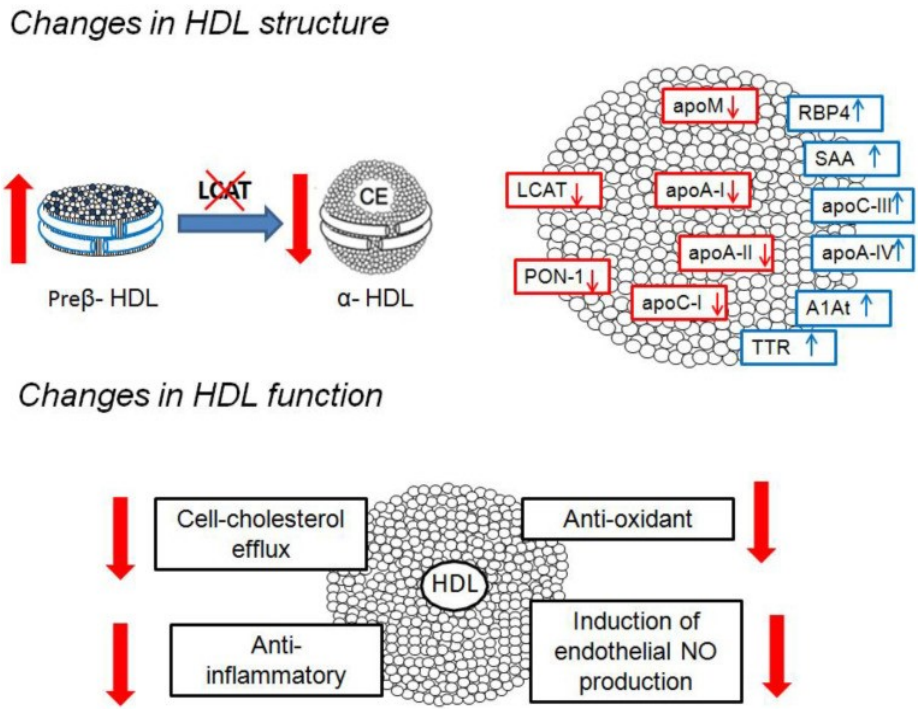

Figure 13. HDL structural and functional modifications in CKD. Upper panel: major alterations in HDL shape and protein composition; lower panel: changes in HDL functions. Abbreviations: LCAT, lecithin–cholesterol acyltransferase; PON-1, paroxonase-1; apoA-I, apolipoprotein A-I; apoA-II, apolipoprotein A-II; apoC-I, apolipoprotein C-I; apoM, apolipoprotein M; apoC-III, apolipoprotein C-III; apoA-IV, apolipoprotein A-IV; SAA, serum amyloid A; A1AT, α-1-antytrypsin; RBP4, retinol-binding protein 4; TTR, transthyretin. The arrows indicate increase or decrease (Strazzella et al., 2021).

In conclusion, the acquired LCAT deficiency in CKD patients leads to a decrease of HDL concentration and functions, with possible consequences on the development of renal damage and on cardiovascular outcome.

3. Renal disease in genetic LCAT deficiency

As previously anticipated, renal disease represents the major cause of morbidity and mortality in FLD patients. However, this clinical manifestation is variable among the carriers, and it can depend on lipid profile, diet and previous kidney disease (*Boscutti et al., 2011*).

Proteinuria is the first symptom of the disease; it can appear in the third and fourth decade of life, with a following development to renal failure with edema and hypertension. The rate of renal disease progression is unpredictable, as some carriers can rapidly degenerate from a mild proteinuria to a fast decline in their renal function even in their 20s. FLD carriers' urine usually contains proteins, erythrocytes and hyaline casts, but the indices of renal function, including serum creatinine and creatinine clearance, remain normal in the first three decades of life (*Boscutti et al., 2011; Miarka et al., 2011*).

The molecular mechanisms of the pathogenesis of renal disease in FLD carriers are not completely understood yet. The most probable hypothesis is that the dramatic changes in lipoprotein profile could be related to the progression of renal disease; in particular it has been demonstrated that the presence of LpX and of possibly large molecular weight LDL (LM-LDL), that accumulate in plasma of FLD patients, play a key role in glomerulosclerosis development (*Imbasciati et al., 1986; Ossoli et al., 2016*). Moreover, this hypothesis is in line with the absence of renal disease in FED, as in these subjects the residual LCAT activity prevents the formation of a significant amount of LpX. However, these abnormal lipoprotein particles are not always detected in FLD patients with renal disease (*Borysiewicz et al., 1982*).

In 2016, a study published by Ossoli et al. demonstrated that in a murine model of LCAT deficiency, the chronic administration of synthetic LpX is directly involved in the onset of both glomerular and tubular damage, confirming that LCAT plays a key role in the remodeling of the abnormal lipoprotein and that the accumulation of LpX is sufficient to explain, at least partially, kidney disease in FLD condition (*Ossoli et al., 2016*)

It has still to be clarified whether the abnormal accumulation of pre-β HDL, typical of FLD carriers' profile, is involved in the renal damage and which the molecular pathogenic mechanisms underlying this condition are.

3.1 Renal damage in genetic LCAT deficiency

Glomerulosclerosis is the typical renal lesion observed in FLD patients. This condition is characterized by a progressive glomerular scarring; at the early stage of the disease, glomerulosclerosis is both focal, which involve a minority of glomeruli, and segmental, that affects a portion of the glomerular globe. As long as the pathology progresses, a more widespread and global glomerulosclerosis develops (*Miarka et al., 2011*).

Renal biopsy of FLD carriers allows a quite accurate diagnosis: through light microscopy analysis it is possible to highlight the characteristic focal segmental glomerular sclerosis (FSGS) with mesangial expansion, the presence of a mild increase in mesangial cellularity, and the irregular thickening of the glomerular capillary walls (*Boscutti et al., 2011*). Moreover, the staining with Oil Red O, which distinguishes neutral lipid, permits to detect some lipid deposits that result in the vacuolization of the glomerular basement membrane with a typical "foamy" appearance. The analysis on isolated glomeruli shows a markedly higher presence of unesterified cholesterol and phospholipids compared to physiological condition (*Boscutti et al., 2011*) (figure 14).

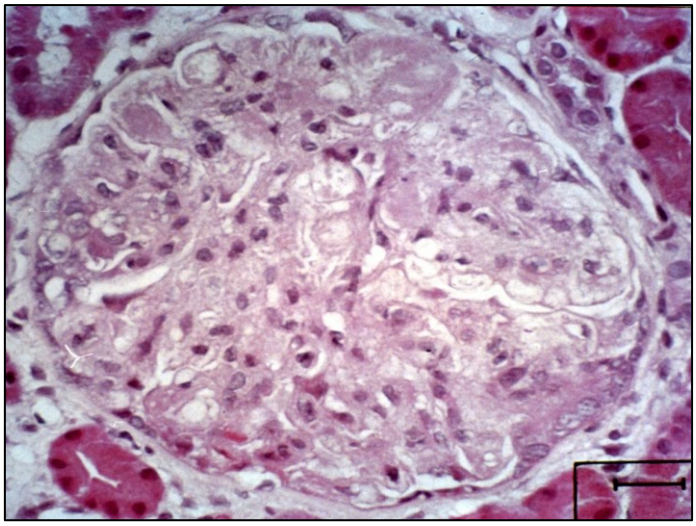

Figure 14. Renal biopsy from FLD patients analyzed by light microscopy: mesangial expansion; basement membrane with "foamy" appearance; foam cells in mesangium and in capillary walls (Levey et al., 2011).

Immunofluorescence microscopy highlights also the presence of IgM deposit and bright granular staining for C3 is detected in the capillary loops, mesangium and arteriolar walls (*Imbasciati et al., 1981; Borysiewicz et al., 1982*). This lipid deposit could be involved in the activation of complement proteins and it can contribute in accelerating the injury.

Through electron microscopy, the presence of typical lipid electron-lucent vacuoles and electron-dense lamellar structures has been detected in different renal departments, including the mesangial matrix, glomerular and tubular basement membrane, and Bowman's capsule (*Lager et al., 1991*). Moreover, the presence of electron-lucent expansion in subendothelium and in subephitelial area, intracitoplasmatic lipid droplet in mesangial and endothelial cells are also detectable. The basement membrane presents an irregular thickening and fused endothelial foot processes. Moreover, the capillary walls are abnormal, showing a reduction of endothelial cells, irregular thickening of the basement membrane, and also fused endothelial foot processes. The mesangial and basement membranes are characterized by "moth-eaten holes" and usually contain lamellar osmiophilic deposits. (*Boscutti et al., 2011; Lager et al., 1991*) (figure 15).

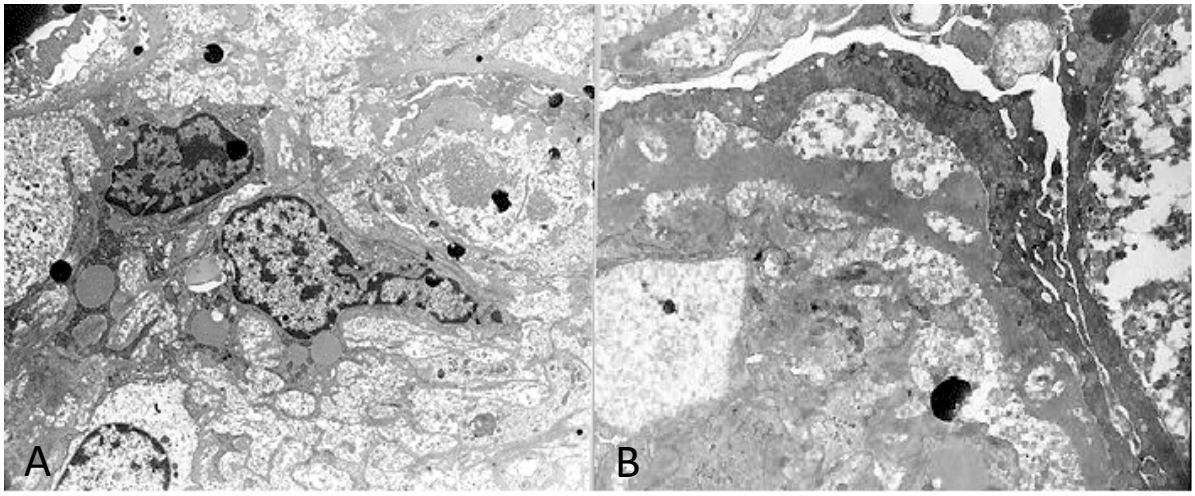

Figure 15. Characteristic lesions of nephropathy associated with LCAT deficiency in electron microscopy. A) Mesangial matrix expansion; mesangial cells nuclei are hypertrophic and irregular; lipid droplets in cytoplasmic region (electron microscopy, x 3000 magnification). B) Basal membranes expansion with irregular bubble aspect (electron microscopy, x 7000 magnification). (Adapted by Boscutti et al., 2011)

Finally, FLD carriers present some glomerular histological lesions and an immunofluorescent glomerular pattern typical of a dense-deposit disease, which is called hypocomplementemia type II membranoproliferative glomerulonephritis (*Sessa et al., 2001*).

Besides the glomerular damage, a case report on two Turkey brothers affected by FLD described a tubular pathology, characterized by a diffuse tubular atrophy with thickening of the tubular basement membranes, associated with focal interstitial fibrosis and mononuclear cells infiltrates (*Stoekenbroek et al., 2013*) (figure 16).

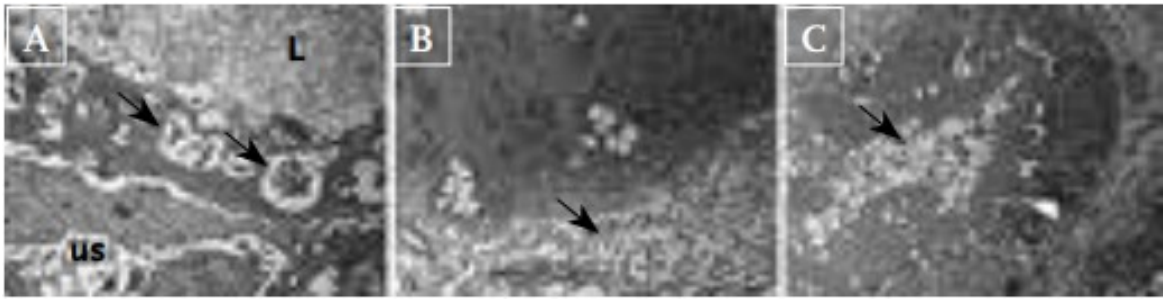

Figure 16. Electron microscopy of renal biopsy of patient 1. A: Glomerular basement membrane with accumulation of lipids. US: urinary space, L: capillary lumen, arrows: osmiophilic structures. B: Tubular basement membrane with osmiophilic structures (arrow). C: Tubule. L: Lumen with osmiophilic structures (arrow) (Stoekenbroek et al., 2013)

Atrophy and interstitial fibrosis at tubular level have been described in a lot of pathologic conditions and this kind of damage is usually associated to a mitochondrial dysfunction with a consequent increase of ROS production and to the accumulation of aggregates of ubiquinated and oxidized proteins, that together can over-stimulate autophagy, ultimately leading to tubular cells dysfunction or death (*Takabatake et al., 2014*).

A possible hypothesis is that a similar process should be involved in the renal disease associated to LCAT deficiency, but further studies to verify this theory are still required.

3.2 Available therapies

Nowadays, a specific treatment for genetic LCAT deficiency is not available and carriers are usually treated just symptomatically. Patients can undergo to corneal and renal transplantation, but the disease usually reoccurs in transplanted tissue. Thus, probably because of the rareness of the disease, therapeutic options for FLD are still poorly defined.

3.2.1 Traditional therapy

The main aim of the therapy for LCAT deficiency nephropathy is to delay the evolution to chronic nephropathy, starting from changes in life style and diet, the control of hypertension, the containment of the proteinuria and control of complications (*Boscutti et al., 2011*).

Among the most used treatments, angiotensin II receptor blockers combined with lipid-lowering drugs, like statins, seems to exert a benefit in blood pressure, lipid abnormalities, proteinuria and also kidney function, probably leading to a delay in the progression to renal failure (*Aranda et al., 2008*).

Moreover, in a case report, a FLD carrier presented a reduction of proteinuria following an amelioration of the lipid profile after a combined treatment with nicotinic acid and fenofibrate; the possible explanation proposed by the authors is that the

reduction of VLDL and chylomicrons, representing the phospholipid pool for LpX formation, leads to a reduction of LpX itself (*Yee et al., 2009*).

Finally, another possibility is the use of corticosteroids in association with angiotensin II receptor blockers or ACE-inhibitors, that seems to ameliorate renal function and proteinuria (*Miarka et al., 2013*).

All these approaches, including renal transplantation in the most severe cases, are not definitive, as the lipid alterations associated with the genetic disorder cannot be completely corrected by treatments, but only delaying the development of the renal disease.

3.2.2 Gene therapy

Gene therapy approach is based on the use of recombinant viruses expressing LCAT in order to treat or prevent dyslipoproteinemia-related diseases, and it was first proposed in 2001 (*Freeman et al., 2020*); starting from that moment, other methods to increase LCAT activity in plasma to prevent or treat atherosclerosis or to treat FLD or FED were patented. This kind of approaches include cell transfection with vectors containing LCAT, the upregulation of *LCAT* gene expression and/or the administration LCAT itself. A study carried out on non-humans primates injected with adenovirus encoding hLCAT has highlighted a sustained increased of HDL-C after a single treatment (*Amar et al., 2007*).

Recently, some AAV vectors with tissue tropism, like for example AAV8, have been developed, reinforcing the idea of *AAV LCAT* gene for the delivery of therapeutics for the treatment of FLD. Some strategies have been used to ameliorate this approach, like the optimization of vectors using the naturally occurring LCAT variants associated with increased activity and codon optimization (*Lagor et al., 2013; Christopher, 2017*).

Anyway, the direct gene therapy presents also potential limitations, including the adequate transfection efficiency of LCAT production to reach physiologic LCAT plasma levels, the presence of pre-existing antiviral vector neutralizing antibodies, and the immunogenicity, especially with high viral infection loads (*Freeman et al., 2020*).

Thus, to overcome these pitfalls, indirect gene delivery has also been developed. This approach is based on the isolation of adipose tissue cells from patients, followed by the transfection with an LCAT expressing vector, and finally by the re-implant of these LCAT-producing cells into the same patient (*Kuroda et al., 2011*). However, also this strategy presents some limitations, that include the not optimal reintegration of the cells in the tissue and a long-term survival and the limited efficiency of LCAT transport from the implanted tissue to the circulation, with possible consequences on the achievement of physiological LCAT concentration (*Freeman et al., 2020*).

A recent study published by Guo et al demonstrates the efficacy of the gene therapy for dyslipidemia, renal injury, and atherosclerosis-related cardiovascular disease in *Lcat*$^{-/-}$ hamsters, using an adeno-associated virus expressing human LCAT (AAV-hLCAT) targeting the liver in these animals. The results obtained show that a single administration of AAV-hLCAT effectively corrects LCAT deficiency for a long period rescue multiple abnormalities, including renal injury, anemia and atherosclerosis in hamsters (*Guo et al., 2021*).

In conclusion, despite all the limitations, the concept of genetically engineered cell therapy for FLD carriers is a valid approach, that in future could potentially be developed and applied to patients.

3.2.3 Recombinant human LCAT enzyme

The enzyme replacement therapy has been a successful approach for several genetic diseases and this set the basis for the recent effort to also develop recombinant human LCAT (rhLCAT) as a therapy. The main potential indications for the use of rhLCAT are for the treatment of FLD and for raising HDL-C as a possible treatment of cardiovascular disease (*Norum et al., 2020*).

A human study on rhLCAT has demonstrated the safety and tolerability of the recombinant enzyme in a cohort of stable coronary heart disease (CHD) and low HDL-C patients in a phase I study (*Shamburek et al., 2015*). In 2016, rhLCAT has been used for the treatment of a single FLD carrier with advanced renal disease and dramatic low HDL-cholesterol levels (*Shamburek et al., 2016*). The patient was treated weekly for approximately 7 months with a dose ranging between 3 and 9

mg/kg. After the treatment with rhLCAT, HDL-cholesterol levels have been normalized until about 3 days after the end of the infusions; a normalization has also been observed in the percent of cholesteryl esters in plasma. The evaluation of renal function has highlighted some minor improvements only during the first month of treatment, with no further benefits during time, probably due to the very compromised condition of the subject (*Shamburek et al., 2016*).

The results collected in this study demonstrate that enzyme replacement therapy with rhLCAT could represent a potential strategy for increasing HDL-C in FLD. However, the effect of rhLCAT on LpX, fundamental for the onset of renal disease in LCAT deficiency, has been studied only in a recent study, in which increasing doses of a more potent formulation of rhLCAT, MEDI6012, have been incubated ex vivo with plasma from an FLD patient. The results obtained show that the incubation of FLD plasma with rhLCAT decreases LpX in a dose-dependent manner (*Freeman et al., 2019*).

In line with the positive results obtained in vivo and ex vivo, the beneficial effect of the treatment with recombinant LCAT has been demonstrated in several animal studies. In one of the most recent works, the researchers have used a mouse model with deleted LCAT gene and with a truncated version of the hepatic SREBP1a gene under the control of a protein-rich/carbohydrate-low (PRCL) diet-regulated PEPCK promoter. This peculiar murine model develops spontaneously abundant amounts of LpX in plasma and it has been injected with rhLCAT to determine whether the treatment with the recombinant could prevent LpX formation and renal injury. The results obtained demonstrate that rhLCAT as able to restore the normal lipoprotein profile, to eliminate LpX in plasma and kidneys and to markedly decrease the proteinuria in these mice (*Vaisman et al., 2019*).

All these considerations, suggest that rhLCAT treatment could represent an effective therapy for the prevention of renal disease in patients with FLD.

Moreover, besides its possible utility for the treatment of FLD, rhLCAT may also exert beneficial effect on cardiovascular disease because of its role in reverse cholesterol transport. Based on this concept, some animal studies have been carried out; for example, both in transgenic rabbits expressing human LCAT (*Amar et al., 2009*) and

in rabbits treated with rhLCAT, a protection against diet-induced atherosclerosis has been shown. However, in mice overexpressing LCAT but with lack of CETP, atherosclerotic process increases, emphasizing the importance of CETP in cholesterol processing following the LCAT reaction (*Hoeg et al., 1996*).

The phase I study on CHD patients, beside the tolerability and safety of rhLCAT, demonstrate that high doses of the enzyme can increase the HDL-C level, decrease preβ-HDL concentration consistently with conversion to larger HDL particles due to cholesterol esterification, and increase the capacity of LDL-depleted serum to promote cholesterol efflux from macrophages (*Shamburek et al., 2016*).

In 2019, Ossoli et al. have demonstrated that, after an acute myocardial infarction, the concentration and the activity of LCAT is reduced and HDL have an impaired ability to promote NO production in endothelial cells. rhLCAT has been tested in vitro and the incubation of the recombinant enzyme with plasma of STEMI patients collected after 48 and 72 hours after the event, restores the HDL ability to promote endothelial NO production, possibly related to significant modification in HDL phospholipid classes. Thus, the impairment of cholesterol esterification system is partially related to HDL dysfunction in acute coronary syndrome, and LCAT can represent a potential therapeutic target for restoring HDL functionality in this pathologic condition (*Ossoli et al., 2019*)

The overall conclusions are that the use of rhLCAT both for preventing renal disease in FLD carriers and for ameliorating cardiovascular disease outcome is a very promising therapeutic strategy, that is still under development.

3.2.4 LCAT activators

Treatment with rhLCAT, at the moment, seems to be the most promising therapeutic approach for FLD carriers, but the use of the recombinant enzyme presents some limitations, as it is expensive, it requires intravenous infusion and in some cases it can cause immunogenicity, which is a relevant issue in chronic treatments.

In this context, small-molecules able to activate LCAT mutants causing FLD could represent a better treatment option.

Compound A (3-(5-(ethylthio)-1,3,4-thiadiazol-2-ylthio)pyrazine-2-carbonitrile)) has been the first small-molecule LCAT activator and it has been discovered by Amgen in a high-throughput screen (*Kayser et al., 2013*). Chen et al. have demonstrated that compound A is able to increase LCAT activity in vitro in plasma of mice, hamsters, rhesus monkeys and humans. After a single dose (20 mg/kg) of compound A, both mice and hamsters have presented an increased plasma esterified cholesterol and HDL-C levels and a significant decreased of non-HDL-C and triglycerides; moreover, the amelioration in lipid profile was enhanced after 2 weeks treatment, characterizing the pharmacological activation of LCAT and the potential impact on dyslipidemia therapies for the first time (*Chen et al., 2012*).

Further studies have investigated the mechanism of LCAT activation by compound A and have assessed whether it can also increase activity of some natural LCAT mutations (*Freeman et al., 2017*). The results show that compound A can activate a subset of FLD mutations through the formation of a hydrophobic adduct with Cys31 near the active site, increasing the apparent V_{max} of LCAT for at least the first step of the reaction.

Cys31 is located in the active site of LCAT (*Glukhova et al., 2015*) and, as a consequence, modifications of this residue can alter LCAT activity. It is well known that the interaction between the enzyme and the lipoproteins provides the bond with the substrates for LCAT but it also causes the displacement of the lid region that blocks the binding pocket (*Ahsan et al., 2014*); in fact, site-directed mutations in Cys31 activating LCAT are associated with an increased movement of the membrane binding domain, mechanism that can potentially explain the increased LCAT activity after compound A treatment. Moreover, also other changes in the lid and substrate binding region of LCAT are correlated with changes in its activity.

In the study published by Freeman et al, the researchers have demonstrated also that compound A is able to activate LCAT in three of the nine FLD mutations analyzed to a level comparable to FLD heterozygotes. Thus, as the FLD heterozygotes do not present any clinical manifestation except for low-normal HDL-C levels, this result indicates that small-molecule LCAT activators could represent a valid therapeutic approach for FLD treatment (*Freeman et al., 2017*)

Recently, a new compound has been developed by Daiichi Sankyo (DS compound). Pavanello et al. have measured the effect of the in vitro incubation of compound DS on cholesterol esterification rate (CER) and on LCAT activity, selecting FLD homozygous carriers belonging to the large Italian cohort. The results demonstrate that DS compound increases CER in 2 of the 5 tested FLD mutations, and LCAT activity in 3 FLD mutations. Only one of the tested mutants, the Pro254---Ser, characterized by a hydrophilic residue within a pack of hydrophobic residues close to the lid loop region likely disrupting LCAT fold, has not been activated by DS compound incubation.

The potential mechanism of DS compound activity is associated to its ability to stabilize the LCAT lid-loop in an open conformation, enhancing the hydrophobicity of the LCAT membrane-binding domain and facilitating its interaction with lipids (*Pavanello et al., 2020*).

It is interesting to underline that DS compound activates Arg147---Trp and Thr274---Ile mutants increasing LCAT activity but not CER, thus suggesting that the molecule influences the ability of the mutant LCAT to esterify cholesterol only on synthetic HDL with no effect on endogenous lipoproteins. On the other side, LCAT mutants Leu372---Arg, located in a region involved in apoA-I recognition (*Manthei et al. 2018*), is the only mutant activated in all tested conditions, including CER, LCAT activity on synthetic HDL, and LCAT activity on apoB-depleted plasma. Finally, the Val309---Met mutant, characterized by a mutation far from the active site and from lipoprotein binding site, is activated only on endogenous substrates, while the activator has no effect on synthetic HDL.

In conclusion, the use of LCAT activators could potentially induce benefits in conditions of secondary LCAT defects, such as acute coronary syndrome (*Lager et al., 1991*), and chronic kidney disease (*Calabresi et al., 2014*) and also in FLD condition. For FLD carriers, all the current studies pose the basis for a personalized therapeutic approach, in order to face the severe clinical complications for which no cure exists.

3.2.4 Synthetic HDL

Despite all the evidences from classical epidemiological association studies which demonstrate that low HDL-C are associated with increased CAD risk (*Gordon et al., 1977*), the therapeutic approaches aimed at raising HDL levels have not been effective in reducing the cardiovascular event risk nor in affecting the development of atherosclerosis (*Rosenson et al., 2016*); in fact, treatments with niacin and CETP inhibitors increased HDL-C in patients treated with statins, but these strategies have repeatedly failed in reducing cardiovascular events, except for Anacetrapib in the REVEAL study (*Karalis et al., 2013; Karalis et al., 2018*).

These controversial results have focused the attention on the functional properties of HDL more than their concentration and in particular the ability of these lipoproteins of stimulating the RCT; it has been demonstrated that cholesterol efflux capacity is a strong predictor for cardiovascular events, independently from HDL levels (*Rohatgi et al., 2014; Khera et al., 2011*). In this context, therapeutic strategies based on the increase of functional HDL particles/HDL efflux rather than simply raising the cholesterol content of the HDL have been developed.

One of the first approaches is based on a naturally occurring mutation of apoA-I, the apoA-I Milano. It has been reported that carriers of this mutation are exceptionally less affected by cardiovascular disease, despite the reduced HDL cholesterol and apoA-I levels (*Franceschini et al.,1985; Sirtori et al., 2001*), thanks to an increase in ABCA-1-mediated cholesterol efflux and anti-inflammatory activity of HDL induced by apoA-I Milano mutation. This mutation induces more ABCA1-mediated cholesterol efflux and exerts superior anti-inflammatory and plaque stabilizing properties (*Karalis et al., 2018*). Starting from the genetic mutation, some formulations containing recombinant apoA-I Milano complexed with phospholipids have been produced. The first molecule tested in a phase II clinical trial, ETC-216 produced by Esperion Therapeutics, has demonstrated to be efficient in inducing a significant regression of coronary atherosclerosis in a small group of patients with ACS, suggesting potential novel approach for the treatment of these subjects, in addition to the therapy with conventional lipid-modulating agents (*Nissen et al., 2003*).

Another compound tested is CSL-112, produced by the Commonwealth Serum Laboratories; this molecule is a reconstituted HDL particle, containing native apoA-I and phospholipids. CSL-112 has been developed because the predecessor compound, CSL-111, led to side effects as hepatotoxicity, despite of an improvement in the plaque characterization index and coronary score measured through quantitative coronary angiography in post ACS patients (*Tardif, 2007*). CSL-112 presents a safety and a tolerability increased compared its predecessor, and induces an increase in acutely enhanced cholesterol efflux, without serious side effects, as demonstrated in AEGIS-I trial on patients with myocardial infarction (*Gibson et al., 2016*). To assess the potential benefit of CSL112 in reducing major adverse cardiovascular events in a group of ACS patients, a large phase III AEGIS-II study is currently ongoing (*Karalis et al., 2018*).

Cerenis Therapeutics has developed another compound called CER-001, a negatively charged lipoprotein complex consisting of recombinant human apoA-I and a combination of two naturally occurring phospholipids, diphosphatidylglycerol and sphingomyelin, which is able to mimic the structure and function of natural discoidal pre-β HDL (*Tardy et al., 2014*). These phospholipids have been chosen for their ability to form a discoidal complex with a strong affinity for cholesterol (*Mattjus et al., 1996*), for the negative charge that reduces the renal clearance and for their ability to be easily recognized by the liver (*Guasch et al., 1993*).

In preclinical studies, CER-001 presented all the biological properties of natural HDL (*Tardy et al., 2014*); in particular, it has been demonstrated that this synthetic particle is able to regress atherosclerotic plaque and to stimulate the cholesterol efflux from macrophages both in mice and in humans in a similar way to HDL3 (*Tardy et al., 2014; Barbaras et al., 2015*). In cellular models, CER-001 has shown a high ability as acceptor of cholesterol and in in vivo studies this molecule is able to mobilize cholesterol in a dose-dependent manner into HDL fraction. Moreover, the phospholipids contained in the formulation can stimulate the LCAT activity, increasing the esterification of cholesterol (*Mattjus et al., 1996*).

CER-001 exerts also an effect on the chronic inflammation, which is a trigger factor in the development and progression of the atherosclerotic plaque, reducing the

secretion of all the cytokines tested in a dose-dependent manner (*Barbaras et al., 2015*).

Based on the promising results of the preclinical studies, some clinical trials using CER-001 infusions have been carried out. Improvements in the carotid wall thickness have been observed both in patients with familial hypercholesterolemia (*Hovingh et al., 2015*) and in patients with hypoalphalipoproteinemia (*Kootte et al., 2015*). In 2014, the CHI-SQUARE study (*Tardy et al., 2014)* has been designed with the aim of assessing the safety and efficacy of CER-001. Patients with coronary atherosclerosis have received infusion of 3, 6, or 12 mg/kg CER-001 for three weeks, and the results shows that despite the dose-related increase in cholesterol mobilization, none of the other parameters indicated a reduction of coronary atherosclerosis in the treated groups compared to placebo. However, a post hoc analysis has demonstrated that patients with a higher baseline atheroma volume percentage have a benefit in terms of atheroma regression from infusions of CER-001 at a dose of 3 mg/kg, while higher concentrations of CER-001 do not exert different effects from the placebo (*Kataoka et al., 2017*). A possible mechanism to explain this observation seems to be related to a downregulation of the ABCA1 transporter mRNA and protein expression at higher doses of CER-001, leading to a reduction of ABCA1-mediated cellular sterol efflux, as demonstrated in *apoE*$^{-/-}$ mice (*Tardy et al., 2015*). Thus, high doses of HDL and CER-001 are less effective in slowing progression of atherosclerotic plaque, describing a U-shaped dose-response curve.

Despite all the promising results from the preclinical and the first clinical studies, it has been recently demonstrated that CER001 is not able to promote the regression of coronary atherosclerosis in a cohort of statin-treated patients with ACS presenting a high plaque burden (*Nicholls et al., 2018*); moreover, the molecule is not effective in reducing carotid vessel wall dimensions and arterial wall inflammation in patients with genetically determined very low HDL-cholesterol (*Zheng et al., 2020*).

Although the treatment with CER-001 in several pathological conditions has given contrasting results, the benefic effects of this molecule has never been tested in genetic LCAT deficiency. Thus, our group has recently designed a study to investigate the effect of the absence of LCAT on catabolic fate of CER-001 and to

estimate the effects of CER-001 on kidney disease in this pathological condition (*Ossoli et al., 2021*) in a mouse model of the disease. The results will be fully discussed in this thesis, but briefly the treatment with CER-001 corrects the dyslipidemia associated with LCAT deficiency and limits renal damage in *Lcat*$^{-/-}$ mice. These results have set the basis for the use of CER-001 for the first time in a FLD patient, in which the treatment has been slightly effective in reducing the renal function decline (*Faguer et al., 2021*).

AIM

Lecithin:cholesterol acyltransferase (LCAT) is the only human enzyme responsible for the synthesis of cholesteryl esters in plasma and biological fluids and it plays a critical role in high density lipoprotein (HDL) metabolism (*Jonas, 2000*). Familial LCAT deficiency (FLD) is a rare genetic and recessive disease characterized by the reduction of plasma HDL-C concentration paralleled by an increase of free cholesterol and a variable hypertriglyceridemia; moreover, plasma lipoprotein profile presents abnormalities, including the accumulation of small and discoidal preβ-HDL particles, as well as the presence of LpX, an abnormal lipoprotein usually absent in normal plasma and detectable only in some pathological cases (*Boscutti et al., 2011; Santamarina-Fojo et al., 2001*). Furthermore, a condition of acquired LCAT deficiency is responsible for the typical reduction of HDL-C observed in chronic kidney disease (CKD) (*Calabresi et al., 2014*).

Renal disease is the major cause of morbidity and mortality in LCAT deficiency carriers but the cause of kidney failure is poorly understood. The rate of progression of renal damage in FLD patients is unpredictable, with some carriers rapidly going from mild proteinuria to a fast deterioration in their renal function even in their early 20s. Histological analyses on kidneys of LCAT deficient carriers highlight the presence of focal and segmental glomerulosclerosis, indicating a glomerular damage typical of this pathological condition; moreover, the presence of osmiophilic structures in basal tubular membrane and in tubule lumen indicates also a tubular alteration (*Boscutti et al., 2011; Stoekenbroek et al., 2013*).

Currently, there are no therapies available for FLD patients, who are treated just symptomatically with pharmacological approaches mainly aimed at correcting the dyslipidemia typically associated with the disease and at delaying the evolution of chronic nephropathy. Patients are also candidates for kidney transplantation, but the pathology reoccurs within few years. At the moment, specific new approaches are under investigation and include the possible use of small molecules activating LCAT (*Pavanello et al., 2020; Manthei et al., 2018*), the use of synthetic HDL (*Tardy et al., 2014; Hovingh et al., 2015*) and the development of a recombinant human enzyme (rhLCAT) (*Shamburek et al., 2016; Ossoli et al., 2019*).

Despite what is already known, there are still a lot of open questions about the onset of renal disease in LCAT deficiency; lipid abnormalities that characterize FLD patients' profile are at least partially responsible for the onset of renal damage (*Ossoli et al., 2016*), but the molecular mechanisms behind this condition are still unknown. Furthermore, there is a urgent need to develop effective therapeutic strategies to prevent the worsening of renal damage in LCAT deficient carriers. Finally, it has still to be established whether a reduction of LCAT concentration could influence renal disease development and progression in general population.

Aim of this project was to analyze these unknown aspects of renal disease in LCAT deficiency; thus, to throw light on the open questions, my project has been divided into 4 work packages, each one focused on a peculiar aspect of LCAT deficiency:

WP 1: Purification and characterization of lipoproteins from plasma of LCAT deficient carriers. The results collected within this aim, obtained in collaboration with professor Kontush's laboratory at the Institut National de la Santé et de la Recherche Medicale (INSERM) in Paris, helped to identify and characterize the alterations in plasma and in HDL composition potentially related to renal damage.

WP 2: Molecular mechanisms investigation with in vitro studies on renal cells. Data from this work package contributed, at least partially, to establish with which mechanisms lipoprotein abnormalities can induce the renal damage at cellular level.

WP 3: Metabolism and effect of synthetic HDL in murine model of LCAT deficiency: CER-001. A formulation of synthetic HDL, CER-001, was tested in murine model of LCAT deficiency in order to study the remodeling and metabolism of the particle in absence of the enzyme and to evaluate the effect of CER-001 on the renal disease associated to the genetic condition.

WP 4: Acquired LCAT deficiency and renal disease in general population. The last part of the project was focused on the study of the relation between the reduction of LCAT levels and renal disease in general population, to establish whether the concentration of the enzyme could represent a predictive factor for renal damage progression in healthy subjects.

MATERIALS AND METHODS

WORKPACKAGE 1: Purification and characterization of lipoproteins from plasma of LCAT deficient carriers

1.1 Subjects enrolled in the study

Nine carriers of *LCAT* gene mutations, including 4 carriers of two mutant LCAT alleles and 5 heterozygotes, and 5 family controls, all belonging to Italian cohort of LCAT deficient families (*Calabresi et al., 2005*), volunteered for the study. All subjects were fully informed of the modalities and the end points of the study and signed an informed consent. Fasting blood was collected and plasma prepared by low speed centrifugation at 4°C. Aliquots were immediately frozen and stored at −80 °C until assayed.

1.2 Lipid and lipoprotein profile measurement

Plasma total (TC) and HDL cholesterol as well as triglyceride (TG) levels were determined with certified methods using a Roche Integra c311 autoanalyzer (Roche Diagnostics). LDL-C concentration was calculated by Friedwald's formula:

$$LDL = TC - \left(\frac{TG}{5}\right) - HDL$$

Plasma concentration of apoA-I, apoA-II and apoB was determined by immunoturbidimetry.

Plasma phospholipid (PL) and unesterified cholesterol (UC) concentration was measured according to colorimetric and enzymatic assays as previously described (*Simonelli et al., 2013*).

The amount of esterified cholesterol (EC) in isolated lipoproteins was calculated as:

$$EC = (TC - UC)x\ 1{,}68$$

1.3 HDL subclass distribution

HDL subclass distribution was evaluated by 2D-electrophoresis. In the first dimension,10 µl of plasma were loaded on a 0.5% agarose gel (Hydragelprotein(e) kit, Sebia PN4120) and lipoproteins were separated by charge; agarose gel strips containing the runs were then transferred to a home-made 3–20%polyacrylamide gradient gel, to separate lipoproteins by size. The second run was performed at 30 mA for 4 hours. Lipoproteins were then blotted on a nitrocellulose membrane and apoA-I-containing particles were detected with anti-human apoA-I antibody (Calbiochem 178422).

Densitometry was performed using Multi-Analyst (Bio-Rad Laboratories) software; concentration of preβ-HDL was calculated as percentage of total apoA-I.

1.4 LpX detection

10 µl of plasma were loaded on a 0.5% agarose gel (Hydragelprotein(e) kit, Sebia PN4120) and electrophoresis was performed at 100 V for 1 hour in a barbital buffer (#B5934-12VL; Millipore Sigma, St. Louis, MO).

Filipin solution was prepared each time by dissolving 50 mg of filipin (Polysciences, Inc., Warrington, PA) in 2 ml of *N*,*N*′-dimethylformamide, and then adding 100 ml 1× PBS containing 0.1% sodium azide. After electrophoresis, gels were washed for 5 min in 1× PBS and then incubated overnight in 30 ml of filipin solution at 4°C under gentle rocking, protected from light. Gels, kept in the dark, were washed for 10 min at room temperature and then again for 1 h with 100 ml of PBS. LpX, which retro-migrates toward the cathode, was detected by UV rays using the Chemidoc™ XRS+ System and Image Lab™ Bio-rad software.

1.5 Evaluation of cholesterol esterification system

The evaluation of cholesterol esterification system was performed by measuring the activity of LCAT on an endogenous substrate (cholesterol esterification rate, CER), on an exogenous substrate (LCAT activity) and the plasma concentration of the enzyme.
LCAT concentration in plasma was measured using a specific competitive enzyme−linked
immunoassay. The plate was coated with a peptide corresponding to C-terminal tail of LCAT at the concentration of 20 µg/ml in carbonate solution, pH 9.6. After the coating, the wells were saturated with a solution of 0.5% of jelly in phosphate solution, pH 7.2, for 1 hour. The calibration curve and the samples, previously diluted 1:4 and mixed with the primary antibody (anti-LCAT 1:1000) were added to the plate and incubated for 1 hour. After the secondary antibody (1:1000 anti-rabbit, Dako) addition, the plate was incubated for 1 hour. Finally, 100 µl of 3,3′,5,5′-Tetramethylbenzidine (TMB) solution were put into wells to start the colorimetric reaction, stopped after 30 minutes with 50 µl of H_2SO_4 1M; plate was read at 450 nm using a microplate reader (Bio-Rad Laboratories).
The procedure to determine plasma cholesterol esterification rate (CER) and LCAT activity is based on the measurement of the difference in UC concentration after incubating each sample for 5 and 65 minutes at 37°C, temperature at which the enzyme activity is optimal. For CER, that reflects the ability of endogenous LCAT to esterify cholesterol within endogenous lipoproteins, the substrate is the entire plasma, while in LCAT activity, that measures the enzyme activity on exogenous HDL, the substrate is represented by synthetic preβ-HDL composed of 1-palmitoil-2-oleoyl-sn-glycero-3-phosphocholine (POPC), human apoA-I and cholesterol in weight ratio of 2.17:1:0.22, according to previously described methods (*Calabresi et al., 2005*).

1.6 ABCA1- mediated cholesterol efflux

To evaluate ABCA1-mediated cholesterol efflux, J774 macrophages were used. Untreated macrophages were used as control, while other macrophages were treated

with cAMP to induce ABCA-1 expression. The cells were grown in RPMI medium containing 10% of FCS, at 37° in controlled atmosphere (5% of CO2). For the experiment, cells were plated in 12 multi-wells plates and used when the confluence was at 80-90%.

Monolayer macrophages were washed with PBS and incubated for 24 hours in RPMI medium added of [1,2-3H] cholesterol (4μCi/ml). Labeled medium contained 1% of FCS and 2μg/ml of ACAT inhibitor, to guarantee that all the labeled cholesterol was unesterified. After 24 hours, cells were washed and incubated with 0,2% of BSA-containing RPMI with or without 0,3mM cpt-cAMP o/n. Basal value (time 0) for total [1,2-3H]cholesterol was obtained by washing some wells with PBS and by extracting the cells with 2-propanol. The other monolayers containing [3H] cholesterol, stimulated or not, were incubated for 4 hours in presence of 5% (v/v) of serum. Cholesterol efflux was quantified after the collection of the medium; the radioactivity of the media was determined by liquid scintillation and the % of labeled cholesterol released (% of efflux) was calculated as: (cpm of the medium after 4 hours/cpm of the medium at time 0) x 100. ABCA-1 mediated efflux was calculated as % efflux of stimulated J774 macrophages - % efflux of non-stimulated macrophages.

1.7 HDL-mediated transfer of cholesterol and phospholipids from TGRL lipolysis

To evaluate the HDL ability to acquire cholesterol and phospholipids from the lipolysis of TGRL, two specific substances were used to label the two lipids, in accordance with described protocols (*Feng et al., 2020; Feng et al., 2021*).

The first step was the isolation of TGRL (d<1.019 g/ml), performed by a single-step ultracentrifugation.

TGRL were labelled with fluorescent 23-(dipyrrometheneboron difluoride)-24-norcholesterol (Avanti Polar Lipids, Alabaster, AL, USA), also known as TopFluor-Cholesterol (TopF), to follow the uptake of UC, or with 1,1′-dioctadecyl-3,3,3′,3′-tetramethylindocarbocyanine perchlorate (DiI; Sigma, France) to highlight PL pathway.

To label TGRL with the fluorescent substances, lipoproteins were added to lipoprotein-deficient plasma (LPDP) at the LPDP:TGRL ratio of 1:100 by volume. The mixture was then filtered and the fluorophores were added as a chloroformic solution followed by overnight
incubation at 37° C under gentle stirring. Labelled TGRL were filtered through a PD-10 Sephadex column and the triglyceride concentration in purified labelled TGRL was measured by photometry (fluorescence registered at the excitation/emission wavelengths
of 500/525nm with a Gemini Microplate Reader (Molecular Devices, USA)).
To evaluate the transfer of TopF and DiI, Tris buffer (0.4 M, pH 8) was mixed on ice with required amounts of TopF of DiI-labelled TGRL and apoB-depleted plasma of the subjects; LPL from Pseudomonas sp. (Sigma, France) was added to start lipolysis at 37° C. At the end of the incubation, the mixture was placed on ice and apoB precipitant composed of phosphotungstic acid and MgCl2, was added. After 15 minutes incubation at room temperature and 10 minutes centrifugation at 13000 rcf, HDL-containing supernatant was filtered and transferred to a black microplate for fluorescence reading. Fluorescence of the standard TGRL sample alone was also measured at a triglyceride concentration employed in the assay and fluorescent values measured in HDL were expressed as a percentage of fluorescence of such standard sample. Moreover, a reference apoB-depleted plasma sample obtained from one healthy donor was included in each measurement and all values obtained in clinical samples were normalized to that observed in the reference plasma.

1.8 HDL isolation by ultracentrifugation

To isolate HDL, a multi-step ultracentrifugation method was employed. Briefly, 800 µl of plasma were mixed with 260 µl of solution d= 1,24 g/ml to adjust the density at 1,063 g/ml. The run lasted 3 hours at 120000 rpm. After removing the top, the density of 500 µl of bottom was adjusted at 1,125 g/ml by adding 270 µl of solution d= 1,24 g/ml and another run was performed for 4 hours and 30 minutes at 120000 rpm. The collected top contained HDL2, while the bottom was adjusted at 1,21 g/ml by mixing

240 µl of d=1,24 g/ml and 200 µl of d=1,21 g/ml solutions. The last run went on for 5 hours at 120000 rpm; the top containing HDL3 was collected. For all the runs, a Beckman SW41 Ti rotor in a Beckman XL70 ultracentrifuge was used. All density solutions contained sodium azide (0.01%), EDTA (0.01%), and gentamicin (0.005%), pH 7.4. To perform lipidomics analysis, half volumes of HDL2 and HDL3 fractions were pooled and the lipoprotein composition was assessed calculating the weight percentage of UC, CE, TG, PL and protein, measured with enzymatic assays as previously described.

1.9 Lipidomics analysis for subjects' plasma and HDL characterization

Lipids were extracted from plasma and HDL isolated by ultracentrifugation according to a modified Bligh and Dyer method: a volume of HDL equivalent to 30 µg of PL or 10 µl of plasma were supplemented with internal standards and the lipids contained in the two matrices were extracted with 2.1 ml methanol/CHCl3 (2:1 v/v) in presence of the antioxidant BHT. 550 µl of HCl 0,005N were subsequently added.

Phase separation was triggered by the addition of 700 µl of $CHCl_3$ and 700 µl of water and the extracted lipids were dried and re-suspended in 50 µl of LC/MS solvent.

After the extraction, lipids were quantified by LC-ESI/MS/MS using a Prominence UFL CandaQTrap4000 mass spectrometer.

4µl of each samples were injected into a Kinetex HILIC 2.6 µm 2.1x 150 mm column. Mobile phases consisted of (A) water containing 30 mM ammonium acetate and 0.2% acetic acid, and (B) acetonitrile with 0.2% acetic acid.

Lipid species were detected using scheduled multiple reaction monitoring (sMRM) in the positive-ion mode reflecting the head group fragmentation of each lipid class (Table 2).

Lipid Class	Lipid Subclasses	No of assayed species	No of quantified species (>LOQ)	ISTD	Parent Ion	MS Experiment
Glycero-phospholipids	Phosphatidylcholine (PC)	27	27	PC(16:0/16:0-d9), PC(15:0/18:1-d7)	$[M+H]^+$	PIS 184m/z
	Lysophosphatidylcholine (LPCsn1)	17	16	LPC(18:1-d7)	$[M+H]^+$	PIS 184m/z
	Lysophosphatidylcholine (LPCsn2)	17	15	LPC(18:1-d7)	$[M+H]^+$	PIS 184m/z
	Phosphatidylethanolamine (PE)	24	24	PE(15:0/18:1-d7)	$[M+H]^+$	NL 141m/z
	Plasmalogen PE (pPE)	18	17	PE(15:0/18:1-d7)	$[M+H]^+$	PIS (RCO+PE)
	Lysophosphatidylethanolamine (LPEsn1)	15	15	LPE(18:1-d7)	$[M+H]^+$	NL 141m/z
	Lysophosphatidylethanolamine (LPEsn2)	15	15	LPE(18:1-d7)	$[M+H]^+$	NL 141m/z
	Phosphatidylinositol (PI)	17	17	PI(15:0/18:1-d7)	$[M+NH_4]^+$	NL 277m/z
	Phosphatidylserine (PS)	14	10	PS(17:0/14:1)	$[M+H]^+$	NL 185m/z
	Phosphatidylglycerol (PG)	13	10	PG(15:0/18:1-d7)	$[M+NH_4]^+$	NL 189m/z
	Phosphatidic acid (PA)	9	8	PA(15:0/18:1-d7)	$[M+NH_4]^+$	NL 115m/z
Sphingolipids	Sphingomyelin (SM)	16	16	SM(d18:1/18:1-d9)	$[M+H]^+$	PIS 184m/z
	Dihydrosphingomyelin (DHSM)	9	8			
	Ceramide (Cer d18:1)	14	13	Cer(d18:1-d7/24:0)	$[M+H]^+$	PIS 264m/z
	Sphingadienines (cer d18:2)	11	10			PIS 262m/z
	Dihydroceramide (Cer d18:0 noted DHC)	11	10		$[M+H]^+$	PIS 266m/z
Total		247	231			

PIS: product ion scan, NL: neutral loss

Table 2. Mass spectrometry analysis conditions

An in-house developed R-script was used to correct for isotopic contribution on MRM signals from HILIC injections. Raw data were expressed as mol percentage of total analyzed lipids, recalculated as mol/g of total protein in HDL and as nmol/µl for both plasma and HDL.

1.10 Statistical analysis

Data of lipid and lipoprotein profile of subjects were reported as mean±SD, unless otherwise stated. Group differences were evaluated by One-Way ANOVA, and comparisons among the groups were evaluated in a post hoc test (Holm-Sidak method); group differences with a P value <0.05 were considered statistically significant. The analyses were carried out using SigmaPlot 12.5 (Systat Software, Inc., San Jose, CA, USA)

For lipidomics data, comparison of two groups (CTL vs HEZ or CTL vs HOZ or HEZ vs HEZ) was done using unpaired Student t-test. One-way ANOVA was performed for all the groups to find features separating the three groups. In all these analysis, a feature is considered significant when the p<0.05 after the Benjamini−Hochberg FDR correction. Statistical analysis was performed using Multi Experiment Viewer (MeV) software version 4.9, while Venn diagram representing the relationship of each

normalization methods was made using VennDIS3; a JavaFX-based Venn and Euler diagram software.

WORKPACKAGE 2: Molecular mechanisms investigation with in vitro studies on renal cells

2.1 Subjects of the study and biochemical analysis

For the in vitro studies, 6 homozygous and 8 heterozygous LCAT deficient carriers, as well as 8 family controls from the Italian cohort (*Calabresi et al., 2005*) were enrolled. All subjects were fully informed of the modalities and end points of the study and signed an informed consent. Fasting blood was collected and plasma prepared by low speed centrifugation at 4°C. Aliquots were immediately frozen and stored at −80 °C until assayed.

2.2 HDL isolation for in vitro studies

3 ml of plasma were used to isolate LDL (d = 1.019-1.063 g/ml) and HDL (d = 1.063-1.21 g/mL) by a multi-step ultracentrifugation using OptimaTM L-100 XP (Beckman Coulter) centrifuge. The initial plasma density (d=1,006 g/ml) was adjusted by KBr addition to a density of 1,063 g/ml, and stratified with a solution with the same density. The conditions of the runs were calculated as

$$Speed\ (rpm) = F\ x\ hours$$

in which F is a tabulated value depending on the density of the solutions and the time is defined by the operator.

The first run separated the LDL from HDL; in homozygous LCAT deficient carriers, LpX floats with LDL, as the particle presents the same density. The LDL fraction was collected in the top of the tube and washed with another run, while the density of the bottom containing HDL was corrected to 1,21 g/ml and stratified with a solution of equal density. After the second ultracentrifugation, HDL were collected in the top and

the fraction underwent to the last wash to remove the interfering plasma proteins, like albumin.
All the density solutions used were prepared starting from saline solutions (NaCl 0,9% p/v in purified water) added of EDTA, sodium azide and KBr, pH=7.4. The density was confirmed with a densitometer. Isolated lipoproteins were subsequently dialyzed and the composition was evaluated with enzymatic techniques.

2.3 Cell culture

In vitro experiments were performed on two different renal cell lines: immortalized human podocytes, cultured in Dulbecco′s Modified Eagle Medium (DMEM) containing 1g/L of glucose supplemented with 10% fetal bovine serum (FBS), 1% L-Glutamine, and 1% antibiotics; immortalized human tubular cells (HK2), grown in DMEM enriched of nutrient mixture F-12 with 10% FBS, 1% L-Glutamine and 1% antibiotics.
For all the experiments, serum at 2% v/v or lipoproteins at 0,25 mg/ml of cholesterol were used.

2.4 Reactive Oxygen Species (ROS) production

To evaluate ROS production, cells were incubated 30 minutes with HEPES buffer containing 5 μM of carboxy-H2DCFDA (Molecular Probes, Invitrogen), which is a carboxyl derivative of fluorescein, before 1 hour incubation with media containing subjects' sera at 2% or 0,25 mg/ml of cholesterol of isolated lipoproteins. Reduced and acetylated forms of dichlorofluorescein are non-fluorescent until the acetate groups are removed by intracellular esterases and the oxidation occurs within the cells. Oxidation of the probe can be detected by monitoring fluorescence at 517-527 nm. After the incubation, cells were lysated and total protein content was measured by microBCA assay (ThermoScientific) to normalize the fluorescent signal.

2.5 Gene expression

Real Time PCR for podocytes and tubular cells proteins was performed using SYBER green method (iTaq Universal SYBR Green Supermix -BioRad); primers have been designed on different exons to avoid the amplification of DNA contaminations eventually present in cDNA preparations and the sequences are reported below (table 3). Briefly, RNA was extracted from cells after incubation with subjects' sera at 2% v/v or 0,25 mg/ml of cholesterol of isolated lipoproteins for 48 hours according to Trizol (Invitrogen) method; 0.8 µg of RNA were retro-transcripted using iScript cDNA Synthesis Kit (BioRad). Real-Time PCR was performed using a thermal cycler MJ MiniTM e il software Opticon MonitorTM 3.1 (Biorad) and the process consisted of an initial denaturation of the samples at 95°C for 3 min, followed by 40 cycles. Each cycle consisted of a denaturation step at 95°C for 10s and 25s annealing step at the 60°C. At the end, melting curve was evaluated from 60°C to 95°C.Results were calculated on the quantification cycle (Cq), determining the expression of each gene calculating $2^{-\Delta\Delta_{C}q}$ normalized for the housekeeping gene.

Gene	Primer forward	Primer reverse
β-actin	CTG GAC TTC GAG CAA GAG ATG	CCA TGC CCA GGA AGG AAG
Podocin	CAT GAG ATC GTG ACC AAA GAC	GAG ACG CTT CAT AGT GGT TTG
Synaptopodin	AAG TCA CAT CCA GCT CCT TC	CTT CTC CGT GAG GCT AGT G
OPA	TGTGAGGTCTGCCAGTC TTTA	TGTCCTTAATTGGGGTCGTTG
MFN2	CTCTCGATGCAACTCTAT CGTC	TCCTGTACGTGTCTTCAAGGAA
MFF	CCAAACGCTGACCTGGA AC	TTTCCTGCTACAACAATCCTCT CC
FIS1	GTCCAAGAGCACGCAGT TTG	ATGCCTTTACGGATGTCATCAT T

Table 3. Primers used for evaluation of gene expression in immortalized human podocytes and tubular cells.

2.6 Evaluation of apoptosis

To evaluate apoptosis, the activity of caspase 3/7 was measured by luminescence using Caspase-Glo® 3/7 reactive (Promega) according to manufacturer's instruction. Renal cells were plated in a 96 wells plate at a density of 20.000 cells/wells, and incubated for 48 hours with sera at 2% v/v from the subjects. After changing the medium, 100 µl of reactive were added and the plates were incubated for 2 hours in the dark, to allow the stabilization of the signal. Plates were read using the multi-wells plate reader Synergy^{TM}H1 Bio-Tek. The measured luminescence was directly proportional to the grade of apoptosis reached in every well and the results were expressed as fold vs untreated cells.

2.7 Expression of autophagy key proteins

To evaluate the protein expression of ATG5, LC3I, LC3II and Beclin, tubular cells were incubated for 48 hours with 2% v/v of serum or with 0,25 mg/ml of cholesterol and then lysed using a lysis buffer (Tris buffer 20 mM, pH 6.8, EDTA 1 mM, 4% p/v of SDS, 20% v/v of glycerol, sodium fluoride 1 mM, sodium vanadate 1 mM, benzamidine 1 mM, trypsin inhibitors 10 µg/mL, leupeptin 1 µg/mL, dithiothreitol 0.5 mM, pefabloc 1 mM). Protein concentration of lysates was evaluated by microBCA (ThermoScientific). 25 µg of protein were loaded on a 8-18% polyacrylamide SDS-gel for the SDS-PAGE. The electrophoresis was performed using a cathodic (Tris 0,1 M, Tricina 0,5 M, pH 8,25 e SDS 0,1%) and anodic (Tris 0,2 M, pH 8,9) buffers, at 80 V for 4 hours.

Then proteins were blotted onto a nitrocellulose membrane for 1 hour at 180 mA in a transfer solution containing 25 mM Tris, 192 mM glicin and 15% (v / v) methanol. Membranes were saturated in 4% milk solution and the immune-detection was performed using ATG5, LC3I, LC3II and Beclin antibodies (Cell signaling) 1:1000 overnight at 4°C and subsequently with a secondary antibody anti-rabbit (Dako) 1:2000 for 1 hour at 37° C. Proteins were visualized by biochem-luminescence (GE

Healthcare Biosciences), quantified with GS-690 densitometer and analyzed by Multi-Analyst software (BioRad Laboratories).

2.6 Statistical analysis

Data are reported as mean±SD, unless otherwise stated. Group differences were evaluated by one-way ANOVA or unpaired t-test; group differences with a P value <0.05 were considered statistically significant. Comparisons to control group were evaluated in a post hoc test (Holm-Sidak method). The analyses were carried out using SigmaPlot 12.5 (Systat Software, Inc., San Jose, CA, USA).

WORKPACKAGE 3: Remodeling and effect of synthetic HDL in a murine model of LCAT deficiency: CER-001

3.1 Murine models and experimental procedures

Lcat$^{-/-}$ mice were generated by knocking down the *Lcat* gene, as previously described (*Lambert et al., 2001*). In order to evaluate CER-001 in vivo remodeling, the first set of experiments was performed by injecting CER-001 at the doses of 2.5, 5,10 mg/kg every other day for 2 weeks (8 injections) in *Lcat*$^{-/-}$ and control C57BL/6 mice. Three randomly assigned animals per group were used. Blood was collected at baseline, at day 14 (end of treatment) and at the 30 min, 1, 4, and 48 h after the first injection, while urine was collected at baseline and 24 h after the last injection.

To develop the second part of the work, that was focused on the evaluation of the effects of CER-001 on kidney function in LCAT deficiency, *Lcat*$^{-/-}$ mice were injected for one month with exogenous LpX to create a mouse model of renal disease (*Ossoli et al., 2016*). At the end of LpX administrations, mice were divided into two groups (6/9 animals each); one was injected with CER-001 (10 mg/kg) three times per week for 1 month (*Tardy et al., 2015*) while the control group (*Lcat*$^{-/-}$ LpX-injected mice)

received the same volume of saline solution. Blood and urine were collected at baseline, at the end of LpX injections and at the end of treatment with CER-001 or saline. Mice were sacrificed through cervical dislocation and kidneys and liver were collected for the following analysis.

All animal procedures were conducted according to institutional guidelines that are in compliance with national (D.L. No.26, March 4, 2014, G.U. No. 61 March 14, 2014) and international laws and policies (EEC Council Directive 2010/63, September 22, 2010:Guide for the Care and Use of Laboratory Animals, United States National Research Council, 2011). The experimental protocol was approved by the Italian Ministry of Health (Protocol#545/2017-PR).

3.2 Evaluation of particle remodeling using 2D-electrophoresis

Plasma particle remodeling was evaluated through 2D-electrophoresis, as described in the first workpackage. The immune-blotting was performed using human (Calbiochem) or murine apoA-I (Meridian) antibodies (*Pedrelli et al., 2014*).

3.3 Evaluation of CER-001 signal in liver and kidney

50 mg of kidney and liver were homogenized in lysis buffer, prepared as previously described (*Valkanova et al., 2005*). 200 ug of proteins, determined by standard BCA method (Pierce™ BCA Protein Assay Kit, ThermoFisher), were separated by SDS-PAGE and transferred to a nitrocellulose membrane. The membrane was blocked for 2 hours at room temperature in 5% milk and incubated overnight with the primary antibody for human apoA-I (1:1000; Calbiochem) and for 1 hour at 37° with the secondary antibody (1:2000; mouse anti-rabbit IgG-HRP, Santa Cruz).

3.4 Blood and urine collection and biochemical analyses

Blood samples were collected from the retro-orbital plexus in EDTA-containing tubes, and then plasma was separated through low-speed centrifugation at 4 °C and stocked at -80°. TC, UC,HDL-C and TG were measured using certified enzymatic techniques using a Rochec-311 auto-analyzer. PL concentration in plasma was evaluated using a colorimetric assay. The content of albumin and creatinine in urine was assessed using commercial assays (Ethos Biosciences, #1011 and #1012) (*Ossoli et al., 2021*).

3.5 Fast protein liquid chromatography analysis

The evaluation of lipoprotein profile was assessed by pooling 250µl of plasma collected at baseline from three *Lcat*$^{-/-}$mice after LpX injection, and after CER-001 at 10 mg/kg or saline; samples were diluted with 250µl of saline solution and injected into a Superose6HR 10/30 column (GE Healthcare, UK). 40 fractions of 0.9 ml were collected and TC, UC, TG and PL were measured using the enzymatic techniques (*Calabresi et al., 2005*).

3.6. Determination of lipid content in glomeruli

For lipid staining, 5 µm frozen kidney sections were fixed with 10% formalin for 5 min, covered with 100% propylene glycol for 5 min and then stained with Oil red O for 9 min at 60°C. All the sections were washed with 85% propylene glycol and subsequently stained for a few seconds with toluidine blue and mounted with aqueous solution. 20 glomeruli for each animal were randomly acquired using bright-field microscopy (ApoTome, Axio Imager Z2, Zeiss,Jena, Germany). Fiji Image J Software (http://imagej.net/Fiji) was used to quantify the number of lipid droplets in each glomerulus. The result was expressed as the mean number of droplets per glomerulus.

3.6 In vitro studies on podocytes

In the first set of experiments, to evaluate the direct effect of CER-001 on intracellular cholesterol content, podocytes were starved in serum-free medium for 2 h and then incubated with synthetic LpX (0.5 mg/ml of cholesterol) for 18 h. Medium was subsequently removed and podocytes were incubated for 4 h with CER-001 at a concentration resembling the in vivo dose of 10 mg/kg (0.15 mg/ml of protein) or with the same volume of saline solution.

In the in vitro study with FLD carrier' plasma, in order to evaluate the effect of drug-induced lipoprotein remodeling on intracellular cholesterol content, podocytes were incubated for 48 h with 2% v/v of subject' plasma collected at different time points (basal condition, after 3, 6 and 12 weeks of treatment). In a second set of experiments of the same study, to assess the direct effect of CER-001 on intracellular cholesterol content, podocytes were pre-treated with baseline patient's plasma for 48 hours and then incubated for 4 h with CER-001 saline at a concentration resembling the dose of 10 mg/kg (0.15 mg/mL of protein) or with the same volume of saline solution. In all the experiments, cells were then washed with PBS and lysed overnight with 1% sodium cholate and 10U/ml DNase. Cholesterol was measured by fluorescence using the Amplex Red Cholesterol Assay kit (Sigma Aldrich) and the results were normalized by protein concentration of the total cell lysate, measured according to Lowry method.

3.7 Evaluation of podocyte markers in glomeruli of *Lcat*$^{-/-}$ mice

For nephrin staining, OCT-frozen kidney sections were fixed with cold acetone and incubated with 1% BSA, after antigen retrieval with citrate buffer. The treated sections were incubated with primary antibody goat anti-nephrin (Santa Cruz Biotechnology, Dallas, TX) and then with donkey anti-goat Cy3-conjugated secondary antibody (1:400; Jackson Immunoresearch Laboratories). Nephrin expression was measured in 15–20 glomerular cross sections using a score between 0 and 3 (0, no staining; 1,

weak staining along the capillary tuft; 2, moderate staining along the capillary tuft; 3, linear and intense staining along the capillary tuft).

Nestin staining was performed using the immune peroxidase method. Duboscq-fixed, 3-µm paraffin-embedded kidney slices were incubated with Peroxidazed 1 (PX968, Biocare Medical) to inhibit endogenous peroxidase, after antigen retrieval in a decloaking chamber with Rodent decloaker (RD913, Biocare Medi-cal). Sections were then incubated with rat anti-nestin (1:300; Abcam) followed by rat-on-mouse HPR polymer (TR517,Biocare Medical) for 30 min at room temperature. Staining was visualized using diaminobenzidine solutions (BDB2004H, BiocareMedical). Slides were counterstained with Mayer's hematoxylin, mounted with Eukitt mounting medium and finally observed using light microscopy (ApoTome, Zeiss). Negative controls were obtained by omitting the primary antibody on adjacent sections. Nestin staining in 15-20 random glomeruli was quantified using a score between 0 and 3 (0–0.5: absent or weak staining in a few podocytes, 1: moderate staining in podocytes with altered distribution, 2: moderate podocyte staining, 3: intense podocyte staining).

3.8 CER-001 in FLD carrier

CER-001 infusion was tested through a compassionate program, approved by the local ethical committee (Approval nr.CEUR-2020-EAP-012-ASUFC) in cooperation with Abionyx Pharma, which provided the study medication. The subject was a 49 years old Italian male with genetically confirmed FLD, due to homozygous Thr274Ile mutation in LCAT, who already underwent to 3 renal transplantations. CER-001 was infused at the dose of 10 mg/kg 3 times per week for 3 weeks, followed by 10 mg/kg 2 times per week for 3 weeks, and then 10 mg/kg once per week for 6 weeks.

3.9 Statistical analysis

Continuous data are reported as median (interquartile range) and categorical data as n (%) unless otherwise stated. The lipid profile modifications after the particles injections at various doses were evaluated using the Spearman correlation coefficient

between plasma lipid levels and CER-001 increasing dose. The effect of CER-001 on the lipid profile, albumin to creatinine ratio, intracellular cholesterol content and podocyte markers was compared to saline using the Wilcoxon rank-sum test. Statistical analysis for cell studies was carried out using SigmaPlot 12.5 (Systat Software, Inc., San Jose, CA, USA); data were expressed as mean±SD and two-tailed paired Student's t-test or a one-way ANOVA for repeated measures were used as appropriate.

WORKPACKAGE 4: Acquired LCAT deficiency and renal disease in general population

4.1 Subjects of the study

The study included a cohort of 164 subjects randomly selected from the PLIC study (*Baragetti et al., 2013*), an epidemiological and prospective large survey of the general population in the northern area of Milan carried out at the Center for the Study of Atherosclerosis, Bassini Hospital (Cinisello Balsamo, Milan, Italy).

The subjects had comparable age and sex, and presented a median basal estimated glomerular filtration rate (eGFR) of 67.51 (60.01 as minimum and 122.03 as maximum) ml/min/1.73 m2.

All participants signed a written informed consent and all procedures were performed according to the Declaration of Helsinki.

The study was approved by the Ethic Committee of the University of Milano (SEFAP/Pr.0003).

4.2 Biochemical analyses

Blood samples were collected after overnight fasting. Plasma and serum samples were stored at –80 °C until analysis. Lipid and lipoprotein profile, plasma LCAT

concentration and pre-β HDL content was evaluated as described in the previous work packages.

4.3 Estimated Glomerular Filtration Rate

The determination of the Estimated Glomerular Filtration Rate (eGFR) has been calculated by
Cockroft-Gault formula, used for the estimation of the renal clearance of creatinine in routine analysis to obtain a reliable approximation of residual renal function.

4.4 In vitro studies

In vitro experiments were performed using two different renal cell lines: immortalized human podocytes, grown in Dulbecco′s Modified Eagle Medium (DMEM) supplemented with 10% fetal bovine serum (FBS), 1% L-Glutamine, and 1% antibiotics; immortalized human tubular cells (HK2), grown in DMEM enriched of nutrient mixture F-12 with 10% FBS, 1% L-Glutamine and 1% antibiotics.
Reactive oxygen species (ROS) production, both in podocytes and tubular cells, and podocin gene expression were measured as previously described.
To evaluate the effect of LCAT in determining the serum ability to promote ROS production, sera from 1st LCAT tertile subjects (*n* = 11) were incubated at 37 °C for 6 h with rhLCAT (*Simonelli et al., 2013*) to reach the final LCAT concentration of 6 µg/mL (identical to the mean LCAT concentration in 3rd LCAT percentile subjects) or with the same volume of saline.
The effect of serum-free rhLCAT (6 µg/mL) was also tested.

4.5 Statistical analysis

Statistical analysis was performed using SPSS® v.23.0 for Windows® (IBM Corporation®, Chicago IL, USA) software. For normally distributed variables, the mean ± standard deviation (SD) is reported and t-test was used for comparisons; for

non-normally distributed variables, the median and inter-quartile range (IQR, as the range between the 25th and the 75th percentile around each median value) are reported and the Mann-Whitney U nonparametric test was performed.

P trend among the three groups were perfomed by the Analysis of Co-Variances (ANCOVA) model. Results of the eGFR changes and in vitro studies were than compared by the Kruskall–Wallis test.

Box plots reporting mean values with 10th to 90th upper and lower bounds, were generated using GraphPad Prism 5® for Windows® (Graphpad Software Inc.®, La Jolla, CA, USA). For all analyses, $p<0.05$ were considered statistically significant.

RESULTS

WORKPACKAGE 1: Purification and characterization of HDL from plasma of LCAT deficient carriers

1.1 Characteristics of the subjects

For the first part of the project, nine carriers of *LCAT* gene mutations on one (heterozygous) or two (homozygous) alleles and 5 healthy subjects matched for sex and age were enrolled.

Clinical manifestations of genetic LCAT deficiency are recessive, meaning that only homozygous carriers can develop the symptoms. In table 4, the main characteristics of the 4 enrolled homozygous carriers are summarized:

Subjects	Mutation	Phenotype	Corneal Opacity	Anemia	Kidney Disease	Cardiovascular Disease
HOZ 1	Leu372--Arg	FLD	YES	YES	YES	NO
HOZ 2	Val309--Met	FLD	YES	YES	YES	YES
HOZ 3	Thr274--Ile	FLD	YES	YES	YES	NO
HOZ 4	Arg147--Trp	FLD	YES	YES	YES	NO

Table 4. Characteristics of homozygous LCAT deficient carriers

All the homozygous subjects carried mutations associated to FLD phenotype, the only one related to renal disease outcome. The most frequent clinical features were corneal opacity and normochromic anemia at various stages of severity, both found in all the carriers.

Moreover, three of the four homozygous had a serious kidney dysfunction that required kidney transplantation. One of the carrier presented only microalbuminuria, thus a starting renal impairment. All the patients were under treatment with ACE inhibitors and two of them with folic acid. None of the homozygous carriers presented cardiovascular diseases, according to what previously demonstrated (*Ossoli et al., 2015*) with the exception of one subject carrying Val309-Met mutation. The woman

showed hypertension, mesenteric and aortic plaques and underwent to surgery for coronary stents implantation, in addition to the renal alterations.

The lipid and lipoprotein profile of the subjects enrolled in the study is reported in table 5:

	HOZ	HEZ	CTRL	P trend
N	4	5	5	-
Sex (m/f)	2/2	3/2	3/2	-
Age	50 ± 8	62 ± 14	47± 9	0,105
TC (mg/dL)	132 ± 62	168 ± 41	201 ± 36	0,128
UC (mg/dL)	117 ± 56§*	47 ± 17	46 ± 14	*0,019*
UC/TC (%)	89 ± 9§*	28 ± 9	23 ± 6	*<0,001*
LDL-C (mg/dL)	85 ± 48	104 ± 35	121 ± 31	0,400
HDL-C (mg/dL)	6 ± 1§*	41 ± 12*	57 ± 12	*<0,001*
TG (mg/dL)	199 ± 128	117 ±32	117 ± 71	0,285
PL (mg/dL)	214 ± 60	207 ± 39	244 ± 87	0,692
ApoA-I (mg/dL)	36 ± 11§*	101 ± 21	131 ± 35	*<0,001*
ApoA-II (mg/dL)	6 ± 3§*	34 ± 6	31 ± 2	*0,023*
ApoB (mg/dL)	48 ± 13§*	97 ± 18	99 ± 26	*0,005*
Preβ-HDL (%)	48 ± 12§*	22 ± 8	15 ± 1	*<0,001*
LpX	Yes	no	no	-

Table 5. Subjects lipid and lipoprotein profile. Data are expressed as mean ± SD. Parameters were analyzed by one- way ANOVA. All pairwise multiple comparison were performed by Holm-Sidak method. (§p<05 vs Hez, *p<0,05 vs Ctrl).

Collected data showed that, in accordance with the literature [*Calabresi et al., 2005*], homozygous carriers had a significant reduction of HDL-C, apoA-I, apoA-II and apoB concentration compared to both heterozygous and controls. The levels of unesterified cholesterol and the ratio UC/TC are significantly increased compared to the other groups; triglycerides concentration presented an enhancement too. Finally, homozygous carriers showed the typical lipoprotein abnormalities of LCAT deficiency

condition, which are the significant increase of preβ-HDL percentage and the accumulation of LpX. The heterozygous presented an intermediated profile, with a significant reduction of HDL-C compared to controls.

To further characterize the subjects, cholesterol esterification system was evaluating by measuring LCAT concentration, the activity on an exogenous substrate (LCAT activity) and the cholesterol esterification rate (CER) (table 6)

	HOZ	HEZ	CTRL	P trend
LCAT mass (µg/mL)	2 ± 1§*	4 ± 1	5 ± 1	*0,011*
LCAT activity (nmol/ml/h)	0 ± 0§*	14 ± 10	34 ± 14	*<0,001*
CER (nmol/ml/h)	0 ± 0§*	41 ± 18	41 ± 19	*<0,001*

Table 6. Evaluation of the esterification system. Data are expressed as mean ± SD. Parameters were analyzed by one-way ANOVA. All pairwise multiple comparison were performed by Holm-Sidak method (§p<05 vs Hez, *p<0,05 vs ctrl).

The results confirmed the expected alterations in the cholesterol esterification system (*Calabresi et al., 2005*) in homozygous carriers, in particular the reduction of LCAT concentration and the absence of LCAT activity on both HDL and LDL.

Thus, the sub-groups of selected subjects well represented the main alterations associated to genetic LCAT deficiency.

1.2 Evaluation of ABCA1-mediated cholesterol efflux

To investigate whether the cardiovascular disease that affected the carrier of Val309-Met mutation (and another unrelated subject carrying the same mutation, not enrolled in the current study) could be linked to alterations in HDL function, the ability of subjects' HDL to promote the ABCA1-mediated cholesterol efflux was assessed in comparison with the described cohort (*Calabresi et al. 2009)* (figure 17).

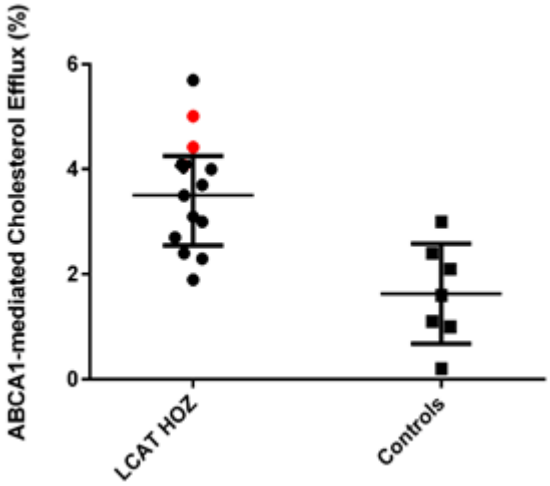

Figure 17. Evaluation of ABCA1- mediated cholesterol efflux in LCAT deficient carriers compared to controls. Red points indicate the carriers of Val309-Met mutation. Scatter-plots show the median values and the interquartile range.

The results demonstrated that Val309-Met mutation did not affect the ability of HDL to promote ABCA1-mediated cholesterol efflux, as the evaluation of this parameter was totally in line with the other homozygous carriers and enhanced compared to controls (*Calabresi et al., 2009*).

1.3 HDL ability to acquired surface lipids derived from TGRL by LPL-mediated lipolysis

The ability of LCAT deficient carriers' HDL to acquire free cholesterol and phospholipids upon the LPL-mediated lipolysis of TGRL was never investigated, thus experiments to evaluate this peculiar HDL function were performed (figure 18):

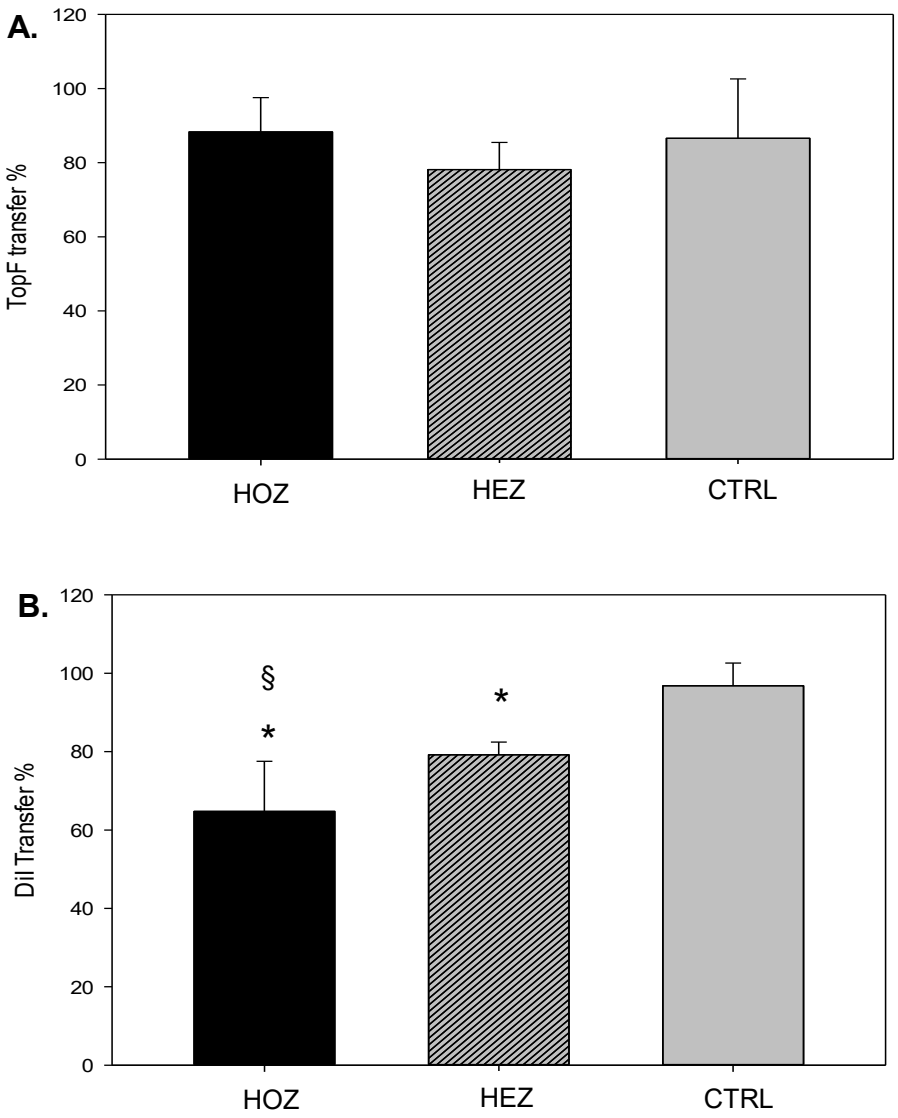

Figure 18: HDL transfer of free cholesterol (A) and phospholipids (B) upon TGRL lipolysis. Data are expressed as mean ± SD. Parameters were analyzed by one-way ANOVA. All pairwise multiple comparison were performed by Holm-Sidak method. ($^{\S}p<05$ vs Hez, $^{*}p<0,05$ vs Ctrl).

The results showed that the HDL- mediated transfer of free cholesterol upon TGRL lipolysis did not present significant differences among homozygous, heterozygous and controls, despite the low level of HDL in LCAT deficient carriers.

On the contrary, the capacity of HDL to acquire phospholipids was significantly impaired in carriers of LCAT gene mutations, with a clear gene dose-dependence trend that reflects the concentration of HDL in the subjects.

1.4 Characterization of LCAT deficient carriers' HDL

Subjects' HDL were isolated by ultracentrifugation and the composition was evaluated (table 7):

	HOZ	HEZ	CTRL	p trend
%UC	16 ± 6§*	5 ± 1	5 ± 1	*0,008*
%TG	8 ± 5	6 ± 1	4 ± 1	0,118
%EC	0 ± 0§*	20 ± 2	25 ±1	*<0,001*
%PL	24 ± 9	20 ± 1	18 ± 0	0,101
%PT	53 ± 14	49 ± 2	47 ± 2	0,771

Table 7. Percentage composition of HDL isolated by ultracentrifugation. Data are expressed as mean ± SD. Parameters were analyzed by one-way ANOVA. All pairwise multiple comparisons were performed by Holm-Sidak method (§p<05 vs Hez, *p<0,05 vs Ctrl).

Homozygous FLD carriers' HDL presented alterations in the total composition, in particular an increased amount of free cholesterol and a the total depletion of esterified cholesterol, paralleled by a less marked increasing trend in phospholipids and proteins percentage compared to heterozygous' and healthy subjects' HDL.

Through lipidomics analysis, phospholipids and sphingolipids in subjects' HDL were analyzed. The main species of phospholipid class evaluated included phosphatidylcholine (PC) and lysophosphatidylcholine (LPC), phosphatidylethanolamine (PE) and lysophosphatidylethanolamine (LPE), phosphatidylethanolamine plasmalogens (Pep), phosphatidylinositol (PI), phosphatidylserine (PS), phosphatidylglycerol (PG) and phosphatidic acid (PA). Among sphingolipids, dihydrosphingomyelin (DHSM), sphingomyelin (SM), ceramides (Cer 18:1), sphingadienines (Cer 18:2) and dihydroceramides (DHC) were evaluated. The distribution of the phospholipids and sphingolipids classes and the most abundant species for each class in controls subjects' HDL are reported in table 8 and 9, as mol% on the total lipid content:

Phospholipid class (mol% tot lipid)	Most abundant species (mol% tot lipid)	Phospholipid class (mol% tot lipid)	Most abundant species (mol% tot lipid)
PC (80,43%)	PC(34:2): 13,4% PC(34:1): 10,2% PC(36:2): 9,54%	**PG (0,2%)**	PG(36:2): 0,008% PG(34:1): 0,005% PG(36:1): 0,006%
PI (2,99%)	PI(36:2): 0,33% PI(36:1): 0,20% PI(36:4): 0,16%	**LPEsn2 (0,09%)**	LPE(20:4)sn2: 0,021% LPE(22:6)sn2: 0,014% LPE(20:3)sn2: 0,011%
LPCsn1 (1,18%)	LPC(16:0)sn1: 0,59% LPC(18:0)sn1: 0,24% LPC(18:2)sn1: 0,13%	**PS (0,07%)**	PS(38:4):0,026% PS(36:1): 0,021 PS(38:3): 0,004%
PE (1,20%)	PE(36:2): 0,26% PE(34:2): 0,11% PE(38:4): 0,18%	**PA (0,08%)**	PA(38:4): 0,027% PA(36:2): 0,016% PA(38:3): 0,007%
PEp (0,55%)	PE(18:0p/20:4): 0,21% PE(16:0p/20:4): 0,06% PE(16:0p/22:5): 0,01%	**LPEsn1 (0,03%)**	LPE(18:0)sn1: 0,008% LPE(18:1)sn1: 0,007% LPE(20:4)sn1: 0,005%
LPCsn2 (0,46%)	LPC(18:0)sn2: 0,12% LPC(16:0)sn2: 0,08% LPC(20:4)sn2: 0,08%		

Table 8. The distribution of the phospholipids classes and the most abundant species for each class in controls subjects' HDL. Data are expressed as mol% on the total lipid content

Sphingolipid class (mol% tot lipid)	Most abundant species (mol% tot lipid)
SM (12,38%)	SM(34:1): 2,84% SM(42:2): 1,73% SM(40:1): 1,05%
DHSM (0,39%)	SM(36:0): 0,046% SM(35:0): 0,029% SM(34:0): 0,27%
Cer 18:1 (0,11%)	Cer(d18:1-24:0): 0,04% Cer(d18:1-22:0): 0,02% Cer(d18:1-23:0): 0,01%

Cer 18:2 (0,01%)	Cer(d18:2-18:0): 0,003% Cer(d18:2-16:0): 0,001% Cer(d18:2-22:0): <0,001%
DHC (0,01%)	Cer(d18:0-24:1): 0,003% Cer(d18:0-16:0): 0,001% Cer(d18:0-22:0): 0,001%

Table 9. The distribution of the sphingolipid classes and the most abundant species for each class in controls subjects' HDL. Data are expressed as mol% on the total lipid content.

The qualitative differences in the content of total lipids classes between homozygous FLD carriers' and control subjects' HDL are reported in table 10, and data were recalculated as mol% of total lipid, as mol/g of total protein or nmol/µl; the recalculations allowed a precise and sure definition of the changes in the quantities of analyzed lipid classes.

Moreover, in table 11, the fold changes in HDL of LCAT deficient carriers' total lipids classes measurements compared to controls are reported.

	Mol % (PL + SL)	mol/g of prot	nmol/µl
Total PC	↔	↑	↓↓
Total LPCsn1	↑	↔	↓↓
Total LPCsn2	↑	↔	↓↓
Total PE	↑↑	↑	↓
Total LPEsn1	↑	↑	↔
Total LPEsn2	↓↓	↓	↓
Total PEp	↓↓	↓	↓↓
Total PI	↔	↔	↓↓
Total PG	↔	↑	↓
Total PS	↑	↑	↔
Total PA	↑	↑	↓
Total SM	↔	↑	↓
Total DHSM	↑	↑	↓
Total DHC	↑↑	↑↑	↑

Total Cer 18:1	↑↑	↑	↑
Total Cer 18:2	↑	↑	↓

Table 10. Qualitative trend of FLD homozygous' HDL total phospholipid and sphingolipid classes measurements compared to controls. (↔): unchanged, (↑) slight increase, (↑↑) strong increase, (↓) slight decrease, (↓↓) strong decrease

	Heterozygous vs controls			Homozygous vs control		
	Mol % (PL + SL)	mol/g prot.	nmol/µl	Mol % (PL + SL)	mol/g prot.	nmol/µl
Total PC	1,00	0,94	0,82	0,98	1,17	*0,51**
Total LPCsn1	1,06	0,99	0,87	1,23	1,04	*0,44**
Total LPCsn2	1,08	1,00	0,88	1,47	1,20	*0,51**
Total PE	*1,33**	1,25	1,11	*1,63**	1,81	0,77
Total LPEsn1	1,07	1,01	0,91	2,29	1,93	0,83
Total LPEsn2	1,08	1,04	0,92	0,43*	0,43	0,19
Total Pep	1,06	0,99	0,87	*0,61**	0,72	*0,31**
Total PI	0,93	0,87	0,77	0,95	1,14	*0,49**
Total PG	0,78	0,73	0,66	1,23	1,36	0,58
Total PS	0,78	0,74	0,66	4,11	2,16	0,90
Total PA	1,10	1,03	0,91	1,26	1,50	0,65
Total SM	0,98	0,92	0,81	1,01	1,25	0,54
Total DHSM	0,86	0,81	0,73	1,21	1,44	0,63
Total DHC	1,50	1,40	1,23	*4,96**	*6,09**	2,71
Total Cer 18:1	1,23	1,14	1,00	*2,33**	2,78	1,21
Total Cer 18:2	0,96	0,90	0,79	1,26	1,61	0,69

Table 11. Fold change of LCAT deficient carriers' total phospholipid and sphingolipid classes measurements in HDL compared to controls. Data were expressed as mol% on total lipids (phospholipids + sphingolipids), as mol/g of total protein or as nmol/ µl. Results were analyzed by paired T-test (p*<0.05 vs ctrl).

The three different ways of expressing the concentration were used to globally define the enrichment/depletion effect observed in the total lipid classes; mol% of total lipids and the recalculation of mol/g of total protein presented nearly the same trend for all the evaluated lipid classes, while the recalculation per volume was influenced by the HDL concentration in plasma, that in homozygous FLD carriers is critically reduced.

The results indicated a significant increase in the total PE both as mol% and per volume (figure 19A), which is a substrate of the LCAT reaction particularly affine to

the enzyme, and in total LPE-sn1 as mol%, in parallel with a significant depletion of LPEsn2 as mol% and per volume, which is a the preferential product of the LCAT reaction (*Pownall et al., 1985*); moreover, total PEp in FLD carriers' HDL was significantly reduced as mol% and per volume compared to controls' ones (figure 19B). Interestingly, the total amount of PC, the main LCAT substrate, as well as the level of LPCsn1 and LPCsn2, classical products of LCAT reaction, did not differ between homozygous and controls' HDL. Moreover, FLD carriers' particles are enriched in total PS. The other minor classes, as PI, PG and PA did not show any significant alteration, despite the reduction when recalculated according to volume, an effect observed in almost all the lipids classes due to the significant reduction of HDL concentration in FLD carriers' plasma.

The analysis of sphingolipids highlighted an enrichment of FLD carriers' HDL of DHC and Cer 18:1 as mol%, that represent minor classes (figure 19C and D). Consistently with these data, DHC and Cer were not reduced in homozygous when recalculated per volume despite the low levels of HDL in these subjects.

Heterozygous' HDL did not presented deep alterations compared to controls, with the exception of the increased amount of PE as mol%.

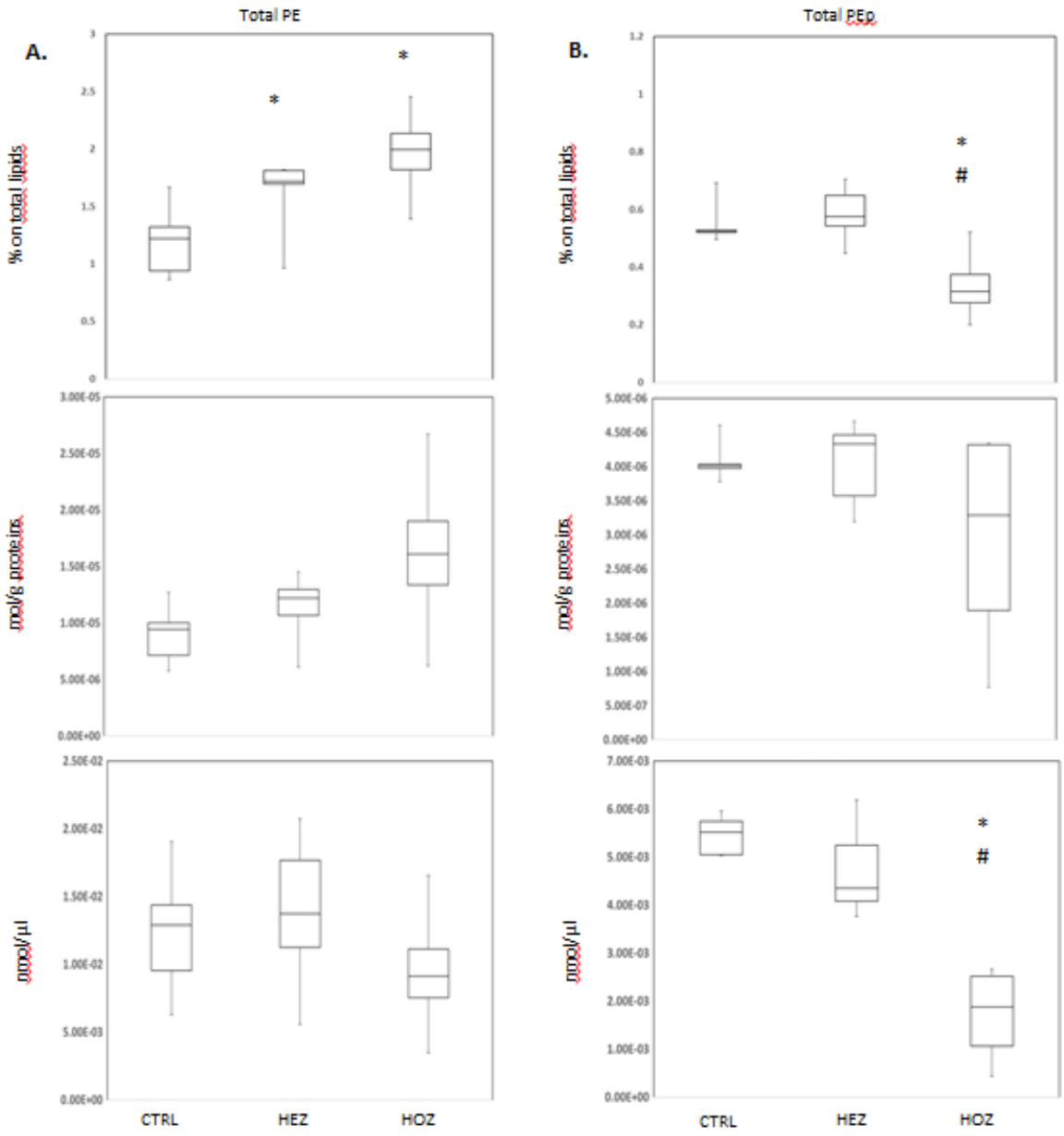
A.
Total PE
% on total lipids
mol/g proteins
nmol/µl
CTRL
HEZ
HOZ
B.
Total PEp
% on total lipids
mol/g proteins
nmol/µl
CTRL
HEZ
HOZ

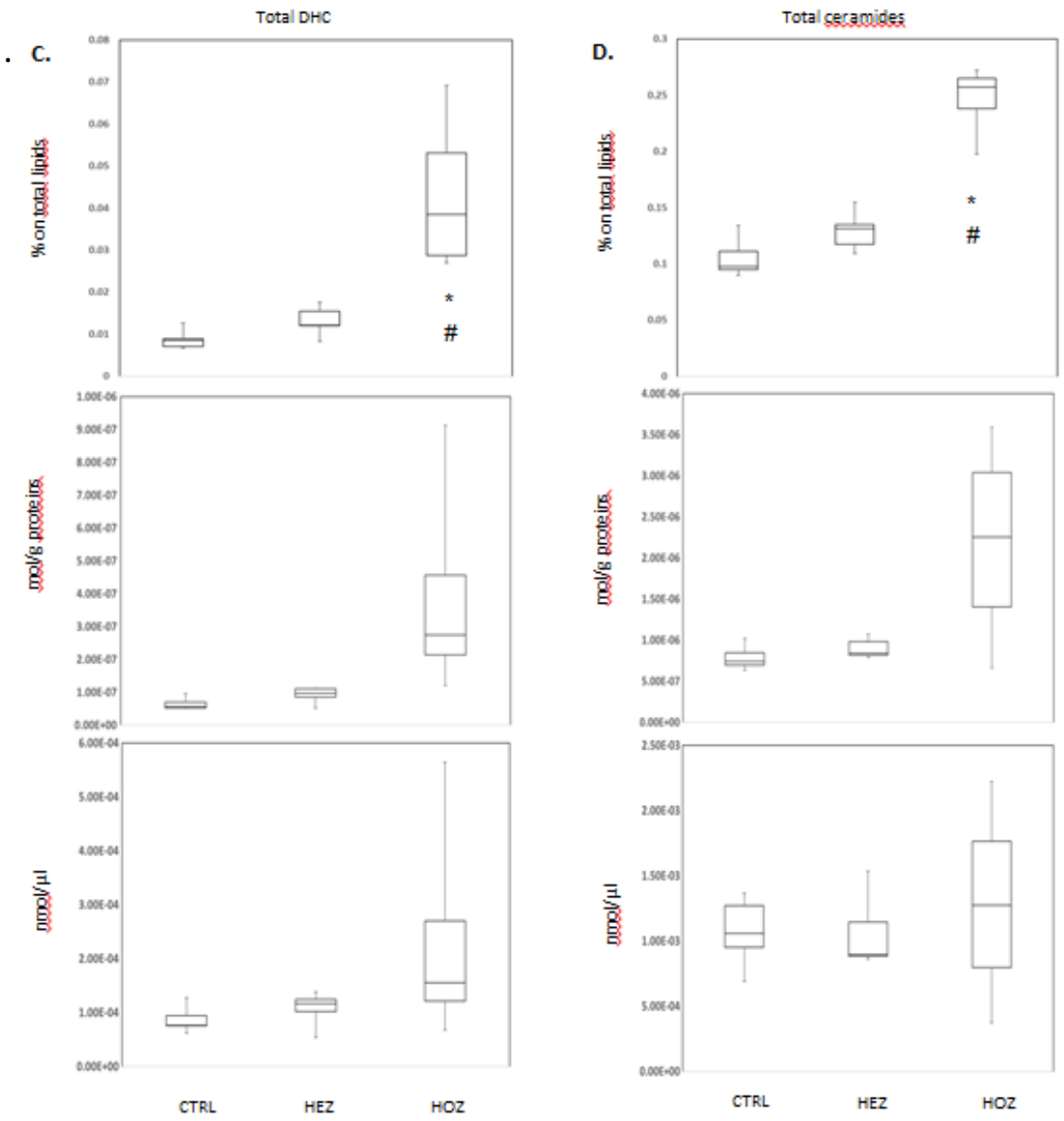

Figure 19. Total PE (A) and PEp (B), DHC (C) and ceramides (D) concentrations expressed as mol%(on PL+SL), nmol/g proteins and nmol/µl. Data are represented as boxplot indicating median and 25th-75th percentile. Results were analyzed by one-way ANOVA (§p<05 vs Hez, *p<0,05 vs Ctrl)

The boxplot clearly showed that in homozygous FLD carriers' HDL, the absence of LCAT led to a significant accumulation of PE and to a strong depletion of PEp. This effect was evident in all the recalculations ways. The amount of DHC and total ceramides was significantly increased with the recalculation as mol%, and the same trend was observed even when the data were expressed as mol/g of total protein, confirming the marked increase in the content of these minor sphingolipids.

To further investigate whether the absence of LCAT could affect not only the amount of polar lipids classes but also the individual lipid species, the fatty acids distribution in LCAT deficient carriers' HDL was compared to controls' one. The result are summarized in the Venn's diagram below (figure 20):

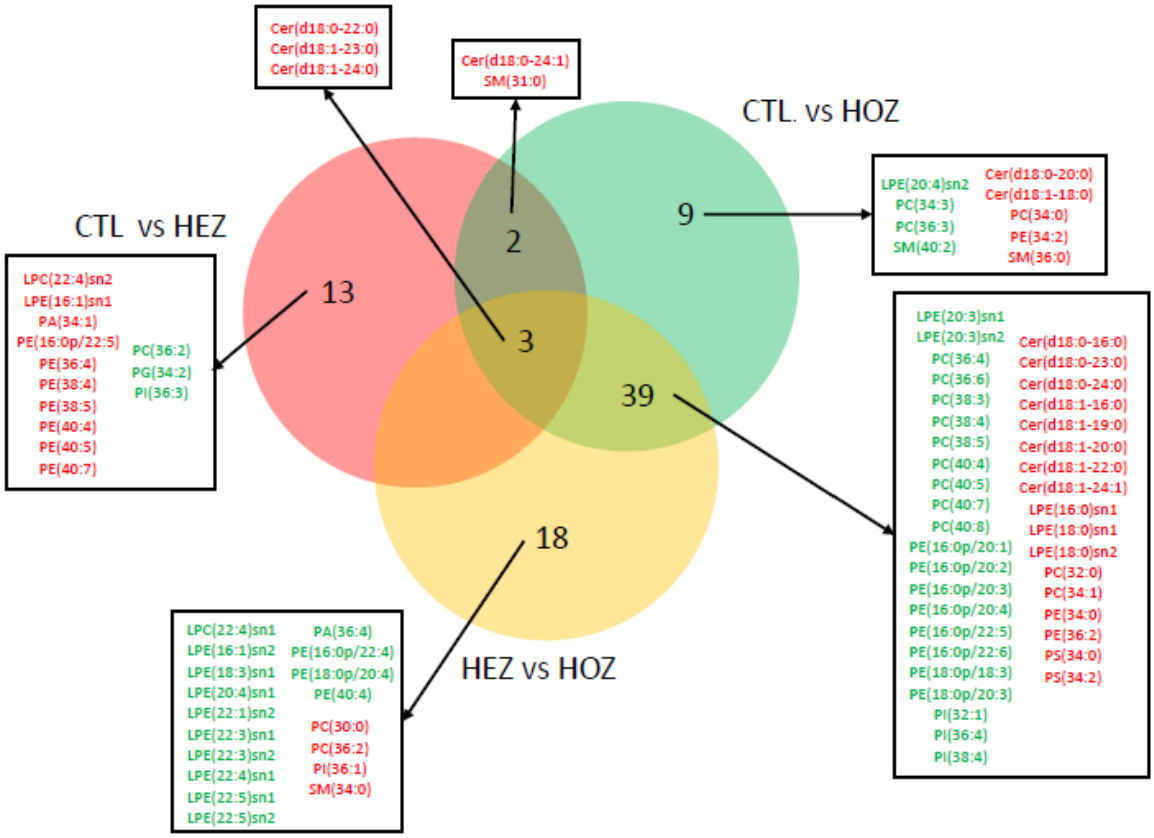

Figure 20. Venn's diagram representing the difference in species amount among FLD homozygous, heterozygous and controls. In green, species depleted; in red, species enriched

The results obtained demonstrated that the lack of LCAT enzyme deeply affects fatty acids moieties of lipid species in HDL; in particular, homozygous FLD carriers' HDL were enriched in short and saturated fatty acid residues, especially among PC, PE, DHC and ceramides species, while being depleted of long polyunsaturated fatty acids (PUFA), the preferred substrates of LCAT in particular in PC and PE species (*Jonas, 2000*). It is interesting to notice that the modifications in the moiety of the fatty acids did not affect the most abundant species in each lipid class. For example, FLD carriers' HDL were enriched in PC and PE containing saturated minor species, like

PC(32:0), PC(34:0), and PE(34:0), while a high number of PUFA species were depleted. Other minor lipid classes presented alterations in the species amount; thus, the amount of saturated PS increased in homozygous' HDL (PS 34:0), while PI PUFA were decreased (PI 36:4 and 38:4).

Heterozygous HDL presented an enrichment in PUFA in PE species compared to controls' HDL, as well as a depletion in PUFA in LPE species respect to homozygous' HDL.

Finally, the esterified cholesterol in subjects' HDL was evaluated (figure 21):

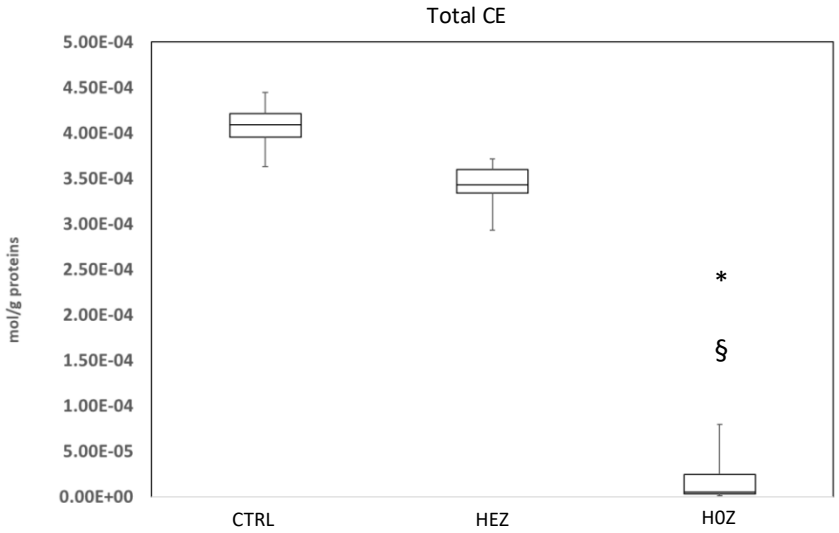

Figure 21. Total esterified cholesterol concentrations in HDL expressed as mol/g protein. Data are represented as boxplot indicating median and 25th-75th percentile. Results were analyzed by one-way ANOVA (§p<05 vs Hez, *p<0,05 vs Ctrl)

The results confirmed the dramatic reduction in total esterified cholesterol in homozygous FLD carriers' HDL compared to controls' and heterozygous' lipoproteins, observed in the preliminary composition analysis.

1.5 Characterization of LCAT deficient carriers' plasma

The evaluation of the total phospholipids and sphingolipids classes was performed also on LCAT deficient carriers' plasma. The normal distribution of the phospholipids and sphingolipids classes and of the most abundant species for each class in control subjects' plasma are reported in table 12 and 13, as mol% on the total lipid content:

Phospholipid class (mol% tot lipid)	Most abundant species (mol% tot lipid)	Phospholipid class (mol% tot lipid)	Most abundant species (mol% on tot lipid)
PC (69,91%)	PC(34:2): 14,0% PC(34:1): 9,85% PC(36:2): 9,48%	**LPE sn2 (0,32%)**	LPE(20:4)sn2: 0,098% LPE(22:6)sn2: 0,064% LPE(22:5)sn2: 0,033%
LPCsn1 (4,92%)	LPC(16:0)sn1: 2,35% LPC(18:2)sn1: 0,88% LPC(20:4)sn1: 0,17%	**PG (0,2%)**	PG(36:2): 0,007% PG(34:1): 0,003% PG(34:2): 0,001%
PI (3,06%)	PI(38:4): 1,56% PI(36:2): 0,33% PI(36:1): 0,20%	**LPEsn1 (0,14%)**	LPE(18:2)sn1: 0,038% LPE(20:4)sn1: 0,030% LPE(22:6)sn1: 0,014%
LPCsn2 (1,48%)	LPC(16:0)sn2: 0,52% LPC(18:0)sn2: 0,26% LPC(18:1)sn2: 0,20%	**PS (0,06%)**	PS(38:4): 0,033% PS(40:6): 0,011% PS(36:1): 0,008%
PE (1,28%)	PE(38:3): 0,040% PE(36:2): 0,24% PE(38:6): 0,17%	**PA (0,03%)**	PA(38:4): 0,010% PA(36:2): 0,006% PA(34:2): 0,005%
PEp (0,66%)	PE(16:0p/22:6): 0,042% PE(18:0p/20:4): 0,26% PE(18:0p/22:6): 0,08%		

Table 12. The distribution of the phospholipids classes and of the most abundant species for each class in controls subjects' plasma. Data are expressed as mol% on the total lipid content

Sphingolipid class (mol% tot lipid)	Most abundant species (mol% tot lipid)
SM (17,45%)	SM(34:1): 5,27% SM(36:1): 1,26% SM(40:1): 1,46%
DHSM (0,41%)	SM(34:0): 0,24% SM(36:0): 0,060% SM(40:0): 0,033%

Cer 18:1 (0,24%)	Cer(d18:1-23:0): 0,033% Cer(d18:1-24:0): 0,11% Cer(d18:1-24:1): 0,042%
DHC (0,03%)	Cer(d18:0-23:0): 0,003% Cer(d18:0-24:0) 0,013% Cer(d18:0-24:1): 0,008%
Cer 18:2 (0,01%)	Cer(d18:2-16:0): 0,001% Cer(d18:2-18:0): <0,001% Cer(d18:2-22:0): 0,007%

Table 13. The distribution of the sphingolipid classes and of the most abundant species for each class in controls subjects' plasma. Data are expressed as mol% on the total lipid content

The qualitative differences in the amount of total lipids classes between homozygous FLD carriers' and control subjects' plasma were assessed and results are reported in table 14; data were recalculated as mol% of total lipid and as noml/ul, again for confirming the changes in the quantities of the analyzed lipid classes.
Moreover, in table 15, the fold changes of plasma LCAT deficient carriers' total lipids classes measurements compared to controls in HDL are reported.

	Mol % (PL + SL)	nmol/µl
Total PC	↑↑	↑
Total LPCsn1	↓	↔
Total LPCsn2	↓	↔
Total PE	↑	↑
Total LPEsn1	↑	↑
Total LPEsn2	↓↓	↓↓
Total Pep	↓↓	↓
Total PI	↔	↔
Total PG	↔	↑
Total PS	↑	↑
Total PA	↔	↑
Total SM	↓↓	↓
Total DHSM	↔	↑

Total DHC	↑	↑
Total Cer 18:1	↑	↑
Total Cer 18:2	↓	↓

Table 14. Qualitative trend of FLD homozygous' plasma total phospholipid and sphingolipid classes measurements compared to controls. (↔): unchanged, (↑) slight increase, (↑↑) strong increase, (↓) slight decrease, (↓↓) strong decrease

	Hez vs ctrl		Hoz vs ctrl	
	Mol % (PL + SL)	**nmol/µl**	**Mol % (PL + SL)**	**nmol/µl**
Total PC	1,03	1,01	*1,09**	1,22
Total LPCsn1	1,00	0,97	0,87	0,98
Total LPCsn2	1,00	0,97	0,79	0,88
Total PE	1,12	1,06	1,51	1,74
Total LPEsn1	1,01	0,97	1,37	1,54
Total LPEsn2	0,98	0,98	*0,18**	*0,20**
Total Pep	0,90	0,88	*0,48**	0,56
Total PI	0,87	0,84	1,06	1,18
Total PG	0,59	0,58	1,12	1,34
Total PS	0,70	0,67	1,21	1,29
Total PA	0,73	0,71	1,09	1,28
Total SM	0,91	0,90	*0,66**	0,79
Total DHSM	1,30	1,29	1,09	1,26
Total DHC	1,05	0,99	1,17	1,33
Total Cer 18:1	1,03	1,00	1,03	1,18
Total Cer 18:2	0,85	0,81	0,80	0,87

Table 15. Fold change of LCAT deficient carriers' total phospholipid and sphingolipid classes measurements compared to controls in plasma. Data were expressed as mol% on total lipids (phospholipids + sphingolipids), as mol/g of total protein or as nmol/ µl. Results were analyzed by paired T-test (p*<0.05 vs ctrl).

The results of the lipidomics analysis on LCAT deficient carriers' plasma highlighted a significant increase in PC as mol% and a less enhanced reduction of LPCsn1 and LPCsn2 as mol%, as expected by the lack of LCAT that catalyzes the transesterification of PC leading to the formation of LPC. The recalculation per volume confirmed the results observed as mol%. Ethanolamine-derived phospholipids are affected by the absence of the enzyme too, as demonstrated by the accumulation

of PE as mol% and per volume and the depletion of LPEsn2 with both recalculations, the main product of the LCAT reaction.

Interestingly, the reduction in PEp class previously observed in FLD homozygous carriers' HDL was confirmed also in plasma, clarifying the specificity of the species for HDL. The minor lipid phospholipids classes amount, including PI, PG and PA did not present alterations in homozygous carriers, while the content of PS tended to increase.

The amount of circulating DHC and Cer 18:1 slightly increased when recalculated per volume, mirroring the enrichment observed in FLD carriers' HDL, while the total SM as mol% was significantly reduced.

To establish if the absence of LCAT could affect fatty acid moieties of the individual lipid species not only in HDL but also in plasma, the fatty acids distribution in LCAT deficient carriers' HDL compared to controls' one. The result are summarized in the Venn's diagram below (figure 22):

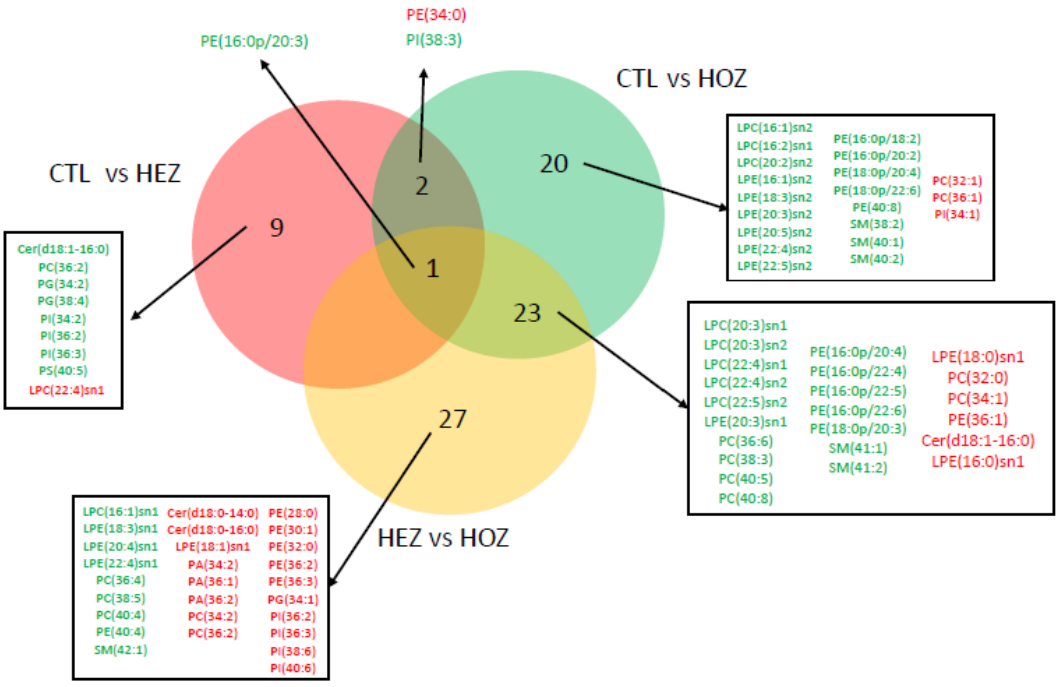

Figure 22. Venn's diagram representing the difference in species amount among FLD homozygous, heterozygous and controls. In green, species depleted; in red, species enriched

Plasma from homozygous deficient carriers presented alterations in lipids species moiety that mirrors the one observed in in HDL, mainly the depletion of long chain PUFA, particularly evident in LPC, LPE and PC classes.

The reduction of almost all PEp species in homozygous plasma strongly support the reduction in the total amount of the class observed in HDL. Homozygous FLD carriers presented also an enrichment in some saturated and monounsaturated species in plasma, as PC (32:0), PC (34:1) and PE and PE (36:1).

Heterozygous plasma showed a depletion of minor lipid species, in particular in PG and PI containing PUFA compared to controls' plasma, and an enrichment in PA, PE, PI and PC containing long and unsaturated fatty acid residues.

Finally, the esterified cholesterol in subjects' plasma was evaluated (figure 23):

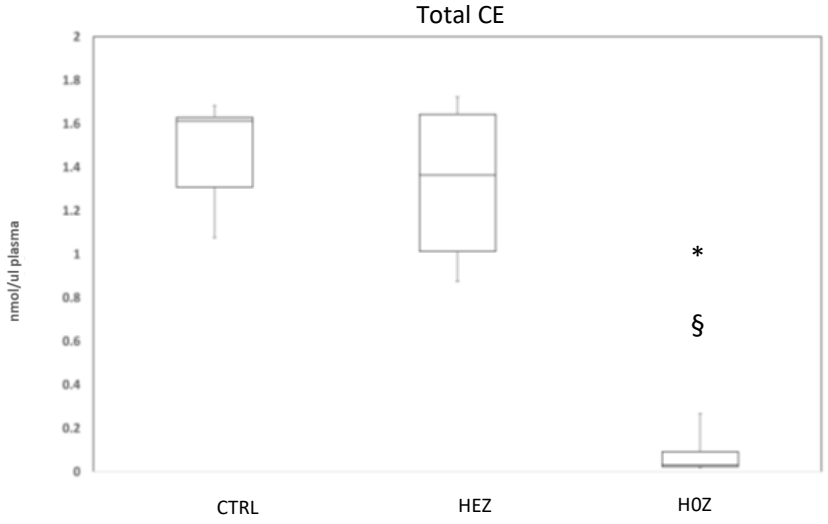

Figure 23. Total esterified cholesterol concentrations expressed as mol/g protein. Data are represented as boxplot indicating median and 25th-75th percentile. Results were analyzed by one-way ANOVA (§p<05 vs Hez, *p<0,05 vs Ctrl)

The results obtained confirmed the strong reduction in total esterified cholesterol previously observed in homozygous FLD carriers' HDL also in plasma, as expected by the lack of LCAT activity on all the substrates.

WORKPACKAGE 2: Molecular mechanisms investigation through in vitro studies on renal cells

In order to identify some potential mechanisms of the onset of renal disease and to assess whether the observed alterations in plasma and lipoproteins of LCAT deficient carriers are involved, in vitro studies were performed incubating renal cells with sera or HDL from a sub-group of carriers and controls selected from the Italian cohort.

2.1 Characteristics of the subjects

For the in vitro studies, a sub-group of subjects from the Italian cohort has been selected.

The characteristic of their lipid and lipoprotein profile are reported in the table 16.

	HOZ	HEZ	CTRL	P trend
N	6	8	8	-
Sex (m/f)	5/1	5/3	4/4	-
Age	37.8 ± 9.3	57 ± 15.1	36.3 ± 7.7	0,1106
TC (mg/dL)	154.3 ± 71	185.9 ± 48.7	194 ± 20.3	0,663
UC (mg/dL)	122 ± 58.1§*	53.5 ± 14.9	26.4 ± 16.9	*0,002*
UC/TC (%)	79.2 ± 15.3§*	29.7 ± 8	14.3 ± 9.9	*<0,001*
LDL-C (mg/dL)	83.2 ± 43.7	119 ± 45.7	115.7 ± 26.4	0,228
HDL-C (mg/dL)	7 ± 1.4§*	38.9 ± 9.9	64.7 ± 20.8	*<0,001*
TG (mg/dL)	321 ± 266.9 §*	139.6 ± 51.8*	73.6 ± 27	*0,007*
PL (mg/dL)	330.4 ± 88.3§*	226.4 ± 39.5	239.7 ± 42.7	*0,017*
ApoA-I (mg/dL)	37 ± 10.8§*	116.1 ± 24.3	120.8 ± 25.2	*<0,001*
ApoA-II (mg/dL)	4.9 ± 1.3 §*	32.6 ± 3.8	29.5 ± 2.1	*<0,001*

ApoB (mg/dL)	62.3 ± 33.1§*	107.3 ± 29.9	93.5 ± 15.1	*0,035*
Preβ-HDL (%)	51 ± 11.5 §*	23.95 ± 3.22	12.13 ± 1.13	*<0,001*
LpX (+/-)	yes	no	no	-

Table 26. Subjects' lipid and lipoprotein profile. Data are expressed as mean ± SD. Parameters were analyzed by one-way ANOVA. All pairwise multiple comparison were performed by Holm-Sidak method (§p<05 vs HEZ, *p<0,05 vs ctrl).

As expected, homozygous carriers presented a significant decrease in HDL-C and a marked increase of UC concentration and, consequently, of UC/TC ratio compared to heterozygous and controls. A significant reduction of apoA-I and apoB in homozygous was particularly evident too. These subjects had also an enhanced concentration of triglycerides and phospholipids compared to the other groups. The % of preβ-HDL, calculated as % of total apoA-I, highlighted a significant increasing gene-dose dependent trend; moreover, the abnormal lipoprototein LpX was detected only in homozygous subjects. Heterozygous carriers showed an intermediate profile between homozygous and controls.

2.2 Subjects' lipoproteins composition

To characterize the subjects' lipoproteins used for the in vitro studies, the composition of fractions isolated by ultracentrifugation was evaluated (table 17):

	LDL+LpX			
	HOZ	**HEZ**	**CTRL**	**p trend**
UC (%)	20 ± 3.9§*	9 ± 1.6	9 ± 2.3	*<0,001*
EC (%)	4 ± 4.2§*	30 ± 10.0	37 ± 5.7	*<0,001*
PL (%)	42 ± 6.4§*	25 ± 4.4	22 ± 5.7	*<0,001*
TG (%)	23 ± 5.1§*	15 ± 3.3*	9 ± 2.3	*0,016*
PT (%)	11 ± 4.8§*	21 ± 4.4	22 ± 6.0	*<0,001*
	HDL			
	HOZ	**HEZ**	**CTRL**	**p trend**
UC (%)	18 ± 2.8§*	4 ± 1.2	4 ± 0.9	*<0,001*
EC (%)	0 ± 0.8§*	16 ± 3.1*	22 ± 3.9	*<0,001*

PL (%)	46 ± 3.1[§*]	29 ± 5.9	32 ± 5.6	*<0,001*
TG (%)	5 ± 2.2	6 ± 1.1	4 ± 1.1	*0,011*
PT (%)	31 ± 3.6[§*]	45 ± 7.6	39 ± 7.3	*0,003*

Table 17. Percentage composition of LDL+LpX and HDL isolated by ultracentrifugation. Data are expressed as mean ± SD. Parameters were analyzed by one- way ANOVA. All pairwise multiple comparisons were performed by Holm-Sidak method ([§]p<05 vs Hez, [*]p<0,05 vs Ctrl).

Lipoproteins from homozygous FLD carriers presented an altered composition compared to heterozygous' and controls' ones. The LDL fraction, containing also LpX in these subjects, presented a significant enrichment of unesterified cholesterol and phospholipids, probably due to the abnormal lipoprotein, as well as an increase of triglycerides amount; on the other side, the percentage of esterified cholesterol and protein was significantly reduced compared to LDL from heterozygous and healthy subjects.

The HDL fraction, that in homozygous carriers contains mainly preβ-HDL particles, showed an increased amount of phospholipids and unesterified cholesterol, while the protein content was significantly reduced compared to heterozygous' and controls' HDL; cholesteryl esters in homozygous' HDL were completely absent, due to the total lack of LCAT activity on its main substrate.

2.3 In vitro studies on podocytes

As the glomerular damage has been largely described in LCAT deficiency and it is the cause of the development of proteinuria and kidney failure, in vitro studies on podocytes have been carried out to identify some possible pathologic mechanisms.

2.3.1 ROS production induced by serum and isolated lipoprotein of LCAT deficient carriers in podocytes

Oxidative stress is known to be associated with a direct glomerular damage in podocytes, leading to consequent dysfunction and apoptosis (*Chen et al., 2013*).;

thus the ability of FLD carriers' sera to induce oxidative stress in immortalized human podocytes was tested (figure 24)

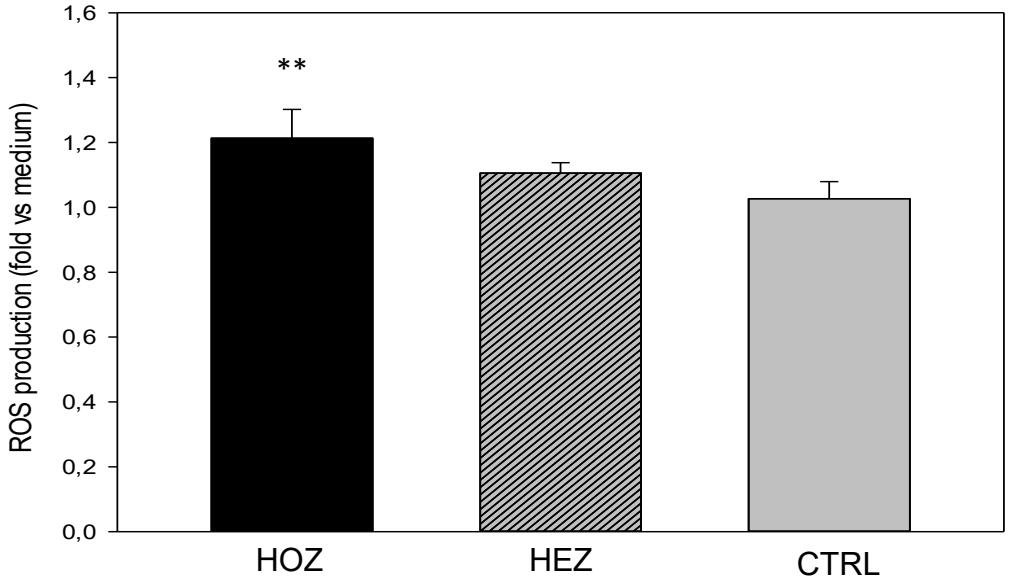

Figure 24. ROS production induced by incubation of podocytes with subjects' sera. Data are expressed as mean±sem. Data were analyzed by one-way ANOVA (P trend <0.05). All pairwise multiple comparisons were performed by Holm-Sidak method (**p<0,01 vs ctrl). HOZ (N=4), HEZ (N=3) and CTRL (N=8)

The results demonstrated that serum of FLD homozygous carriers induced a significant increased ROS production compared to healthy donor (+18,2% *hoz vs ctrl*, p=0,001), confirming the induction of an oxidative damage at glomerular level with a gene-dose dependent trend.

To assess whether the accumulation of LpX and preβ-HDL, the lipoprotein abnormalities present only in homozygous' plasma, could be directly associated to the enhanced oxidative stress, LDL and HDL fractions isolated from homozygous' and controls' plasma were used to incubate podocytes and the consequent ROS production was measured (figure 25).

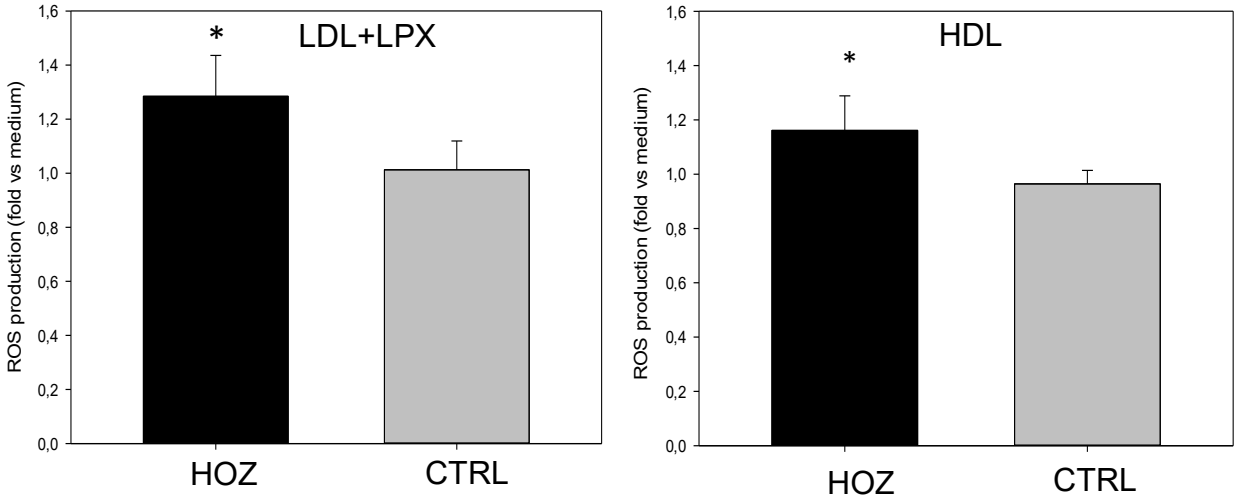

Figure 25. ROS production induced by incubation of podocytes with LDL+LpX (left panel) and HDL (right panel) isolated from homozygous' and controls' plasma. Data are expressed as mean±sem. Results were analyzed by paired T-test (P* <0.05). HOZ (N=4), CTRL (N=4)

The incubation of podocytes with both LDL+LpX and HDL fractions from homozygous FLD carriers increased significantly the oxidative stress compared to lipoproteins isolated from control subjects (+26,82% *LDL+LpX hoz vs ctrl,* p=0,026; +20,4% *HDL hoz vs ctrl*, p=0,018), confirming that LpX and preβ-HDL play a direct role in inducing the oxidative damage at glomerular level in LCAT deficiency.

2.3.2 Gene expression of podocytes' key proteins induced by serum and isolated lipoproteins of LCAT deficient carriers

Because of the central role of podocytes in ultrafiltration process, subjects' sera were incubated with podocytes to assess the effect on the expression of key proteins fundamental for the correct slit-diaphragm function, podocin and synaptopodin (*Haraldsson et al., 2008*) (figure 26).

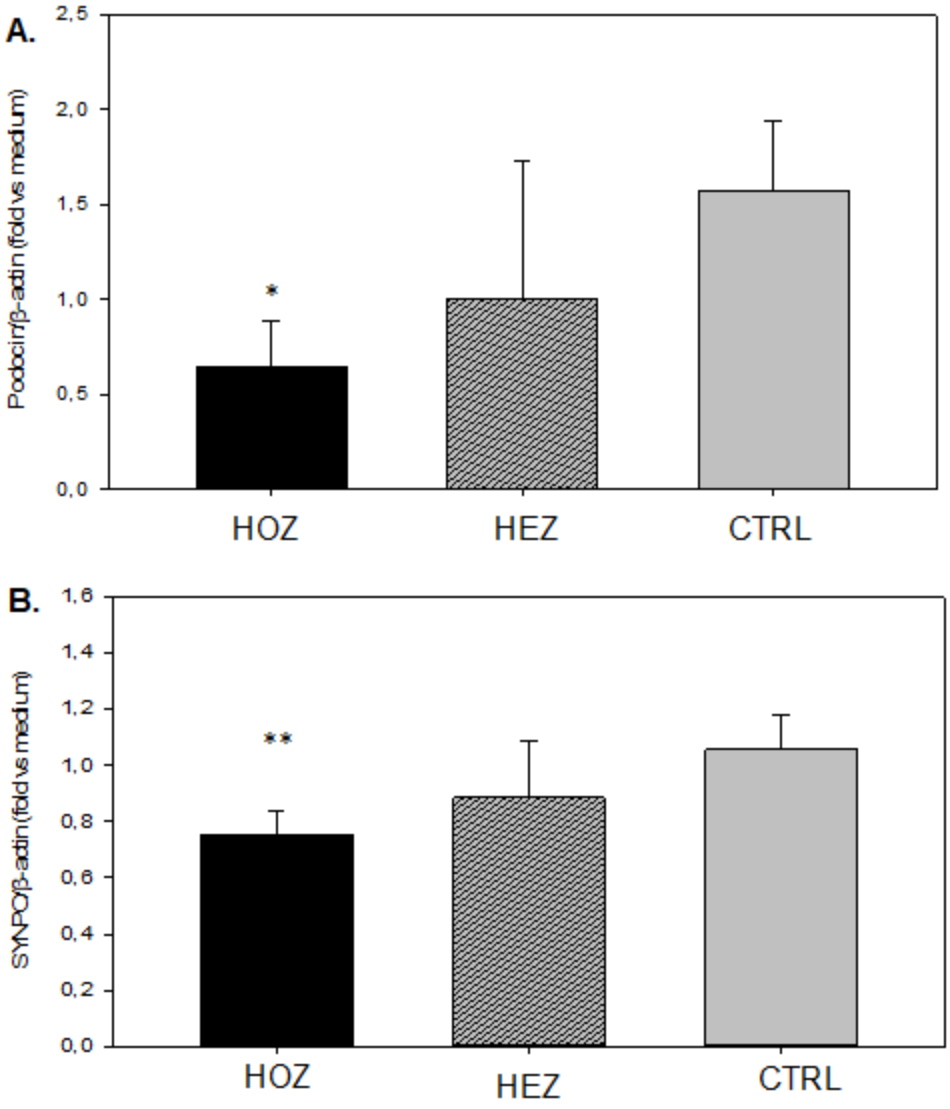

Figure 26. Podocin (A) and synaptopodin (B) gene expression induced by incubation of podocytes with subjects' sera. Data are expressed as mean ± sem. Data were analyzed by one-way ANOVA (P trend <0.05). All pairwise multiple comparisons were performed by Holm-Sidak method. (*p<0,05, **p<0,01 vs ctrl). HOZ (N=5), HEZ (N=4) and CTRL (N=6)

The incubation with sera from LCAT deficient carriers induced a reduction in the gene expression of both proteins with a gene-dose dependent trend, significant in homozygous (podocin -59,3%, *hoz vs ctrl,* p=0,026; synaptopodin -28,6% *hoz vs ctrl,* p=0,008).

To determine whether the reduction of podocin and synaptopodin expression and the consequent loss of podocytes functionality could be explained by lipoprotein

abnormalities in sera of homozygous FLD subjects, cells were incubated with isolated LDL+LpX or HDL fractions from these subjects' and healthy donors' plasma (figure 27).

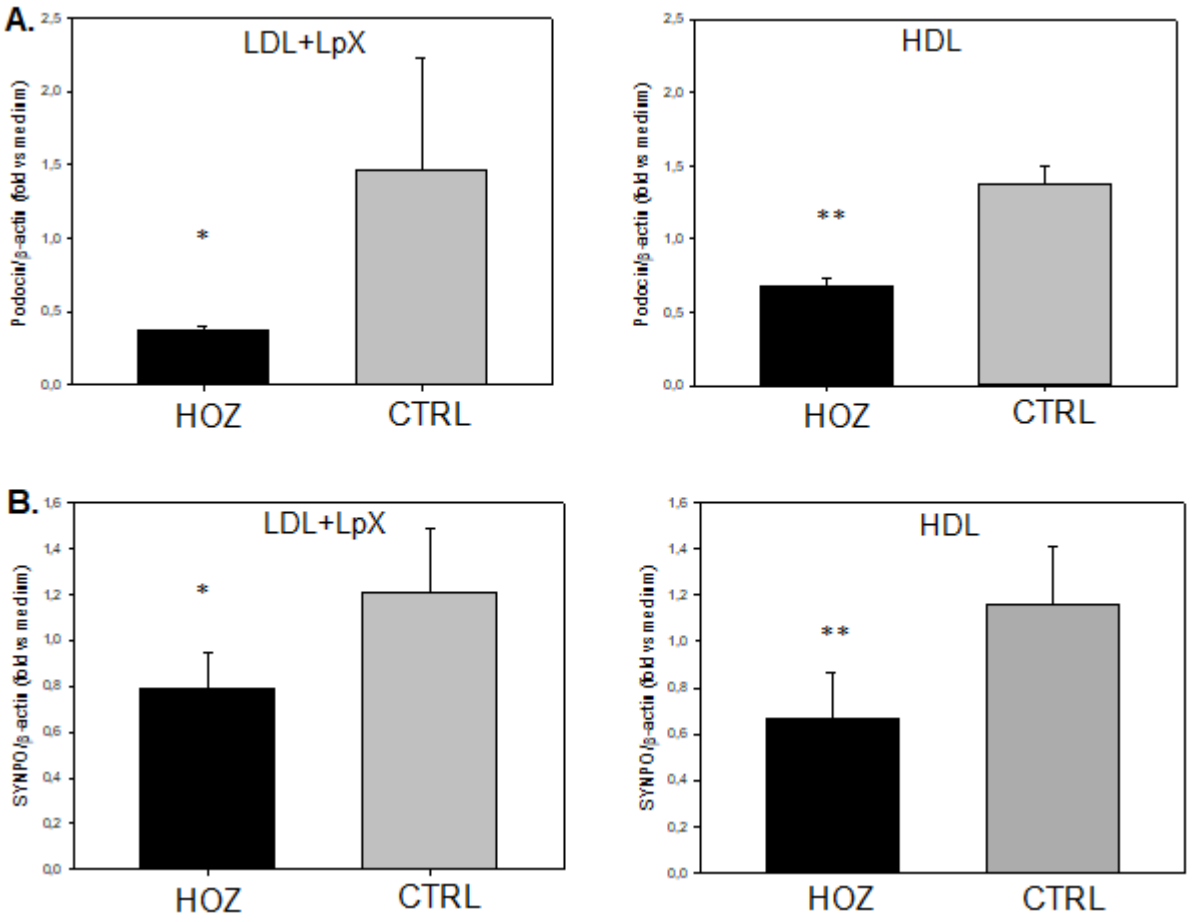

Figure 27. Podocin (A) and synaptopodin (B) gene expression induced by incubation of podocytes with subjects' isolated lipoproteins. Data are expressed as mean±sem. Results were analyzed by paired T-test (p*<0.05, p**<0.01 vs ctrl). HOZ (N=4), CTRL (N=4)

The results obtained showed that the incubation of podocytes with LDL+LpX and HDL fractions isolated from homozygous FLD carriers significantly reduced the gene expression of both podocin (-71,1% *LDL+LpX hoz vs ctrl*, p= 0,028; -50,9% *HDL hoz vs ctrl*, p<0,01) and synaptopodin (-29,3% *LDL+LpX hoz vs ctrl*, P=0,045; -42,4% *HDL hoz vs ctrl* p=0,014) highlighting the direct involvement of lipoprotein abnormalities typical of LCAT deficiency in the impairment of glomerular function.

2.3.3 Apoptosis induced by serum of LCAT deficient carriers in podocytes

To verify whether the increased oxidative stress and the alterations in podocytes function induced by serum of homozygous FLD carriers could affect cells detachment and viability, apoptosis was evaluated after the incubation of podocytes with subjects' sera (figure 28):

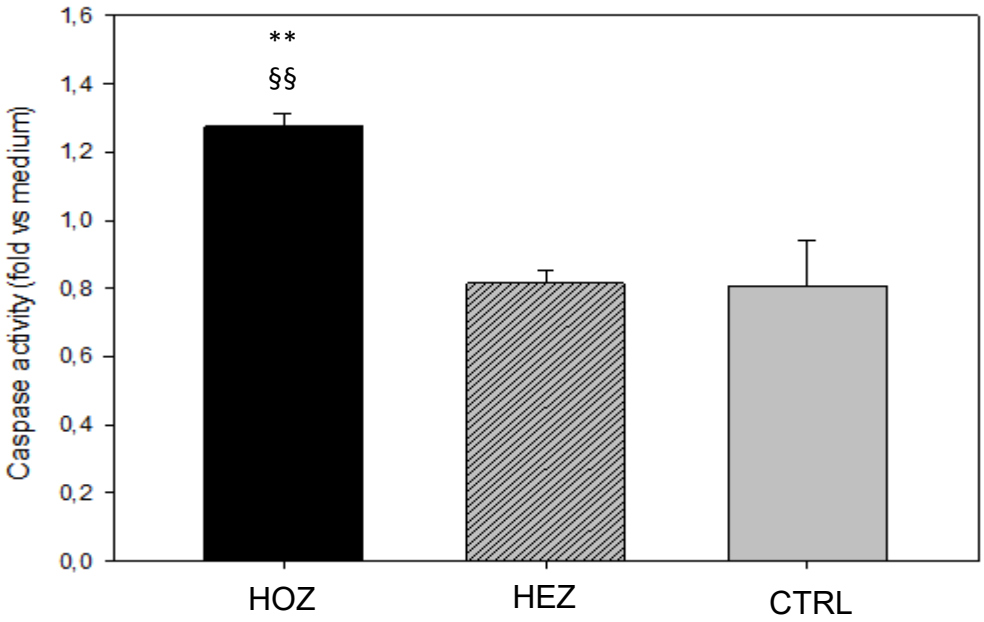

Figure 28. Caspase 3/7 activity induced by incubation of podocytes with subjects'sera. Data are expressed as mean±sem. Data were analyzed by one-way ANOVA (P trend <0.01). All pairwise multiple comparisons were performed by Holm-Sidak method (§§p<0,01 vs HEZ, **p<0,01 vs ctrl). HOZ (N=5), HEZ (N=5) and CTRL (N=3)

The results demonstrated that the incubation of podocytes with homozygous FLD carriers' sera induced a significantly higher apoptosis compared to heterozygous' and healthy donors' serum (+56,2% *hoz vs hez*, p=0,001; +30,5% *hoz vs ctrl*, p<0,001), confirming that renal damage that affects homozygous LCAT deficient subjects is characterized also by an increased cell death and podocytes depletion.

3.3 In vitro studies on tubular cells

In addition to the glomerular damage, the presence of tubular alterations in carriers of FLD has been described (*Stoekenbroek et al., 2013*). As tubular damage

characterizes a lot of renal diseases and it is usually associated with a mitochondrial impairment with a consequent increase of ROS production and to cellular dysfunction or death (*Takabatake et al., 2014*), in vitro studies on immortalized tubular cells were performed to assess the possible contribution of FLD carriers' lipid alterations in the onset of damage at tubular level.

3.3.1 ROS production induced by serum and isolated lipoprotein of LCAT deficient carriers in tubular cells

Oxidative stress is present since the early stages of CKD, playing a key role in the pathogenesis of renal failure, impairing both glomerular and tubular functions (*Duni et al., 2019*). On the basis of this assumption and of the observed pro-oxidant effect induced by FLD carriers' sera in podocytes, the in vitro study on tubular cells was repeated in the same conditions. Tubular cells were incubated with subjects' sera and ROS production was measured (figure 29)

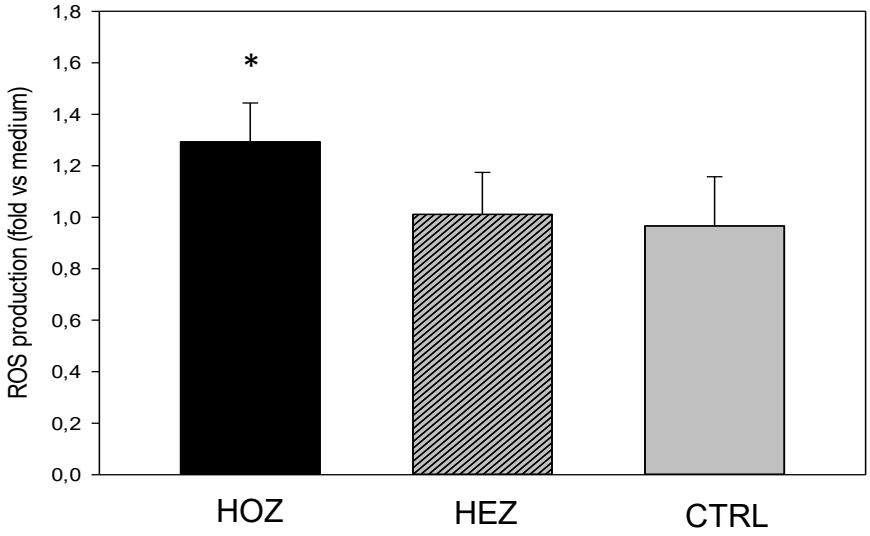

Figure 29. ROS production induced by incubation of tubular cells with subjects' sera. Data are expressed as mean±sem. Data were analyzed by one-way ANOVA (P trend <0.05). All pairwise multiple comparison were performed by Holm-Sidak method (*p<0,05 vs ctrl). HOZ (N=4), HEZ (N=4) and CTRL (N=6)

The incubation of tubular cells with serum from homozygous FLD carriers induced a significant increased ROS production compared to healthy donors' one (+33,8% *hoz*

vs ctrl, p=0,038), confirming an oxidative damage mediated by homozygous LCAT deficient subjects' serum alterations not only in glomeruli but also at tubular level.
To further confirm that the increased oxidative stress at tubular level observed only in homozygous FLD was associated with the accumulation of LpX and preβ-HDL, tubular cells were incubated with LDL+LpX and HDL fractions and ROS production were evaluated (figure 30).

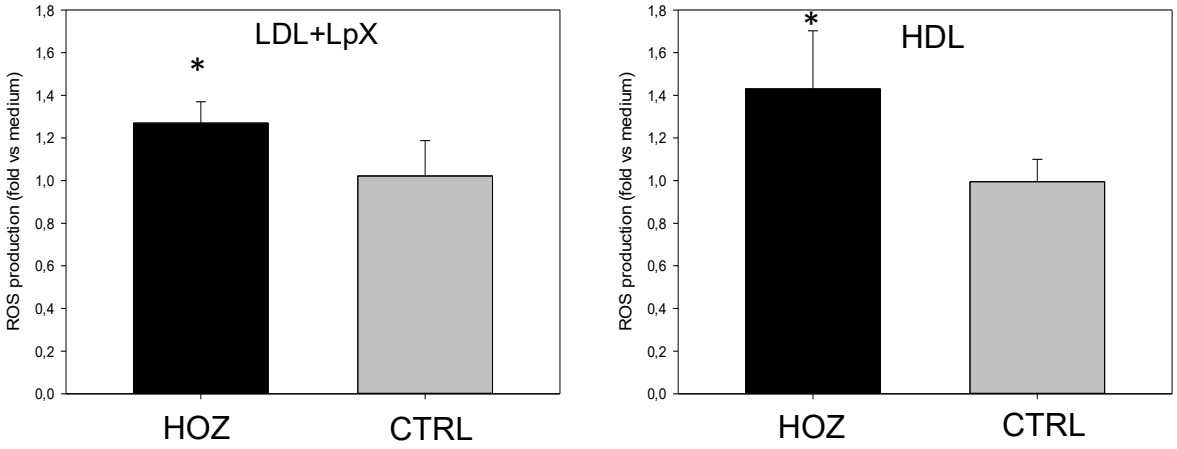

Figure 30. ROS production induced by incubation of tubular cells with LDL+LpX (left panel) and HDL (right panel) isolated from homozygous' and controls' plasma. Data are expressed as mean±sem. Results were analyzed by paired T-test (p* <0.05). HOZ (N=4), CTRL (N=4)

The results collected within these experiments confirmed that both LpX and preβ-HDL, that are largely contained in FLD carriers' isolated lipoprotein fractions, are involved in the increased oxidative stress at tubular level in homozygous LCAT deficient carriers (+18,5% *LDL+LpX hoz vs ctrl*, p=0,045; +43,8% *HDL hoz vs ctrl,* p=0,029).

3.3.2 Apoptosis and mitochondrial alterations induced by serum of LCAT deficient carriers in tubular cells

To verify whether the increased oxidative stress observed in tubular cells after the incubation with FLD carriers' plasma could be linked to alterations in mitochondria function, two genes codifying for fusion (optic atrophy 1, OPA, and mitofusin 2, MFN2) and fission proteins (mitochondrial fission factor, MFF, and mitochondrial fission 1 protein, FIS1) were evaluated (figure 31).

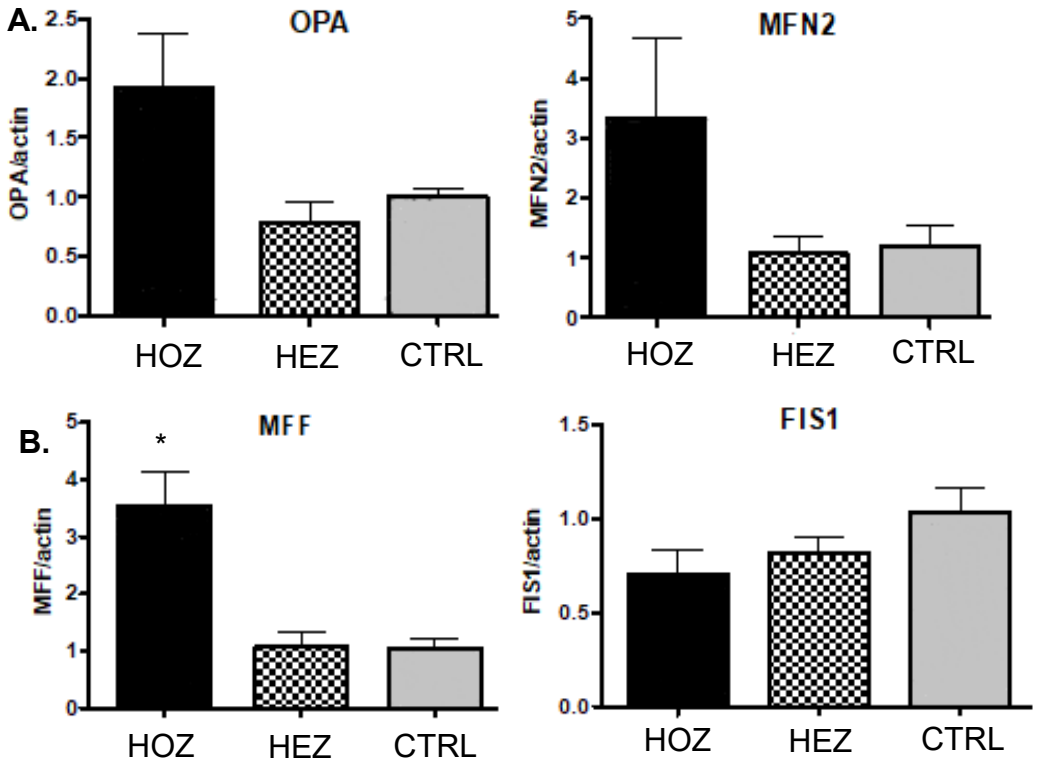

Figure 31. Fusion (A) and fission (B) proteins gene expression induced by incubation of tubular cells with subjects' sera. Data are expressed as mean±sem. Data were analyzed by one-way ANOVA and compared to control group in a post hoc test (Kruskal Wallis test) (p*<0,05 vs ctrl). HOZ (N=3), HEZ (N=2) and CTRL (N=3)

The results showed an increase in fusion proteins OPA (+90% *hoz vs ctrl*, p=0,065) and MFN2 (+220% *hoz vs ctrl*, p=0,104) induced by homozygous FLD carriers' sera and a significant enhanced expression of the fission protein MFF (+250% *hoz vs ctrl*, p<0,05). The higher expression of these genes mirrors an alteration in mitochondria normal function; as mitochondrial impairment and oxidative stress are associated with increased cellular death (*Sheng et al., 2018*), apoptosis in tubular cells was evaluated by measuring the activity of caspase 3/7 after the incubation with subjects' sera (figure 32):

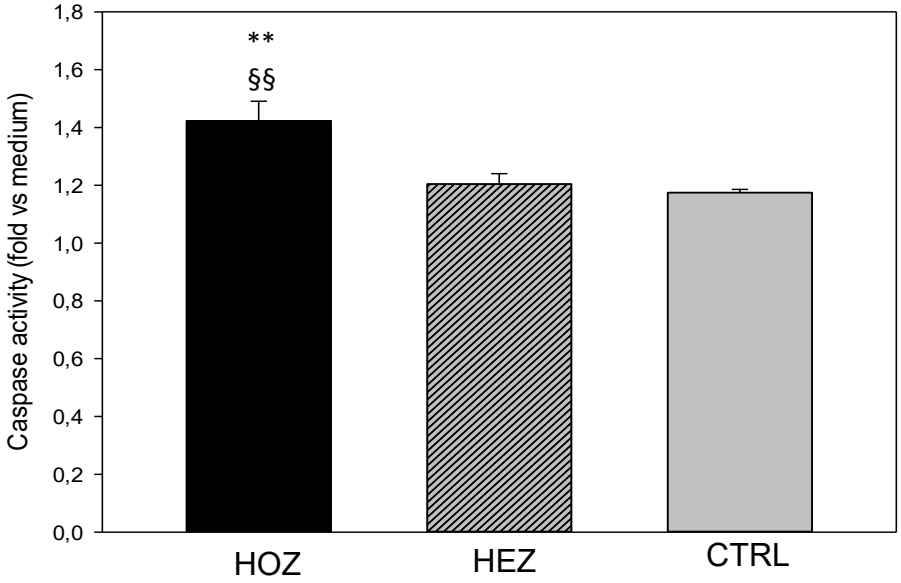

Figure 32. Caspase 3/7 activity induced by incubation of tubular cells with subjects' sera. Data are expressed as mean±sem. Data were analyzed by one- way ANOVA (P trend<0,01). All pairwise multiple comparisons were performed by Holm-Sidak method (§§p<0,01 vs HEZ, **p<0,01 vs ctrl). HOZ (N=5), HEZ (N=5) and CTRL (N=3)

The incubation of tubular cells with homozygous FLD carriers' sera induced a significant higher apoptosis compared to heterozygous' and controls' serum (+18,2% *hoz vs hez*, p=0,01; +21,2% *hoz vs ctrl*, p=0,009), in line with the observed increased impairment of mitochondria activity and the increased oxidative stress.

3.3.3 Autophagy process evaluation in tubular cells

Autophagy is a recycling process including self-degradation and reconstruction of damaged organelles and proteins, critical in kidney physiology and homeostasis.
Among the key proteins of this process, autophagy-related protein 5 (ATG5) is involved in phagosome elongation, and microtubule-associated protein 1 light chain 3 (LC3) is responsible for phagosome maturation. As induction of autophagy could serve as a protective strategy in several kidney diseases by increasing LC3 cleavage (LC3-II/LC3-I ratio) and enhancing Atg5 protein expression (*Lin et al., 2019*), this process was evaluated after the incubation of tubular cells with the sera of

homozygous FLD carriers, the only presenting alterations in oxidative stress and apoptosis, and of healthy subjects (figure 33).

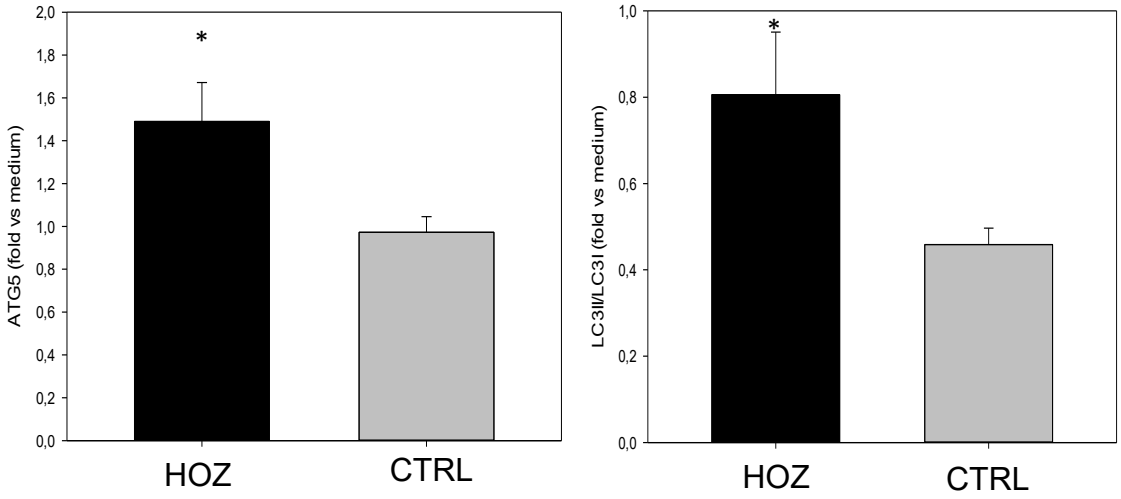

Figure 33. ATG5 (left panel) and LC3II/LC3I (right panel) protein expression induced by incubation of tubular cells with homozygous' and controls' sera. Data are expressed as mean ± sem. Results were analyzed by paired T-test (P* <0.05). HOZ (N=4), CTRL (N=4)

The incubation of tubular cells with homozygous FLD carriers' sera increased the expression of both ATG5 and LC3II/LC3I (+42,9% *hoz vs ctrl*, p=0,027; +75,1% *hoz vs ctrl*, p=0,016 respectively), mirroring an enhancing autophagy activation probably as a compensatory response to the damage induced by lipoprotein abnormalities typical of LCAT deficiency in tubular cells.

WORKPACKAGE 3: Remodeling and effect of synthetic HDL in a murine model of LCAT deficiency: CER-001

3.1 CER-001 in vivo remodeling

The first part of the work was focused on the evaluation of the in vivo remodeling and metabolism of CER-00, a discoidal HDL composed of apoA-I, sphingomyelin and dipalmitoylphosphatidylglycerol (*Tardy et al., 2014*), in absence of LCAT. In order to evaluate this aspect, 2D electrophoretic analysis was performed on plasma collected basal condition, at 30 minutes, 1, 4 and 48 hours from the first injection and at the end of the treatment (figure 34).

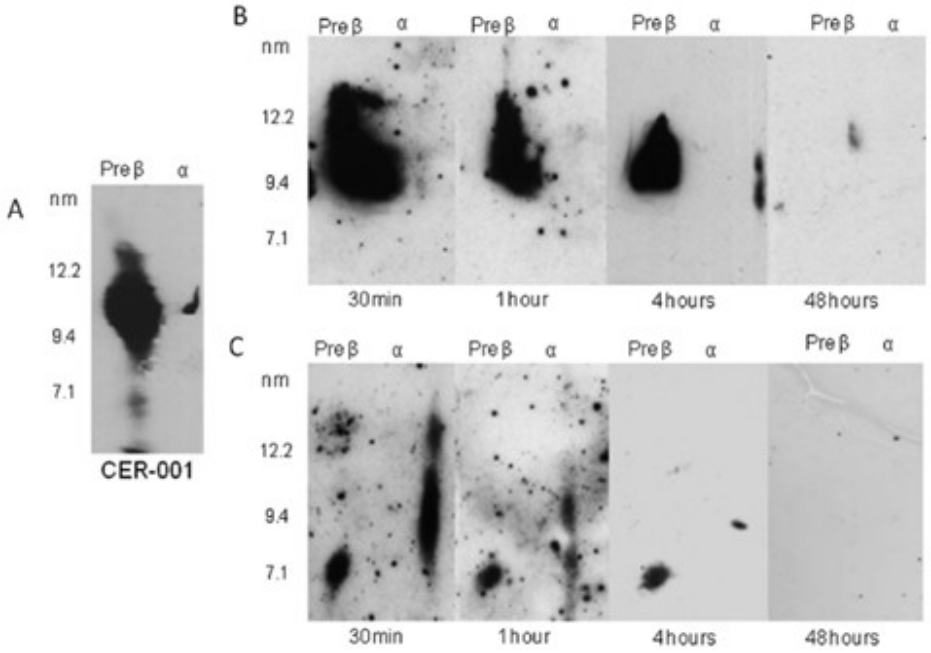

Figure 34. CER-001 in vivo remodeling. CER-001 (A) was injected at 10 mg/kg in WT (B) and *Lcat*$^{-/-}$(C) mice, and blood was collected after 30 min, 1, 4, and 48 h. HDL were separated by 2D-electrophoresis followed by immune-detection with an anti-human apoA-I antibody (Ossoli et al., 2021).

The signal of CER-001 identified the molecule as a large and discoidal particle migrating to the pre-β position (figure 34A).

The results of the 2D-electrophoresis in WT mice showed that the signal of CER-001, detected as as human apoA-I, was unchanged until 4 hours after administration and

disappeared within 48 hours (figure 34B), while in *Lcat*$^{-/-}$ mice the particle was just detectable in the pre-β and weakly α-position 30 min after the administration and disappeared completely 4 hours after injection (figure 34C) (*Ossoli et al., 2021*), probably because of a rapid execration of as they cannot mature.

To further investigate the fate of CER-001 and how the molecule influences the endogenous lipoprotein remodeling pathway in absence of LCAT, the 2D-electrophoresis was followed by an immunodetection with an antibody specific for murine apoA-I (figure 35).

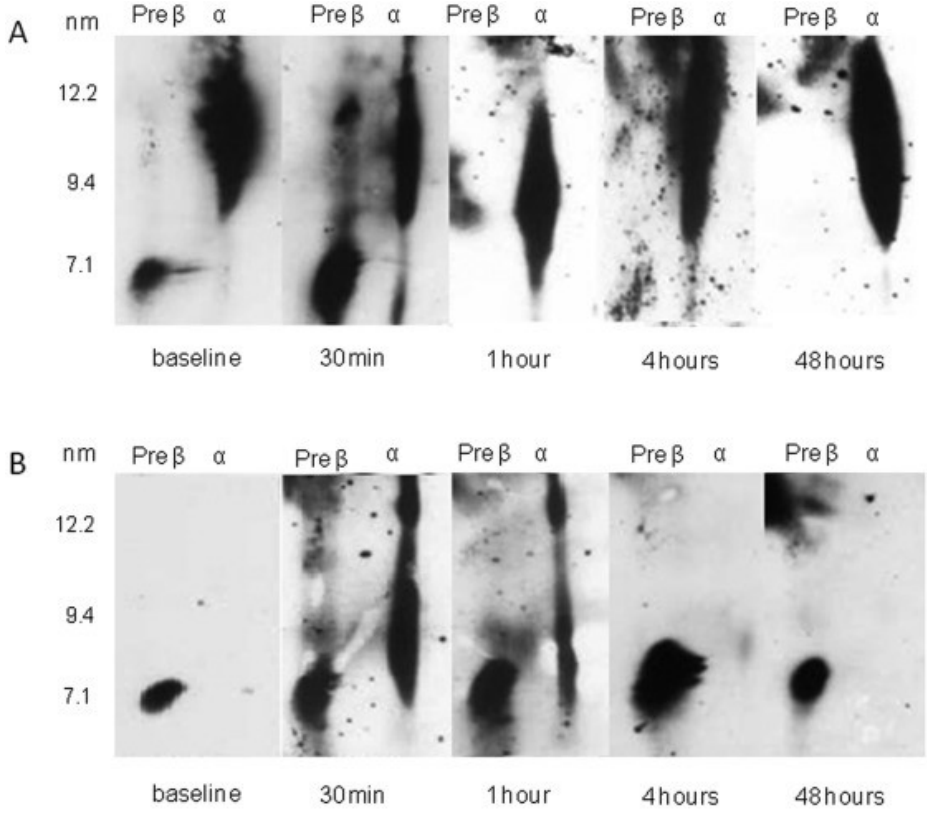

Figure 35. HDL subclass distribution after CER-001 treatment. HDL subclasses in WT (A) and *Lcat*$^{-/-}$ (B) mice treated with CER-001 at 10mg/kg (Ossoli et al., 2021).

The results showed that CER-001 enters in HDL remodeling pathways in different ways depending of the model; in fact, in WT mice, after 30 minutes from CER-001 injection, the majority of apoA-I signal was detectable in preβ position. However, after 1 hour, the signal in preβ disappeared, because of the LCAT-mediated maturation of the particles into α-HDL; after 4 hours and 48 hours, the signal in α position was still detectable and it was even shifted toward larger particles (figure 35A).

On the contrary, *Lcat*$^{-/-}$ mice at baseline presented the majority of apoA-I signal in preβ; until 1 hour after CER-001 injection in these animals, the murine apoA-I was detectable also in α position. The signal in preβ remained enhanced up to 4 hours, to return comparable to baseline after 48 hours (figure 35B). The signal in α position observed after the injection could not be due to the activity of LCAT, which in these mice is not expressed, but it was likely explained by surface lipid charge modifications induced by the interaction of phospholipids contained in CER-001 with murine apoA-I (*Davidson et al., 1994*).The quick return to the basal profile confirmed the rapid catabolic fate of the molecule in absence of LCAT. The fast metabolism of CER-001 was further supperted by the detection of the particle in the kidney and, to a lesser extent, in the liver after 30 minutes and 1 hour from the injection, while the signal disappeared completely after 24 hours later (Figure 36).

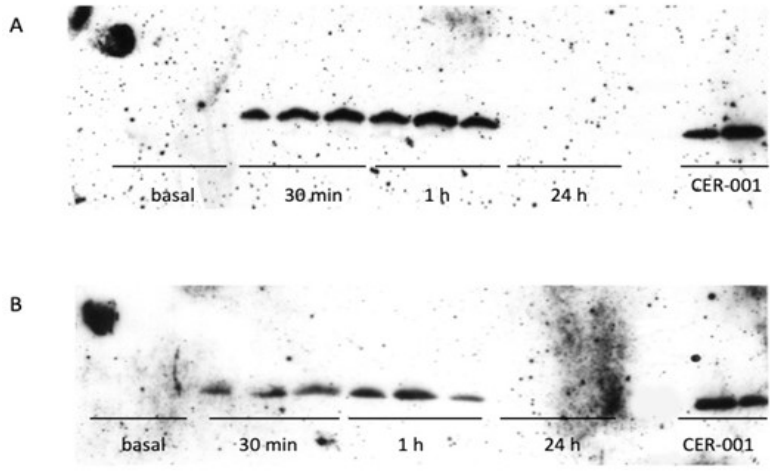

Figure 36. CER-001 catabolism. Western blot showing the signal of human apoA-I in kidney (A) and liver (B) of *Lcat*$^{-/-}$ mice collected at the basal, 30 minutes, 1 hour, and 24 hours after CER-001 administration. 200 µg of total protein was loaded in each lane. CER-001 (0.05 µg) was loaded as reference (Ossoli et al., 2021).

3.2 Effect of CER-001 treatment on lipid profile

The evaluation of the effects of CER-001 at different doses on plasma lipids in the absence or presence of LCAT is reported in table 18.

	Lcat$^{-/-}$					*C57Bl/6 wild-type*				
	Basal	**2.5 mg/kg**	**5 mg/kg**	**10 mg/kg**	**r; *P***	**Basal**	**2.5 mg/kg**	**5 mg/kg**	**10 mg/kg**	**r; *P***
TC (mg/dL)	31.1 (26.9–36.5)	23.1 (18.4–23.4)	21.9 (21.2–24.3)	24.4 (19.4–25.6)	−0.663; *0.003*	71.9 (69.0–73.0)	71.6 (68.2–73.0)	68.0 (67.9–104.7)	58.4 (56.3–68.9)	−0.406; *0.094*
HDL-C (mg/dL)	1.1 (0.4–1.4)	1.5 (1.2–3.9)	1.1 (1.0–1.5)	2.4 (1.6–3.1)	0.544; *0.019*	58.4 (54.6–63.2)	66.9 (63.8–69.6)	64.0 (63.5–75.4)	52.8 (52.7–64.4)	0.149; *0.567*
PL (mg/dL)	117.7 (101.7–145.1)	82.2 (78.4–91.1)	66.5 (55.2–72.5)	45.8 (43.6–51.8)	−0.803; *<0.001*	157.4 (141.4–176.0)	176.8 (166.8–211.1)	108.6 (103.4–143.2)	84.9 (68.9–85.7)	−0.590; *0.010*
TG (mg/dL)	135.5 (104.9–174.3)	126.8 (111.5–166.1)	116.3 (67.4–141.3)	42.2 (33.0–74.9)	−0.569; *0.014*	78.6 (64.5–132.9)	125.5 (113.1–144.8)	73.9 (38.8–94.8)	41.0 (33.4–55.4)	−0.436; *0.070*

Table 18. Lipid profile after CER-001 injections Data are expressed as median (interquartile range). Basal group $n = 9$, 2.5, 5 and 10 mg/kg $n = 3$ for each group. Spearman correlations between lipid concentration and CER-001 dose were performed, correlation (r) and *P* values are reported (Ossoli et al., 2021).

The results demonstrated that in *Lcat*$^{-/-}$ mice TC levels decreased at all doses in a dose-dependent manner and in parallel HDL-C levels increased significantly with an opposite trend. In WT mice, TC and HDL-C levels remained almost unchanged at all tested doses. Phospholipids concentration decreased significantly in both murine models with a dose-dependent way. Finally, triglyceride levels decreased significantly in *Lcat*$^{-/-}$ mice after the treatment with CER-001 in correlation with the dose administered; a similar trend was observed also in WT mice.

3.3 Effect of CER-001 on lipid and lipoprotein profile in a murine model of renal disease in LCAT deficiency

The second part of the work was focused on the evaluation of the effect of CER-001 on the renal disease associated with LCAT deficiency.

To achieve this aim, a mouse model of the disease was created, injecting *Lcat*$^{-/-}$ mice with exogenous LpX for one month, to induce the renal damage. After the end of the

LpX injections, mice were divided into two groups, one receiving CER-001 at 10 mg/kg three times a week for 4 weeks and one receiving the same volume of saline solution.

The lipid profile was evaluated at all the conditions, and the results are resumed in table 19:

	Basal	End LpX	End Saline	End CER-001 10 mg/kg	P values saline vs CER-001
TC (mg/dl)	24.6 (20.9–28.5)	32.8 (28.9–38.9)	30.8 (27.6–34.9)	30.0 (27.3–36.2)	0.952
HDL-C (mg/dl)	6.3 (4.9–7.3)	8.5 (7.6–9.9)	6.8 (5.8–8.7)	8.3 (7.7–10.4)	0.064
TG (mg/dl)	120.4 (80.1–175.0)	98.0 (59.7–162.7)	124.9 (64.9–173.8)	62.1 (36.9–93.1)	0.111
PL (mg/dl)	49.1 (44.2–68.9)	108.1 (61.7–137.6)	117.2 (99.7–127.3)	113.1 (92.0–136.8)	0.981

Table 19. Lipid profile after CER-001 treatment in a mouse model of renal disease. Data are expressed as median (interquartile range). For basal and LpX N= 10, for CER-001 and saline groups N= 6/9. Comparison between saline and CER-001 was analyzed by Wilcoxon rank-sum test (Ossoli et al., 2021).

As reported in the table, the treatment with CER-001 tended to increase the HDL-C concentrations and to reduce triglycerides compared to saline, confirming the ameliorative effect of the treatment observed in *Lcat*$^{-/-}$ mice without renal damage.

The analysis of HDL subclass at basal condition, after the end of LpX and at the end of treatment with CER-001 or saline did not show any significant difference in murine apoA-I distribution among the conditions (figure 37).

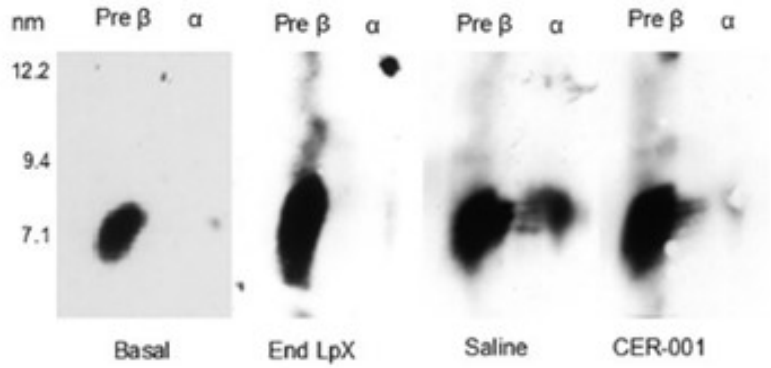

Figure 37. Representative images of HDL subclass distribution. 2D-electrophoresis followed by immunodetection of murine apoA-I at basal condition, at the end of LpX injections and after the treatment with CER-001 10 mg/kg or saline (Ossoli et al., 2021).

Lipoprotein profile was then evaluated by Fast Protein Liquid Chromatography (FPLC) (figure 38).

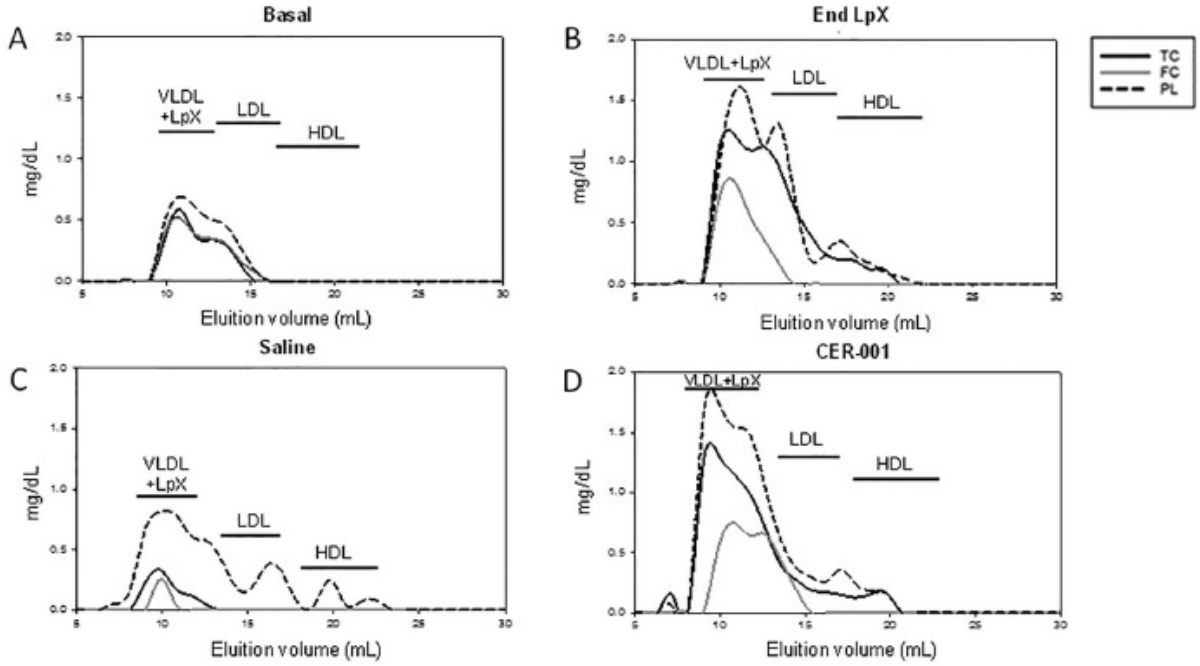

Figure 38. Lipoprotein profile after CER-001 treatment. Plasma of *Lcat*$^{-/-}$ mice (n=3) at basal condition (A), at the end of 4-weeks LpX injection (B), and after saline (C) or CER-001 treatment (Ossoli et al., 2021).

The comparison among the elution profile obtained highlighted the presence of a peak of phospholipids and cholesterol at the end of LpX injection (figure 38B) compared to basal (figure 38A), attributable to the LpX itself, which has the same size of VLDL and eluites in the same fractions of these lipoproteins.

After the end of saline injection, lipoprotein profile tended to return similar to the baseline (figure 38C), while on the contrary the peak was still detectable at the end of the treatment with CER-001, but it was shifted toward larger particles compared to the ones present after LpX injection (figure 38D).

3.4 CER-001 removes lipids accumulated in glomeruli after LpX injections

The ability of CER-001 to remove lipids from glomeruli was confirmed by Oil red-O staining on section of kidney from LpX-injected *Lcat*$^{-/-}$ mice; the treatment with CER-001 largely reduced the lipid droplets accumulation in glomeruli compared to saline injections (figure 39).

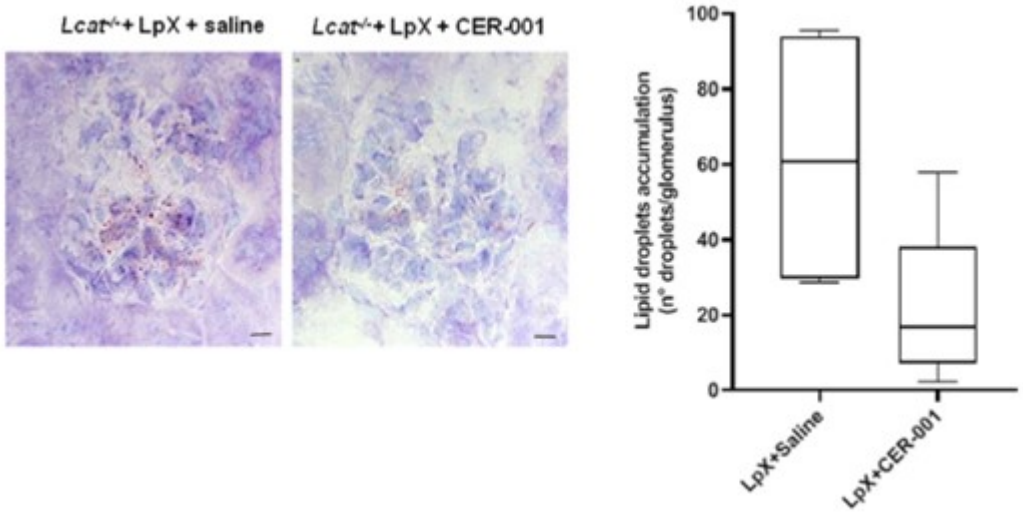

Figure 39. CER-001 limits the lipid accumulation in kidney. Images and quantification of lipid droplet accumulation after Oil Red O staining in the glomeruli of LpX-injected *Lcat*$^{-/-}$ mice after treatment with saline (n =4) or CER-001 at 10 mg/kg (n =6). Scale bars:10 µm. Box Plots indicate median, interquartile range and 5th-95th percentile and were analyzed using Wilcox on rank-sum test, P=0.069 (Ossoli et al., 2021).

The ability of CER-001 to remove lipids accumulated in glomeruli was further confirmed by an in vitro experiment, in which immortalized human podocytes were incubated with LpX and then treated with CER-001 at a concentration resembling the in vivo dose of 10 mg/kg or the same volume of saline solution (figure 40).

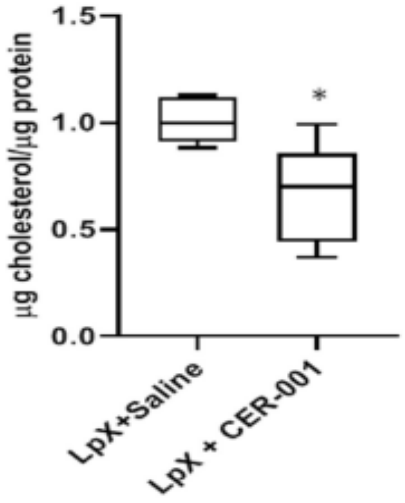

Figure 40. In vitro evaluation of CER-001 ability to remove intracellular cholesterol in podocytes loaded with LpX and treated with saline solution or CER-001 at a concentration corresponding to the 10 mg/kg dose. Box Plots indicate median, interquartile range and 5th– 95th percentile and were analyzed using exact Wilcox on rank-sum test,*P<0.05 (Ossoli et al., 2021).

The treatment with CER-001 significantly decreased the intracellular cholesterol content in podocytes compared to saline, confirming the particle ability to reduce lipid accumulation in kidney.

3.5 CER-001 treatment ameliorates the altered renal function in *Lcat*$^{-/-}$ mice

In order to evaluate whether the normalization of the lipid and lipoprotein profile and the reduction of lipid accumulation in glomeruli were associated with an amelioration of the renal function, urine albumin to creatinine ratio (ACR) was measured at basal condition, after LpX injection and at the end of treatment with CER-001 10 mg/kg or saline (figure 41).

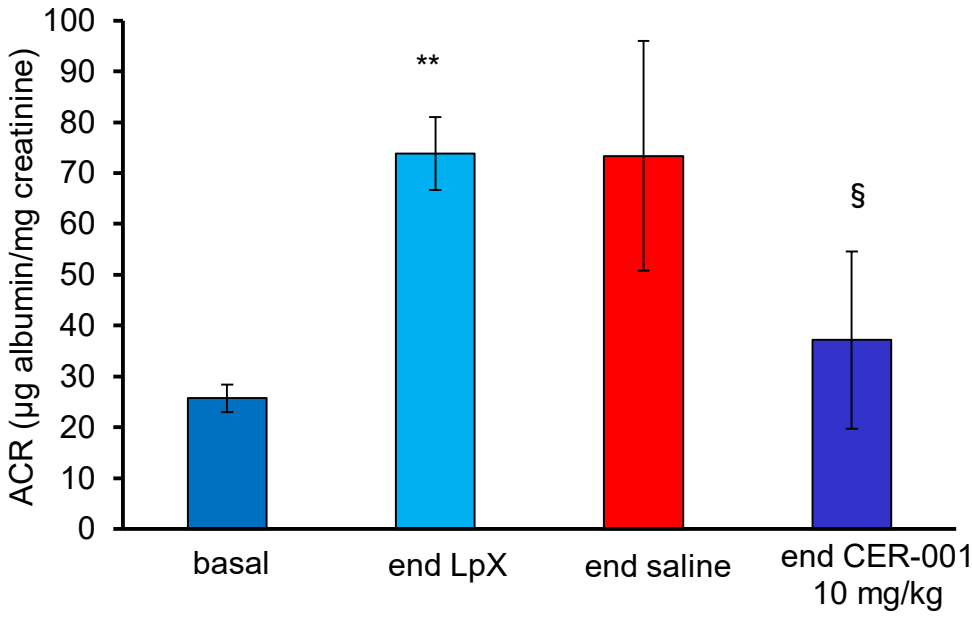

Figure 41. Albumin to creatinine ratio analyzed at basal, at the end of LpX injections and at the end of treatment with saline or CER-001 10 mg/kg. N= 10 for basal and LpX, n= 6/9 for CER-001 and saline groups. Data were analyzed by paired-T test **P<0.01 end LpX vs basal, while the comparison between saline vs CER-001 was analyzed using Wilcoxon rank-sum test § P<0.05 vs saline. (Adapted from Ossoli et al., 2021)

The results demonstrated that after the end of LpX injections, as expected, the ACR was significantly increased compared to basal condition (+145% *basal vs LpX*, p<0,001), confirming the induced impairment of renal function; interestingly, the treatment with CER-001 significantly reduced the ACR compared to saline injections (-71% *end saline vs CER-001*, p=0,034), demonstrating the role of CER-001 in ameliorating the renal function, compromised by LpX accumulation

Based on the anti-albuminuric effect observed after CER- 001 treatment, the evaluation of podocyte damage was assessed by measuring the expression of two key proteins for podocytes function: nephrin, which is an essential component of the slit diaphragm that maintains the slit pore integrity and renal filtration capacity (*Zoja et al., 2006; Martin et al., 2018*), and nestin, a cytoskeleton- associated filament protein also involved in the maintenance of normal podocyte function (*Michalczyk et al., 2005; Zoja et al., 2012*) (figure 42).

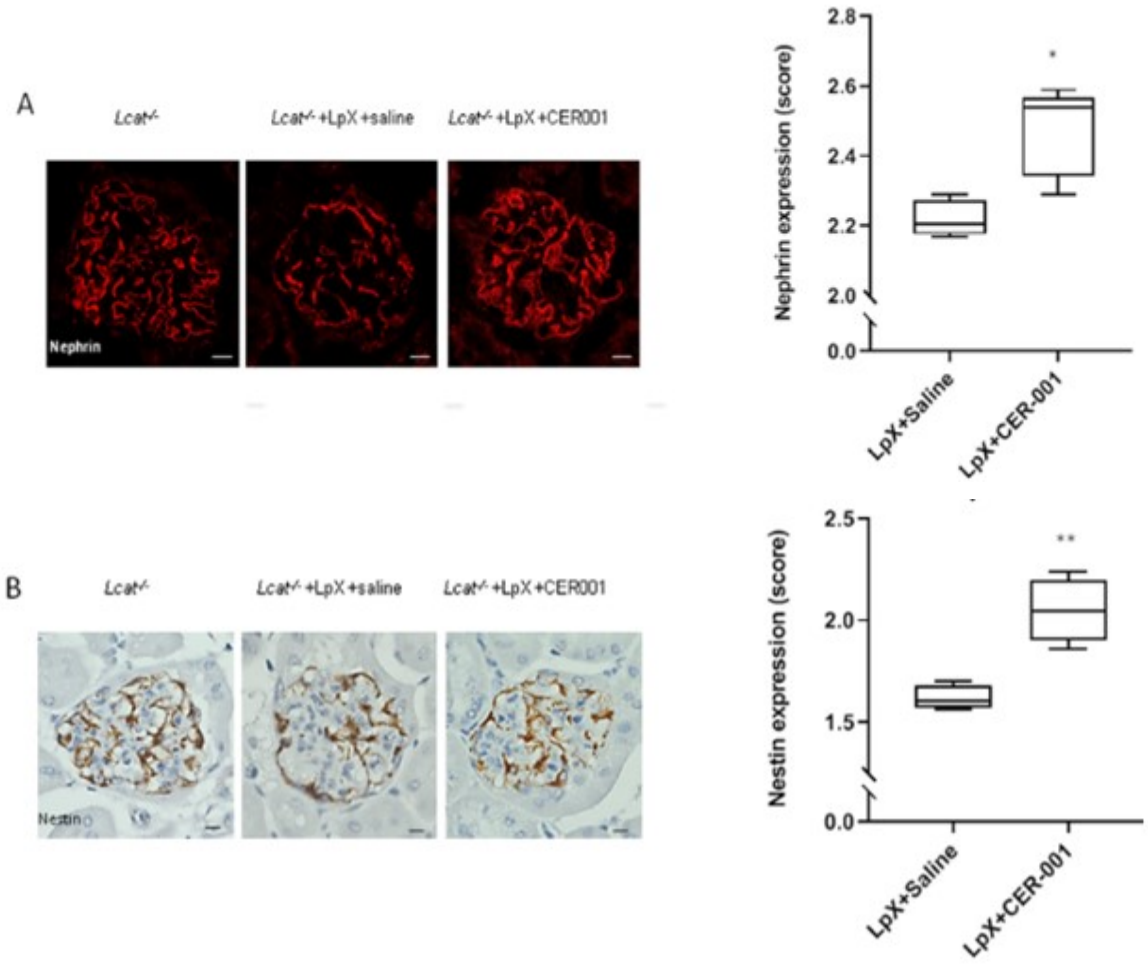

Figure 42. CER-001 limits podocyte dysfunction in LpX-injected *Lcat*$^{-/-}$ mice. Images and quantification of nephrin (A) and nestin (B) in LpX-injected *Lcat* $^{-/-}$ mice injected with saline (n=4) or CER-001 at 10mg/kg (n=6). Scalebars:10 µm. Box Plots indicate median and inter quartile range and 5th–95th percentile and were analyzed using exact Wilcox on rank-sum test, *P < 0.05 and **P<0.01 (Ossoli et al., 2021).

The results obtained showed that LpX-injected *Lcat*$^{-/-}$ mice treated with CER-001 at 10mg/kg presented a significantly increased nephrin (figure 42A) and nestin (figure 42B) expression compared to saline-treated mice. It is also important to underline that LpX saline-treated *Lcat*$^{-/-}$ mice exhibited a reduced intensity of the signal of nephrin and nestin compared to untreated *Lcat*$^{-/-}$ mice used as controls, indicating a podocytes function impairment induced by LpX.

3.6 CER-001 treatment in a FLD carrier: lipid removal from podocytes

These result set the basis for the potential use of CER-001 in FLD carriers; in fact, the beneficial use of the synthetic HDL on renal outcome was recently described in a case report of a French FLD carrier (*Faguer et al., 2021*), but with unknown mechanisms.

Thus, in this part of the work, in vitro studies were performed in order to assess the effect of CER-001 at cellular level in a FLD carrier from the Italian cohort (*Calabresi et al., 2005*)

To evaluate the effect of CER-001-induced plasma lipoprotein remodeling, podocytes were incubated with 2% of serum collected at basal condition (before the beginning of the treatment), after 3, 6 and 12 weeks (end of treatment, EOT) and the intracellular content was measured (figure 43).

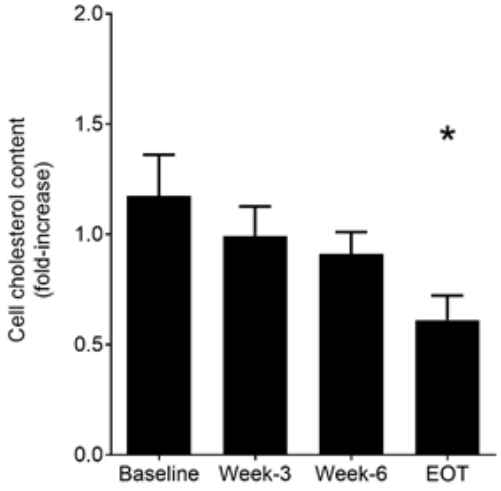

Figure 43. CER-001 limits cholesterol deposition in cultured podocytes through lipoprotein remodeling. Data are presented as mean ± sem. Podocytes were incubated with plasma from patient collected at different time-points. Data were analyzed by one- way ANOVA for repeated measures followed by Bonferroni's post hoc test. (*p<0.05 vs baseline).

The intracellular cholesterol content was progressively reduced with a time-dependent trend of treatment, reaching the significancy at the end of treatment compared to basal condition (-48,7% *EOT vs baseline*, p<0,05) and conferming that CER-001 influences the remodeling of the endogenous lipoproteins. The following

step was to assess the direct effect of CER-001 on LpX-induced deposit in glomeruli. Podocytes were incubated with FLD carrier's basal serum, which is enriched of LpX, and then treated with CER-001 in a concentration that resemble the in vivo dose of 10 mg/kg or the same volume of saline solition (figure 44).

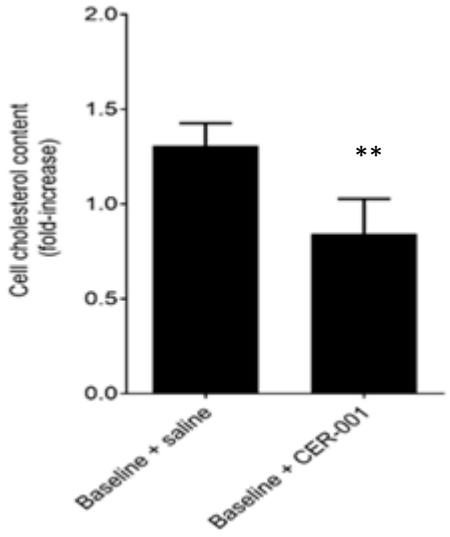

Figure 44. CER-001 limits cholesterol deposition in cultured podocytes by direct cholesterol efflux. Podocytes were incubated with patient's plasma and then treated with saline solution or CER-001. Data are presented as mean ± SD. Data were analyzed by paired Student's t-test. (**p<0.01 vs saline).

The results obtained showed a significant reduction of the intracellular content in podocytes after the incubation with CER-001 compared to saline (-35,8% *saline vs CER-001*, p=0,001), confirming the direct action of the synthetic HDL in favoring the cholesterol efflux.

.

WORKPACKAGE 4: Acquired LCAT deficiency in general population

4.1 Subjects' characteristics at basal visit

To determine whether LCAT concentration could be a predictor of the impairment of kidney function in the general population, 165 subjects with basal eGFR over 60 mL/min/1.73 m^2 were selected among the PLIC study cohort and followed for up to 84 months (*Baragetti et al., 2020)*.

The cohort was divided into three tertiles according to plasma LCAT concentration at the baseline (table 20); subjects in the 1st tertile presented a reduced enzyme concentration, with a median value of 3.89 µg/mL (3.34–4.21), while individuals in the 3rd tertile had normal to high LCAT concentration (6.01 µg/mL (5.00–6.34)); subjects in 2nd tertile presented normal values, with a median of 4.82 µg/mL (4.67–5.09).

	LCAT TERTILES			
LCAT (µg/mL) Mean (Range)	**1st (n = 54) 3.89 (3.34–4.21)**	**2nd (n = 56) 4.82 (4.67–5.09)**	**3rd (n = 55) 6.01 (5.00–6.34)**	***p* trend**
Age (years)	69 (66–73)	67 (65–72)	69 (66–72)	0.742
Gender (men, n (%))	26 ± 48.1	27 ± 48.2	27 ± 49.1	0.994
BMI (kg/m^2)	26.49 (24.37–29.15)	25.85 (24.16–29.25)	26.33 (24.86–28.07)	0.949
eGFR (mL/min/1.73 m^2)	68.71 (63.78–74.67)	68.14 (63.74–74.36)	66.52 (62.02–72.05)	0.178
TC (mg/dL)	223.4 ± 48.7	237.2 ± 45.9	237.8 ± 38.8	0.112
TG (mg/dL)	96.5 (73.2–131.0)	98.0 (76.0–133.2)	84.0 (61.0–106.0)	*0.039**§
LDL-C (mg/dL)	142.0 ± 42.9	157.5 ± 43.0	158.9 ± 36.1	0.080
HDL-C (mg/dL)	54.5 (48.0–67.2)	55.0 (48.2–61.7)	59.0 (51.0–68.0)	0.209

ApoA-I (mg/dL)	152.3 ± 21.9	151.0 ± 23.9	157.7 ± 21.1	0.160
ApoB (mg/dL)	115.4 ± 37.3	126.6 ± 36.9	127.4 ± 31.0	0.111

Table 20. Lipid profile of subjects from the PLIC cohort. Data are reported as mean±SD or median (Interquartile range, as the range between the 25th and the 75th percentile around each median value). (*p < 0.05 vs. 1st LCAT tertile; § p < 0.05 vs. 2nd LCAT tertile) (adapted from Baragetti et al., 2020)

As reported in Table 17, the mean value of eGFR at baseline did not differ significantly among the three groups; moreover, the analysis of the lipid and the lipoprotein profile showed that the concentration of HDL-C, LDL-C, apoA-I and apoB did not present any differences, with the exception of triglycerides concentration, which was significantly reduced in the 3rd tertile (high LCAT) compared to the other two groups.

4.2 Annual EGFR reduction

In order to assess whether reduced LCAT concentration is predictive for faster eGFR reduction in general population, the annual eGFR reduction, calculated as the difference between the eGFR at the follow up and at the baseline, was plotted according to LCAT tertiles at baseline (figure 45):

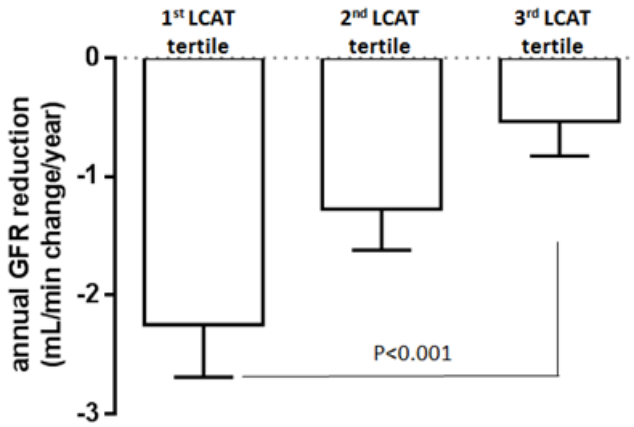

Figure 45. Low plasma LCAT concentration predicts fast renal function decline in the general population. Bar plots showing changes in GFR (annual variation between GFR at basal evaluation and GFR at follow-up) by LCAT tertiles. P<0.001 indicates post-hoc significant difference between the 1st and the 3rd LCAT tertile (adapted from Baragetti et al., 2020)

The results clearly showed that subjects in the 1st tertile, with a reduced LCAT concentration in basal condition, presented a significantly faster progression of kidney impairment compared to subjects in the 3rd tertile, presenting higher LCAT concentration at the baseline This fundamental result demonstrates the importance of LCAT concentration in predicting the onset of renal disease in general population.

4.3 Serum from subjects with low LCAT concentration induces ROS production in renal cells and rhLCAT reduces serum pro-oxidative effect

In order to establish whether low plasma LCAT concentration can induce renal cellular damage before the occurrence of changes in kidney function and to identify possible molecular mechanisms, in vitro studies on podocytes and tubular cells were performed.

Sera from a representative group of subjects from the PLIC cohort belonging to the 1st LCAT tertile (*n* = 11) and to the 3rd LCAT tertile (*n* = 11) were used to incubate renal cells to evaluate serum-mediated podocin expression in podocytes and ROS production in both cell lines. In table 18, the characteristic of subjects used for the in vitro study are summarized (table 21):

	1st LCAT tertile	3rd LCAT tertile	P value
N total	11	11	
Age (years)	68 ± 6	68 ± 3	1.000
Gender (men, n,(%))	5 (45)	4 (36)	1.000
BMI (Kg/m^2)	26.12 ± 2.86	27.12 ± 1.44	0.313
LCAT mass (μg/ml)	2.94 ± 0.44*	6.01 ± 1.00*	*<0.001*
eGFR (mL/min/1.73 m^2)	70.40 ± 5.74	68.42 ± 5.12	0.403
TC (mg/dL)	239.6 ± 57.4	241.1 ± 38.6	0.943
UC (mg/dL)	51.3 ± 12.3	46.4 ± 10.1	0.403

UC/TC	0.21± 0.01*	0.19 ± 0.03*	*0.022*
TG (mg/dL)	116.7 ± 60.8	80.8 ± 43.7	0.127
LDL-C (mg/dL)	160.5 ± 51.6	161.4 ± 38.7	0.964
HDL-C (mg/dL)	55.8 ±13.2	63.5 ± 12.8	0.180
ApoA-I (mg/dL)	146.7 ± 22.5	161.1 ± 16.6	0.103
ApoB (mg/dL)	130.3 ± 47.1	126.1± 25.5	0.797
Pre-β HDL (% of total apoA-I)	22.4 ± 4.9*	15.9 ± 5.8*	*0.015*

Table 21. Characteristics of subjects enrolled in the in vitro studies. Data are expressed as mean±SD. Data were analyzed with paired-T test (*p<0,05 vs 3r^{d} tertile)(adapted from Baragetti et al., 2020).

The two groups presented significant differences, in particular an increase of UC/TC ratio and percentage of preβ-HDL in subjects from 1st tertile compared with 3rd tertile, in line with the reduction of LCAT concentration in this group.

The podocytes incubation with serum of subjects in 1st LCAT tertile induced a marked reduction of podocin expression compared to serum from subjects in the 3rd LCAT tertile (-53,2% *1st tertile vs 3rd tertile*, p<0,05), suggesting a reduction in podocyte functionality under low LCAT concentration conditions (figure 46).

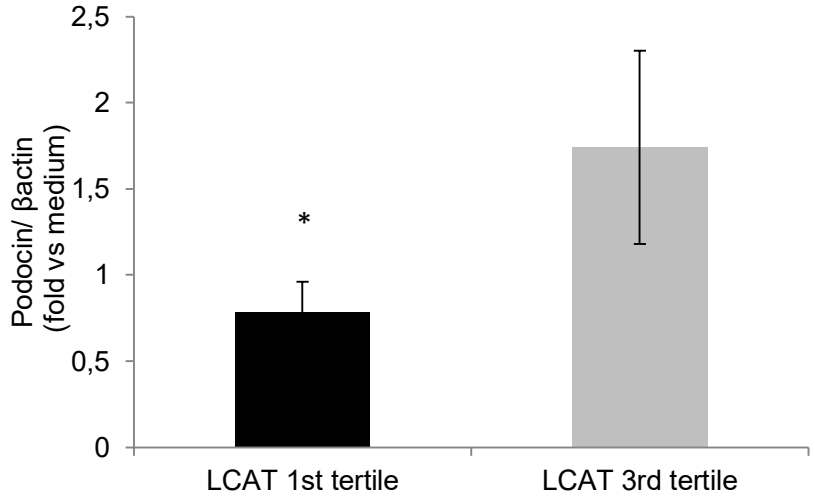

Figure 46. Podocin expression after incubation of podocytes with sera from subjects of the 1st LCAT tertile and 3rd LCAT tertile. Data are expressed as mean ± SD. Data were analyzed by paired-T test (*p<0.05 vs LCAT 3rd tertile) (adapted from Baragetti et al., 2020)

In parallel, the incubation of renal cells with serum of subjects in 1st LCAT tertile increased significantly ROS production compared to serum from subjects in the 3rd LCAT tertile, both in podocytes (figure 47a) and in tubular cells (Figure 47b).

To assess whether the increased oxidative stress in both cell lines was due to low LCAT concentration, serum from subjects in the 1st LCAT tertile was incubated with recombinant human LCAT (rhLCAT), in order to restore a concentration of the enzyme comparable to the subjects' one in the 3rd tertile. The proper HDL remodeling after incubation with rhLCAT was confirmed from the significant reduction of unesterified/total cholesterol ratio and significant 50% reduction in preβ-HDL percentage compared to non-incubated sera (table 22).

	-rhLCAT	+rhLCAT	P value
N	**11**	**11**	
TC(mg/dL)	239.6 ± 57.4	239.4 ± 58.2	0.992
UC (mg/dL)	51.3 ± 12.3	44.1 ± 10.3	0.152
UC/TC	0.21 ± 0.01*	0.19 ± 0.02	<0.001
LDL-C (mg/dL)	160.5 ± 51.6	158.8 ± 51.8	0.940
HDL-C (mg/dL)	55.8 ± 13.2	57.0 ± 13.5	0.833
Non-HDL-C (mg/dL)	183.8 ± 51.0	182.4 ± 51.5	0.948
TG (mg/dL)	116.7 ± 60.9	117.2 ± 60.6	0.985
ApoA-I (mg/dL)	146.7 ± 22.5	147.1± 22.7	0.968
ApoB (mg/dL)	130.3 ± 47.0	128.9 ± 46.8	0.948
Pre-β HDL (% of total apoA-I)	22.4 ± 4.9*	11.0 ± 1.4	0.004

Table 22. Lipid profile after incubation of plasma with or without rhLCAT. Data are expressed as mean ± SD. Data were analyzed with paired-T test (*p<0.05 vs +rhLCAT). (adapted from Baragetti et al., 2020).

The incubation of sera from subjects in the 1st tertile with rhLCAT led to a reduction in serum-mediated ROS production in podocytes to a level similar to the one observed

with sera from 3rd LCAT tertile subjects (figure 47a) in both cell lines, with a more evident effect in tubular cells (figure 47b).

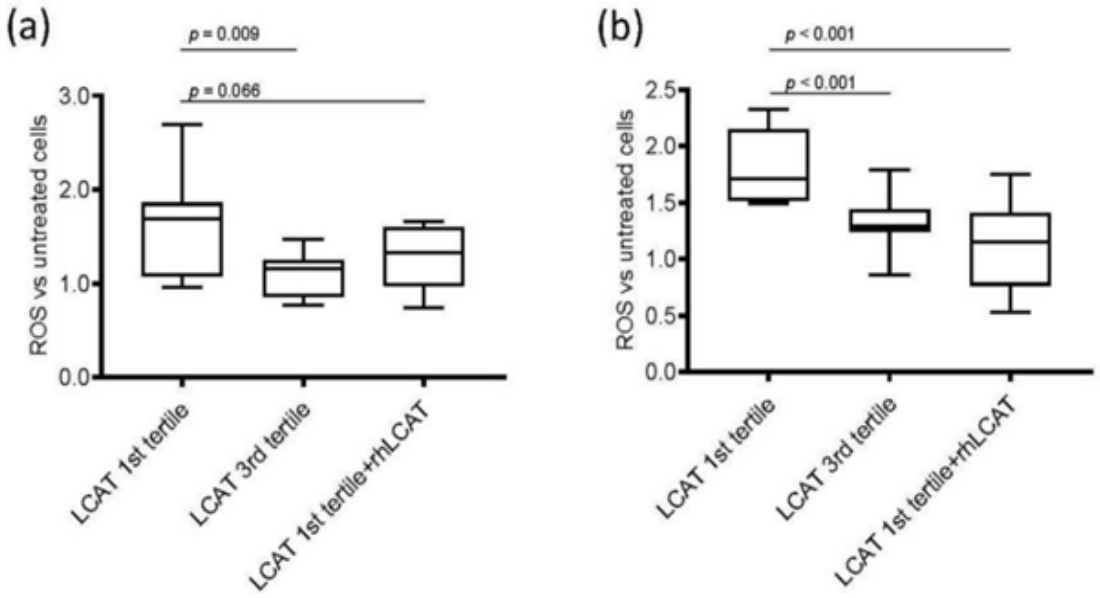

Figure 47. **Oxidative stress in renal cells**. Data are presented as box-plots indicating median and 10th–90th percentile around the median. p-values were calculated the Kruskall–Wallis test for comparison between each group. (Baragetti et al., 2020).

Taken together, the results collected in the last part of the work highlight the relevance of compromised plasma cholesterol esterification renal damage and kidney function impairment in general population.

DISCUSSION

Familial LCAT deficiency (FLD) is a rare genetic disease characterized by the total inactivity of lecithin:cholesterol acyltransferase (LCAT), which is the only enzyme that esterifies cholesterol in plasma. The typical lipid and lipoprotein profile of carriers presents a reduction of HDL-C concentration with an increase of free cholesterol and a variable hypertriglyceridemia; moreover, plasma lipoprotein profile is characterized by typical alterations, including the accumulation of small and discoidal preβ-HDL particles, as well as the presence of LpX, an abnormal lipoprotein mainly composed of phospholipids and free cholesterol (*Boscutti et al., 2011; Santamarina-Fojo et al., 2001*).

Despite what is already known, many aspects of this pathologic condition need further investigation, including the deep characterization of plasma and lipoproteins of FLD carriers, the identification of the nephrotoxic pathways involved in the onset of renal disease, the potential treatments and the evaluation of the impact of a non-genetic LCAT reduction on the worsening of renal function. Thus, aim of the work was to analyze these unknown aspects about the kidney disease in LCAT deficiency.

The first part of the project was focused on the composition and function of carriers' HDL, with the aim of achieving a complete insight of plasma and lipoprotein alterations in these subjects. To this aim, a sub-group of LCAT deficient carriers (homozygous and heterozygous) and healthy subjects was selected from the Italian cohort; the cholesterol esterification system and the lipid and lipoprotein profile of the LCAT deficient subjects were representative of the typical alteration of the disease (*Calabresi et al., 2005*). All the homozygous patients presented corneal opacity and anemia, which are the most common symptoms, and, except for one, all of them showed serious renal impairment and underwent to renal transplantation. Interestingly, the carrier of Val309—Met mutation presented also the cardiovascular disease. This outcome was observed also in another unrelated carrier of the Italian cohort presenting the same mutation. The cardiovascular disease typically does not affect FLD carriers, because despite the reduction of HDL cholesterol, cholesterol efflux is favored by the preβ-HDL, that are best acceptors through ABCA1 (*Favari et al., 2004*). The ABCA-1-efflux process in the carriers of Val309—Met mutations was

enhanced as in all the homozygous carriers, thus the cardiovascular disease was not due to alterations in the substrate but in some intrinsic activity of LCAT, as the anti-oxidant one (*McPherson et al., 2007; Vohl et al., 1999*).

It has been demonstrated that also extremely high HDL-C concentrations are responsible for an elevated cardiovascular risk, resulting in a U-shape relationship between HDL-C and cardiovascular disease (*Madsen et al.2017*). Recently, Feng et al demonstrated that the ability of HDL to transfer free cholesterol, but not phospholipids, upon TGRL lipolysis seems to inversely underlying this U-shape relationship, suggesting a potential link among HDL-C, triglyceride metabolism and atherosclerosis (*Feng et al., 2020; Feng et al., 2021*). This peculiar activity of HDL in LCAT deficient carriers was never evaluated before and it has been tested in this work. The HDL-mediated transfer of free cholesterol upon TGRL lipolysis did not present any significant differences among homozygous, heterozygous and controls, despite the low level of HDL in LCAT deficient carriers. This result is in line with what previously published by Feng et al., in which the exogenous inhibition of LCAT led to an enhanced transfer from TGRL and accumulation of unesterified cholesterol on HDL, impairing the exchange of cholesteryl esters via CETP to TGRL for the subsequent esterified cholesterol elimination. The genetic defect of LCAT confirmed the accumulation of unesterified cholesterol despite the low level of HDL-C concentration, highlighting the link between the reverse cholesterol transport (RCT) and reverse remnant-cholesterol transport (RRT). Moreover, the capacity of HDL to acquire phospholipids in carriers of LCAT gene mutations resulted impaired; according to literature, HDL concentration represents a major determinant of phospholipid transfer from TGRL to HDL upon lipolysis, while LCAT activity does not influence this process; the collected data are therefore consistent with this view (*Feng et al.,2021*).

LCAT is a key enzyme for metabolism and correct maturation of HDL, thus it is not surprising that genetic defect of the protein is associated to deep alterations in HDL composition, enhanced in case of homozygosis. LCAT catalyzes the reaction between a phospholipid and unesterified cholesterol to produce lysophospholipid and esterified cholesterol, through two different activities: phospholipase A2 and the

acyltransferase activity. The first one is responsible for the cleavage of the fatty acid in sn2 position of the phospholipid and its transfer to Ser181 on the enzyme generating lysophospholipid, while the acyltransferase activity permits the fatty acid transesterification to the free 3-β-hydroxyl group of cholesterol, forming cholesteryl esters (*Jonas, 2000*).

The lipidomics analysis of the main polar lipid classes in HDL of homozygous FLD carriers highlighted an accumulation of phosphatidylethanolamine (PE), an important structural phospholipid that accounts for approximately 1 wt% of HDL lipids and that is a substrate of LCAT with a very high affinity for the enzyme (*Pownall et al., 1985; Kontush et al., 2013*). In line with the inactivity of LCAT, a strong depletion of lysophosphatidylehanolamine sn2 (LPEsn2), the preferential product of the LCAT reaction, was observed. On the contrary, the amount of LPEsn1, a very minor species which does not derive directly from the LCAT reaction, tended to increase. This result could be potentially explained by the increased activity of other lipases, such as PAF-AH, that in FLD carriers' plasma is slightly higher than in normal plasma (*Itabe et al., 1999*).

Phosphatidylcholine (PC) is the principal plasma phospholipid in HDL and it is one of the main LCAT substrates; however, despite the key role of this lipid in the LCAT reaction, the total abundance of PC and of its products lysophosphatidylcolines sn1 and sn2 (LPCsn1 and LPCsn2) was not modified in LCAT deficient carriers' HDL. LPC represent a quantitatively important subclass of phospholipids in HDL and it is particularly abundant on HDL for the predominance of LCAT reaction on these lipoproteins (*Kontush et al., 2013*). Plasma LPC are mainly generated by the action of secretory phospholipases A2 (sPLA2) (*Fuchs et al, 2009*), by the action of endothelial and hepatic lipase on lipoproteins and during lipoprotein oxidation (*Knuplez et al., 2020*). Moreover, despite being a product of LCAT reaction, LPC can also represent a substrate for another enzyme activity; in fact LCAT reacylates a certain amount of LPC (*Czarnecka et al., 1993*). This process on HDL is substantial and requires the presence of LDL, probably as donors of the acyl group (*Subbaiah et al., 1980*).

Despite quantitative alterations in total PC and LPC were not observed, the fatty acids distribution in the substrates and products of the LCAT reaction was significantly

affected by the lack of the enzyme; indeed, homozygous LCAT mutants' HDL were enriched in short and saturated lipids (mainly in PC and PE classes) and depleted in polyunsaturated fatty acids (PUFA), more specifically ω6 fatty acids mostly in PC species. In PE and PC classes, PUFA depletion seems to affect mainly the species presenting the longer and/or more unsaturated lipid chains. Modifications in fatty acids distribution, especially in PC, can alter the surface lipid monolayer fluidity of HDL, which is influenced by the ratio of saturated and monounsaturated fatty acids (to PUFA); decreasing relative content of PUFA can diminish the fluidity of the surface lipid monolayer of HDL, leading to the loss of some HDL properties, like the anti-oxidant one (*Kontush et al., 2013*).

The results obtained through the lipidomics analysis clearly highlighted a depletion in a minor class, PE plasmalogens (PEp), that are present in HDL at approximately 1 wt % of lipid; these phospholipids exert anti-oxidative properties (*Kontush et al., 2013; Maeba et al., 2003),* thus a decrease of PEp can be associated to a loss of anti-oxidant activity of HDL.

Other minor phospholipids classes, such as phosphatidylserine (PS) and phosphatidylinositol (PI), presented alterations in fatty acids distribution, including the enrichment in saturated fatty acids in PS and PUFA depletion in PI.

Sphingolipids analysis highlighted a strong increase in dihydroceramide (DHC) and ceramides in FLD carriers' HDL. LCAT reaction does not employ directly sphingolipids, but it can be influenced by sphingomyelin, which is an inhibitor of the enzyme (*Subbaiah et al., 1993).* A potential explanation of this compositional alteration can be likely found in the catabolism of ceramides at cellular level, that could be impaired in case of renal disease (*Yokota et al., 2021*), frequently associated with LCAT deficiency; the products of the process are PE and fatty aldehyde (*Harayama et al., 2018*), and it is possible that the reaction can be sensitive to product inhibition effect, leading to the accumulation of the DHC and ceramides in renal cells. HDL could acquire DHC and ceramides that are stored in the renal cells as a protective mechanism, explaining the enrichment of these lipids in the particles, which, after the plasma remodeling in absence of LCAT, tend to re-accumulate in the kidney, increasing the renal damage in a vicious circle. Indeed, ceramides and DHC

accumulation is associated to an increased cell death by enhancing the pro-apoptotic and pro-autophagic effects and reducing the cellular growth (*Hannun et al., 2018*).
The majority of alterations observed in FLD carriers' HDL can be found in a lesser extent also in the plasma of these subjects, even if these effects are obviously influenced by the dilution and the other lipoproteins composition. Contrary to what observed in HDL, also the amount of PC in plasma was slightly but significantly increased and the LPC classes showed a decreasing trend in homozygous, as expected by the absence of LCAT; the results confirmed that the main substrates (PC and PE) and the main products (LPE and LPC, particularly sn2) of the LCAT reaction are altered in LCAT deficiency. An analogue result in plasma was observed in patients with an acquired LCAT defect (*Gillette et al., 2001*). The reduction in total PEp was also found in plasma, consistent with the specificity of this lipid class for HDL. Plasma from homozygous carriers, moreover, presented a reduction in total SM content, a strong LCAT inhibitor, and deep alterations similar to the ones observed in homozygous carriers' HDL, including above all the depletion of long and polyunsaturated chains in the major lipid classes, such as PC, PE and LPC.
Finally, the measurement of total esterified cholesterol showed a strong depletion of all the cholesteryl esters species in both HDL and plasma from homozygous FLD carriers, consistent with the total inactivity of LCAT in these subjects.
The results collected within this aim demonstrated that the lack of LCAT can largely impact on HDL and plasma lipid composition, affecting both the quantity and the quality of the fundamental polar lipids classes. Moreover, these alterations can potentially account for the harmful effect of HDL at renal level in genetic LCAT deficiency.

The second part of the work was focused on the investigation of molecular mechanisms underlying the onset of renal disease in genetic LCAT deficiency.
The renal damage associated to LCAT deficiency is characterized by focal segmental glomerulosclerosis (FSGS). Lipid deposits are responsible for the vacuolization of glomerular basement membrane with the typical "foamy" appearance and the lipid analysis of isolated glomeruli showed a markedly higher amount of unesterified

cholesterol (*Boscutti et al., 2011*). ROS production has been associated to podocyte damage in several in vitro models, including diabetic nephropathy, membranous nephropathy, minimal change disease and FSGS (*Chen et al., 2013*). Moreover, the accumulation of non-esterified fatty acids in kidney in chronic kidney disease (CKD) is especially harmful for podocytes and proximal tubular epithelial cells, by boosting the production of ROS and lipid peroxidation (*Gai et al., 2019*). As some of these pathologic conditions affect also LCAT deficient subjects (*Boscutti et al., 2011*); ROS production was evaluated in podocytes; the increased oxidative stress induced by LDL and HDL fractions of homozygous carriers, which contain LpX and preβ-HDL respectively, confirmed that lipoprotein abnormalities induce an oxidative damage at glomerular level. The loss of HDL anti-oxidant propriety can potentially be explained by the depletion of PUFA in phospholipids (PE and PC), that can disrupt lipid monolayer fluidity of HDL and consequently affect this function, as well as the depletion of the anti-oxidant PEp observed in carriers' lipoproteins (*Kontush et al., 2013*).

Subjects affected by glomerulopathy usually present a reduced expression of podocin and synaptopodin, fundamental molecules for the correct ultrafiltration process as they are involved in the maintenance of slit-diaphragm function, which is the main unit of the ultrafiltration barrier (*Haraldsson et al., 2008*); mutations on the genes codifying for these proteins have been identified in several families with autosomal recessive FSGS, in most of familial nephrotic syndromes with recessive inheritance and in HIV-associated nephropathy (*Caridi et al., 2005; Yu et al., 2016*). The expression of podocin and synaptopodin resulted reduced in podocytes incubated with LDL and HDL from homozygous FLD carriers, suggesting that lipoprotein abnormalities can directly cause an impairment of the ultrafiltration process. Finally, the evaluation of apoptosis demonstrated that homozygous FLD carriers' serum induced renal damage by increasing cell death and podocytes depletion; this result was in line with what previously observed in primary and secondary forms of FSGS, in which the depletion of podocytes represents the central manifestation of chronic progressive glomerular diseases. The increased apoptosis could be explained by the enrichment of carriers' HDL of DHC, known to act as a pro-apoptotic factor (Hannun et al., 2018); apoptosis

in podocytes could be mediated by TGF-β1 and Smad7, as demonstrated at early stages in the course of progressive glomerulosclerosis, or due to CD36-mediated ROS production associated with lipid accumulation, like in diabetic nephropathy (*Schiffer et al., 2001; Hua et al., 2015*).

Despite the glomerular damage that characterizes renal disease in LCAT deficiency, the presence of tubular alterations in carriers of FLD has been described too (*Stoekenbroek et al., 2013*).

Oxidative stress can directly affect also tubular cells in acute kidney injury and in tubule-interstitial fibrosis, inducing the production of renal pro-oxidant enzymes with an excessive generation of ROS and accumulation of dityrosine-containing proteins (*Duann et al., 2016; Duni et al., 2019*). The evaluation of ROS production induced by LDL and HDL from homozygous FLD carriers revealed an oxidative damage at tubular level mediated by lipoproteins of these subjects.

Oxidative stress is closely linked to the activity of mitochondria, of which the cytoplasm of tubular cells is enriched because of the high energy request derived from the active reabsorption process. Mitochondria are the main source of ROS production and, physiologically, undergo to constant fusion and fission processes, important for the stress mitigation and for the removal of damage organelles to facilitate apoptosis (*Vakifahmetoglu-Norberg et al., 2017*). ROS production could origin from mitochondria dysfunction and it has been demonstrated that oxidative stress induces mitochondrial fission in tubular cells, activating the pro-apoptotic pathway (*Sun et al., 2020; Tait et al., 2013*). Data collected from the evaluation of these processes showed an increase in fusion proteins expression and an enhanced expression of the fission protein MFF induced by homozygous FLD carriers' sera. MFF is a mitochondrial outer-membrane receptor for DRP1 (*Toyama et al., 2016*), which can be responsible for mitochondrial oxidative stress, increasing mPTP opening, to finally start mitochondria-dependent cellular apoptosis (*Sheng et al.,2018*). The higher expression of these genes could potentially mirror an alteration in mitochondria normal function mediated by lipoprotein abnormalities contained in homozygous FLD carriers' sera, resulting also into an enhanced apoptotic process, in concert with the enrichment in ceramides amount of FLD carriers' HDL.

In tubular cells, after acute kidney injuries characterized by oxidative stress and mitochondrial dysfunction, autophagy acts protecting from apoptosis, stimulating cellular regeneration. Moreover, also the enrichment of carriers' HDL in DHC can stimulate this mechanism (*Hannun et al., 2018*); the process resulted enhanced after the incubation of tubular cells with homozygous FLD carriers' sera, probably as a protective mechanism unable to contrast the tubular damage (*Lin et al., 2019*).

As previously anticipated, no effective therapies are available for FLD carriers. Among the specific approaches under investigation, synthetic HDL are biological drugs currently under development to treat cardiovascular diseases.

CER-001 is a discoidal HDL composed of apoA-I, sphingomyelin and dipalmitoylphosphatidylglycerol (*Tardy et al., 2014*). This formulation has already been tested in several clinical trials in patients with acute coronary syndrome (*Andrews et al., 2017; Kataoka et al., 2017*), familial hypercholesterolemia (*Hovingh et al., 2015*) and also in carriers of HDL defects, including apoA-I deficiency and Tangier Disease (*Kootte et al., 2015; Zheng et al., 2020*); however, CER-001 has never been tested in carriers of FLD.

Thus, this part of the project had a double aim: to investigate whether the absence of LCAT affects the remodeling and metabolism of CER-001 in mice, as well as to evaluate the effects of CER-001 on the kidney disease associated with LCAT deficiency.

The results collected demonstrated that the absence of LCAT affected the metabolism of CER-001 in vivo; when injected into WT mice, the particles remained in circulation for hours, probably exchanging lipids with endogenous murine HDL, that could convert into larger spherical particles. On the contrary, in *Lcat*$^{-/-}$ mice, because of the absence of the enzyme, CER-001 could not be properly remodeled in circulation and it accumulated quickly in the kidney and slightly in the liver for a rapid catabolism.

The evaluation of the lipid profile showed an amelioration after CER-001 injections into both murine models with a decrease in total cholesterol paralleled by an increase in HDL-C, particularly evident and with a dose-dependent trend in *Lcat*$^{-/-}$ mice.

Plasma phospholipids concentration was significantly reduced in both WT and *Lcat*$^{-/-}$ mice; an explanation could be found in the measurement of this parameter, that evaluates phosphatidylcholine amount. CER-001 contains only sphingomyelin and dipalmitoylphosphatidylglycerol; these lipids could form a new pool of phospholipids for HDL formation, replacing phosphatidylcholine. Trygliceride were significantly and dose-dependently decreased after CER-001 injection. The result is meaningful, as hypertriglyceridemia in *Lcat*$^{-/-}$ mice reflects the condition of LCAT deficient carriers; moreover, this effect is opposite to what had been observed in animal models treated with other synthetic HDL made of phosphatidylcholine, apoA-I and cholesterol, which induced an increase in triglycerides level (*Kempen et al., 2013*)

Lipid profile of *Lcat*$^{-/-}$ mice resembles FLD carriers' one, but the animals do not develop spontaneously the renal injury. To create the murine model of renal disease, *Lcat*$^{-/-}$ mice were injected with synthetic LpX for one month (*Ossoli et al., 2016*) and the beneficial effects of CER-001 were tested in comparison with saline.

The concentration of total cholesterol and phospholipids, enhanced after LpX injections, did not decrease after CER-001 treatment, probably because of the proven ability of the particle to remove the lipid component of LpX accumulated in glomeruli from the kidney. This hypothesis was supported by the removed lipids reassembling into large lipoproteins with a similar size of VLDL, explaining the shifted peak observed in FPLC profile, and by the reduced lipid content in glomeruli of *Lcat*$^{-/-}$ mice after the treatment with CER-001. This theory was also confirmed with an in vitro experiment, in which podocytes loaded with LpX showed a decreased cholesterol content after incubation with CER-001. The lipids efflux could be mediated by ABCA1, highly expressed in podocytes and involved in lipid accumulation in the kidney, as demonstrated by the glomerular accumulation of lipids in diabetic nephropathies characterized by decreased ABCA1 expression (*Herman-Edelstein et al., 2014, Merscher-Gomez et al., 2013*).

To evaluate whether the reduction of lipid accumulation in glomeruli leads to an amelioration of the renal function, urine albumin to creatinine ratio (ACR) was measured: treatment with CER-001 at 10 mg/kg showed a beneficial effect on kidney function, by reducing of 50% the ACR compared to the end of LpX condition. As

saline did not show any effect, the results suggested that kidney injury induced by LpX is not spontaneously reversible and the amelioration was due to the treatment with CER-001.

In CKD, podocyte dysfunction has been associated with proteinuria and contributes to glomerular sclerotic damage (*Mundel et al., 2002*). Nephrin is a key molecule for the slit-diaphragm integrity and is critical for glomerular function in glomerular diseases (*Li et al. 2015*). Nestin plays an important role in normal podocyte function and can be reduced in kidney diseases (*Su et al., 2007*). CER-001 was able to restore nephrin and nestin expression decreased after LpX injection. The beneficial effect of CER-001 on the kidney disease in LCAT deficiency, through the reduction of ACR and the recovery of nestin and nephrin expression, set the basis for the use of the molecule in FLD carriers. The first treated patient showed slight amelioration of renal function (*Faguer et al., 2021*).

To define whether the removal ability of CER-001 could be associated with the beneficial effect on kidney also in humans, in vitro experiments on podocytes were performed after the collection of one FLD carrier' plasma from the Italian cohort treated with the molecule through a compassionate program. Patient's plasma at baseline induced cholesterol deposition in podocytes, due to the accumulation of LpX, while during CER-001 treatment the accumulation of cholesterol progressively reduced.

This result confirmed that CER-001 is able to accept cholesterol from LpX and corrects lipoproteins remodeling; moreover, the molecule could exert its positive effect through a direct efflux of cholesterol from renal cells, as confirmed by in an vitro experiment showing that CER-001 was able to reduce intracellular cholesterol content in cultured podocytes loaded with patient's plasma collected at baseline, enriched in LpX.

All the collected results obtained in this part of the project, from the in vivo and in vitro studies and from the first FLD carrier, support the use of CER-001 in LCAT deficiency, even if not as a curative approach, being unable to correct the causative defect, but possibly ameliorating the compromised renal function.

The last part of the project was focused on the relationship between LCAT concentration and development of renal disease in general population, facing the non-genetic condition.

It has been previously demonstrated that decreased HDL-C concentration is the most typical lipid alteration both in mild-to-moderate CKD (*Baragetti et al., 2013*) and in hemodialysis patients (*Calabresi et al. 2014*). The reduction of HDL level in these subjects is mainly due to a decrease of the concentration and activity of LCAT (*Calabresi et al. 2014*). Moreover, HDL from CKD patients are characterized by alterations in their composition and function induced by the inflammatory and uremic state (*Strazzella et al., 2021*).

It is important to notice that CKD patients' HDL profile mirrors the one of genetic LCAT deficient carriers (*Calabresi et al., 2005*), probably because of the acquired LCAT deficiency in CKD. Since the genetic absence of LCAT is associated with the alterations in the lipid/lipoprotein profile involved in the pathogenesis of renal disease (*Ossoli et al., 2016*), the aim of the work was to assess whether reduced plasma LCAT concentration can predict CKD incidence and evolution in general population as well as to investigate the possible involved mechanisms underlying this process.

Subjects from the PLIC cohort (*Baragetti et al.,2013)* with normal values of eGFR were divided into tertiles according to the LCAT concentration evaluated at the baseline and were followed for 84 months. eGFR was measured at the baseline and at the follow up. When these data were plotted together, the result demonstrated that the subjects with a reduced concentration of LCAT at the baseline presented a faster renal function impairment during the years compared to the subjects with a normal-high level of the enzyme, measured as annual eGFR reduction.

This relevant finding suggests that the alterations in lipid and lipoprotein profile in subjects with low LCAT concentration, characterized by an increased unesterified/total cholesterol ratio and accumulation of discoidal preβ-HDL, and the concentration of the enzyme are involved in the development of renal damage even in general population. The lipid alterations, even if to a less extent, mirror the ones of LCAT deficient carriers (*Calabresi et al., 2005*)

In order to identify some molecular mechanisms behind the renal impairment, in vitro studies on renal cells were performed. According to the results obtained in workpackage 2, the pro-oxidative effect on podocytes and tubular cells exerted by sera of subjects with low LCAT concentration was confirmed; moreover, sera from these subjects caused a reduction in podocin expression, potentially contributing to the impairment of renal function observed later on in these individuals. The causal relation between low LCAT level and the increased ROS production was confirmed by the in vitro addition of rhLCAT to sera of low LCAT concentration subjects; the incubation with the recombinant enzyme led to the correction of HDL abnormalities and consequently to the reduction of serum-mediated ROS production in renal cells. The incubation with serum-free rhLCAT had a neutral effect on ROS production in both cell lines, suggesting that the anti-oxidant function was likely due to LCAT-induced modifications in lipoproteins, specifically in HDL, and not directly mediated by the recombinant enzyme. In conclusion, the results collected support the pharmacological modulation of LCAT as a potential therapeutic approach, improving the abnormal HDL phenotype and reducing serum pro-oxidative effects associated with low LCAT concentration.

In conclusion, collected data described for the first time the alterations in lipid composition of FLD carriers' HDL and plasma, which could potentially explain some of the nephrotoxic effect induced by the lipoprotein abnormalities typical of carriers' profile in renal cells. Moreover, the treatment with a synthetic HDL, CER-001, exerted a beneficial effect on renal function in a mouse model of kidney disease, setting the basis for testing this formulation in FLD carriers.

Finally, the evaluation of the relationship between low LCAT levels and progression of renal disease revealed that LCAT concentration can predict renal kidney injury in general population.

BIBLIOGRAPHY

- ✓ Adimoolam, S.; Jonas, A. Identification of a domain of lecithin-cholesterol acyltransferase that is involved in interfacial recognition. *Biochem Biophys Res Commun*. **1997**; 232(3); 783-7.
- ✓ Ahsan, L.; Ossoli, A.F.; Freeman, L.A.; Vaisman, B.; Amar, M.J.; Shamburek, R.D.; Remaley, A.T. Role of lecithin: cholesterol acyltransferase in HDL metabolism and atherosclerosis, in The HDL Handbook: Biological Functions and Clinical Implications (Komoda T. ed), London: Academic Press; 2014. 2nd ed, p. 159–194.
- ✓ Albers, J.J.; Bergelin, R.O.; Adolphson, J.L .and Wahl, P.W. Population-based reference values for lecithin-cholesterol acyltransferase (LCAT). *Atherosclerosis* **1982;** 43(2); 369-379.
- ✓ Albers, J.J.; Marcovnia, S.M. and Christenson, R.H. Lecithin cholesterol acyltransferase in human cerebrospinal fluid: reduced level in patients with multiple sclerosis and evidence of direct synthesis in the brain. *Int J Clin Lab Res* **1992**; 22(1-4); 169-172.
- ✓ Amar MJ, Shamburek RD, Vaisman B, et al. Adenoviral expression of human lecithin-cholesterol acyltransferase in nonhuman primates leads to an antiatherogenic lipoprotein phenotype by increasing high-density lipoprotein and lowering low-density lipoprotein. *Metabolism* **2009**; 58; 568–575.
- ✓ Andrews,J.; Janssan, A.; Nguyen, T.; Pisaniello, A.D.; Scherer, D.J.; Kastelein, J.J. et al. Effect of serial infusions of reconstituted high-density lipoprotein (CER-001) on coronary atherosclerosis: rationale and design of the CARAT study. *Cardiovasc Diagn Ther*. **2017**; 7(1); 45–51.
- ✓ Aranda, P.; Valdivielso, P.; Pisciotta, L.; Garcia, I.; Garcã A-Arias, C.; Bertolini, S. et al. Therapeutic management of a new case of LCAT deficiency with a multifactorial long-term approach based on high doses of angiotensin II receptor blockers (ARBs). *Clin Nephrol.* **2008**; 69(3); 213-8.
- ✓ Asztalos, B.F.; Schaefer, E.J.; Horvath, K.V.; Yamashita, S.; Miller, M.; Franceschini, G.; Calabresi, L. Role of LCAT in HDL remodeling: investigation of LCAT deficiency states. *J Lipid Res*. **2007**; 48(3); 592-9.

- ✓ Baragetti, A.; Norata, G.D.; Sarcina, C.; Rastelli, F.; Grigore, L.; Garlaschelli, K. et al. High density lipoprotein cholesterol levels are an independent predictor of the progression of chronic kidney disease. *J Intern Med.* **2013**; 274(3); 252-62.
- ✓ Baragetti, A.; Ossoli, A.; Strazzella, A.; Simonelli, S.; Baragetti, I.; Grigore, L. et al. Low plasma lecithin: cholesterol acyltransferase (LCAT) concentration predicts chronic kidney disease. *J Clin Med*. **2020**; 9(7); 2289.
- ✓ Barbaras, R. Non-clinical development of CER-001. *Front Pharmacol*. **2015**; 6;220.
- ✓ Biemesderfer, D. Regulated intramembrane proteolysis of megalin: linking urinary protein and gene regulation in proximal tubule? *Kidney Int* **2006;** 69; 1717–1721.
- ✓ Bonelli, F. S., and Jonas, A. Reaction of lecithin cholesterol acyltransferase with water-soluble substrates. *J Biol Chem* **1989**; 64(25); 14723-14728.
- ✓ Borysiewicz, L.K.; Soutar, A.K.; Evans, D.J.; Thompson, G.R., Rees, A.J. Renal failure in familial lecithin: cholesterol acyltransferase deficiency. *Q J Med* **1982**; 51(204); 411–26.
- ✓ Boscutti, G.; Calabresi, L.; Pizzolitto, S.; Boer, E.; Bosco, M.; Mattei, P.L. et al. LCAT deficiency: a nephrological diagnosis. *G Ital Nefrol* **2011;** 28(4); 369-382.
- ✓ Braschi, S.; Neville, T.A.; Vohl, M.C.; Sparks, D.L. Apolipoprotein A-I charge and conformation regulate the clearance of reconstituted high density lipoprotein in vivo. *J Lipid Res* **1999**; 40; 522-32.
- ✓ Breznan, D.; Veereswaran, V.; Viau, F.J.; Neville, T.A.; Sparks, D.L. The lipid composition of high-density lipoprotein affects its re-absorption in the kidney by proximal tubule epithelial cells. *Biochem J* **2004**; 379; 343–349.
- ✓ Brown, J.M.; Bell, T.A. 3rd; Alger, H.M.; Sawyer, J.K.; Smith, T.L.; Kelley, K. et al. Targeted depletion of hepatic ACAT2-driven cholesterol esterification reveals a non-biliary route for fecal neutral sterol loss. *J Biol Chem* **2008**; 283; 10522–10534.
- ✓ Brundert, M.; Heeren, J.; Merkel, M.; Carambia, A.; Herkel, J.; Groitl, P. et al. Scavenger receptor CD36 mediates uptake of high density lipoproteins in mice and by cultured cells. *J Lipid Res* **2011**; 52; 745–758.

- ✓ Calabresi L.; Simonelli, S.; Gomaraschi, M.; Franceschini, G. Genetic lecithin:cholesterol acyltransferase deficiency and cardiovascular disease. *Atherosclerosis* **2012**; 222(2); 299-330.
- ✓ Calabresi, L.; Baldassarre, D.; Castelnuovo, S.; Conca, P.; Bocchi, L.; Candini, C. et al. Functional lecithin:cholesterol acyltransferase is not required for efficient atheroprotection in humans. *Circulation* **2009**; 120; 628–35.
- ✓ Calabresi, L.; Favari, E.; Moleri, E.; Adorni, M.P.; Pedrelli, M.; Costa, S. et al. Functional LCAT is not required for macrophage cholesterol efflux to human serum. *Atherosclerosis* **2009**; 204; 141-6.
- ✓ Calabresi, L.; Gomaraschi, M.; Franceschini G. High-Density Lipoprotein Quantity or Quality for Cardiovascular Prevention*? Current Pharmaceutical Design* **2010**; 16; 1494-1503.
- ✓ Calabresi, L.; Pisciotta, L.; Costantin, A.; Frigerio, I.; Eberini, I.; Alessandrini, P. et al. The molecular basis of lecithin:cholesterol acyltransferase deficiency syndromes: a comprehensive study of molecular and biochemical findings in 13 unrelated Italian families. *Arterioscler Thromb Vasc Biol*. **2005**; 25(9); 1972-8.
- ✓ Calabresi, L.; Simonelli, S.; Conca, P.; Busnach, G.; Cabibbe, M.; Gesualdo L. et al. Acquired lecithin:cholesterol acyltransferase deficiency as a major factor in lowering plasma HDL levels in chronic kidney disease. *J.Intern.Med*. **2014**; 277; 552–561.
- ✓ Caridi, G.; Perfumo, F.; Ghiggeri, G.M. NPHS2 (Podocin) mutations in nephrotic syndrome. Clinical spectrum and fine mechanisms. *Pediatr Res*. **2005**; 57 (5 Pt 2); 54R-61R.
- ✓ Cedó, L.; Metso, J.; Santos, D.; García-León, A.; Plana, N.; Sabate-Soler, S. et al. LDL receptor regulates the reverse transport of macrophage-derived unesterified cholesterol via concerted action of the HDL-LDL Axis: insight from mouse models. *Circ Res.* **2020**; 127(6); 778-792.
- ✓ Chang, T.Y.; Li, B.L.; Chang, C.C.; Urano, Y. Acyl-coenzyme A:cholesterol acyltransferases. *Am J Physiol Endocrinol Metab* **2009**; 297(1); E1–9.
- ✓ Chen, S.; Meng, X. F. and Zhang, C. Role of NADPH oxidase-mediated reactive oxygen species in podocyte injury. *Biomed Res Int.* **2013**; 2013;839761.

- ✓ Chen, Z.; Wang, S.P.; Krsmanovic, M.L.; Castro-Perez, J.; Gagen, K.; Mendoza, V, et al. Small molecule activation of lecithin cholesterol acyltransferase modulates lipoprotein metabolism in mice and hamsters. *Metabolism*. **2012**; 61(4); 470-81.
- ✓ Chisholm, J.W.; Burleson, E.R.; Shelness, G.S.; Parks, J.S. ApoA-I secretion from HepG2 cells. Evidence for the secretion of both lipid-poor apoA-I and intracellularly assembled nascent HDL. *J Lipid Res* **2002**; 43; 36-44.
- ✓ Cho, K.H.; Durbin, D.M.; Jonas, A. Role of individual amino acids of apolipoprotein A-I in the activation of lecithin:cholesterol acyltransferase and in HDL rearrangements. *J Lipid Res* **2001**; 42(3); 379–89.
- ✓ Christensen, E.I.; Nielsen, S.; Moestrup, S.K.; Borre, C.; Maunsbach, A.B.; de Heer, E. et al. Segmental distribution of the endocytosis receptor gp330 in renal proximal tubules. *Eur J Cell Biol* **1995**; 66; 349–364.
- ✓ Christopher, D.M. Pre-clinical development of AAV-mediated gene therapy for familial lecithin cholesterol acyltransferase deficiency. Publicly accessible Penn Dissertations. 2228. Philadelphia, PA: University of Pennsylvania; 2017.
- ✓ Chung, B.H. and Dashti, N. Lipolytic remnants of human VLDL produced in vitro. Effect of HDL levels in the lipolysis mixtures on the apoCs to apoE ratio and metabolic properties of VLDL core remnants. *J. Lipid Res*. **2000**; 41; 285–297.
- ✓ Clay, M.A.; Newnham, H.H.; Forte, T.M.; Barter, P.J. Cholesteryl ester transfer protein and hepatic lipase activity promote shedding of apoA-I from HDL and subsequent formation of discoidal *HDL. Biochim Biophys Acta* **1992**; 1124; 52-8.
- ✓ Cogan, D.G.; Kruth, H.S.; Datilis, M.B.; Martin, N. Corneal opacity in LCAT disease. *Cornea* **1992**; 11(6); 595–9.
- ✓ Cohn, J.S.; Batal, R.; Tremblay, M.; Jacques, H.; Veilleux, L.; Rodriguez, C. et al. Plasma turnover of HDL apoC-I, apoC-III, and apoE in humans: in vivo evidence for a link between HDL apoC-III and apoA-I metabolism. *J Lipid Res* **2003**; 44; 1976–1983.
- ✓ Czarnecka, H.; Yokoyama, S. Regulation of lecithin-cholesterol acyltransferase reaction by acyl acceptors and demonstration of its "idling" reaction. *J Biol Chem*. **1993**; 268(26); 19334-40.

- ✓ Daniil, G.; Phedonos, A.A.; Holleboom, A.G.; Motazacker, M.M.; Argyri, L.; Kuivenhoven, J.A.; Chroni, A. Characterization of antioxidant/anti-inflammatory properties and apoA-I-containing subpopulations of HDL from family subjects with monogenic low HDL disorders. *Clin Chim Acta.* **2011**; 412(13-14); 1213-20.
- ✓ Davidson, W.S.; Sparks, D.L.; Lund-Katz, S.; Phillips, M.C. The molecular basis for the difference in charge between pre-beta- and alpha-migrating high density lipoproteins. *J Biol Chem*. **1994**; 269 (12) ; 8959-65.
- ✓ Dikkers, A.; Tietge, U.J. Biliary cholesterol secretion: More than a simple ABC. *World J Gastroenterol* **2010**; 16; 5936–5945.
- ✓ Duann, P.; Lianos, E.A.; Ma, J.; Lin, P.H. Autophagy, innate immunity and tissue repair in acute kidney injury. *Int. J. Mol. Sci*. **2016**; 17; 662.
- ✓ Dugue-Pujol, S.; Rousset, X.; Chateau, D.; Pastier, D.; Klein, C.; Demeurie, J. et al. Apolipoprotein A-II is catabolized in the kidney as a function of its plasma concentration. *J Lipid Res* **2007**; 48; 2151–2161.
- ✓ Duni, A.; Liakopoulos, V.; Roumeliotis, S.; Peschos, D.; Dounousi, E. Oxidative stress in the pathogenesis and evolution of chronic kidney disease: untangling Ariadne's thread. *Int J Mol Sci*. **2019**; 20(15); 3711.
- ✓ Edelstein, C.; Gordon, J. I; Toscas, K.; Sims, H. F.;. Strauss, A. W. and Scanu, A. M. In vitro conversion of proapoprotein A-I to apoprotein A-I. Partial characterization of an extracellular enzyme activity. *J. Biol. Chem* **1983**; 258; 11430–11433.
- ✓ El Khoury, P.; Plengpanich, W.; Frisdal, E.; Le Goff, W.; Khovidhunkitc, W.; Guerin, M. Improved plasma cholesterol efflux capacity from human macrophages in patients with hyperalphalipoproteinemia. *Atherosclerosis* **2014**; 234; 193–199.
- ✓ Emmanuel, F.; Steinmetz, A.; Rosseneu, M.; Brasseur, R.; Gosselet, N.; Attenot, F. et al. Identification of specific amphipathic alpha-helical sequence of human apolipoprotein A-IV involved in lecithin:cholesterol acyltransferase activation. *J Biol Chem*. **1994**; 269(47); 29883-90.
- ✓ Escolà-Gil, J.C.; Marzal-Casacuberta, A.; Julve-Gil, J.; Ishida, B.Y.; Ordóñez-Llanos, J.; Chan, L. et al. Human apolipoprotein A-II is a pro-atherogenic

molecule when it is expressed in transgenic mice at a level similar to that in humans: evidence of a potentially relevant species-specific interaction with diet. *J Lipid Res*. **1998**; 39(2); 457-62.

- ✓ Faguer, S.; Chauveau, D.; Colombat, M.; Delas, A.; Bernadet-Monrozies, P.; Beq, A. et al. Administration of the high-density lipoprotein mimetic CER-001 for inherited lecithin-cholesterol acyltransferase deficiency*. Ann Intern Med*. **2021;** Epub ahead of print.
- ✓ Favari, E.; Calabresi, L.; Adorni, M.P.; Jessup, W.; Simonelli, S.; Franceschini, G.; Bernini, F. Small discoidal pre-beta1 HDL particles are efficient acceptors of cell cholesterol via ABCA1 and ABCG1. *Biochemistry* **2009**; *48*: 11067-74.
- ✓ Favari, E.; Lee, M.; Calabresi, L.; Franceschini, G.; Zimetti, F.; Bernini, F.; Kovanen, P.T. Depletion of pre-beta-high density lipoprotein by human chymase impairs ATP-binding Cassette Transporter A1- but not Scavenger Receptor Class B Type I-mediated lipid efflux to high density lipoprotein. *J Biol Chem* **2004**; 279; 9930–6.
- ✓ Feister, H.A.; Auerbach, B.J.; Cole, L.A.; Krause, B.R.; Karathanasis, S.K. Identification of an IL-6 response element in the human LCAT promoter. *J. Lipid Res.* **2002**; 43(6); 960-970.
- ✓ Feng, M., Darabi, M., Lhomme, M., Tubeuf, E., Canicio, A., Brerault, J. et al. Phospholipid transfer to high-density lipoprotein (HDL) upon triglyceride lipolysis is directly correlated with HDL-cholesterol levels and is not associated with cardiovascular risk. *Atherosclerosis* **2021**; 324; 1-8.
- ✓ Feng, M.; Darabi, M.; Tubeuf, E.; Canicio, A.; Lhomme, M.; Frisdal, E. et al. Free cholesterol transfer to high-density lipoprotein (HDL) upon triglyceride lipolysis underlies the U-shape relationship between HDL-cholesterol and cardiovascular disease. *Eur J Prev Cardiol.* **2020**; 27(15);1606-1616.
- ✓ Foley R.N.; Parfrey, P.S.; Sarnak, M.J. Clinical epidemiology of cardiovascular disease in chronic renal disease. *Am. J. Kidney Dis*. **1998**; 32; 112–119.
- ✓ Franceschini, G.; Calabresi, L.; Colombo, C.; Favari, E.; Bernini, F.; Sirtori, C.R. Effects of fenofibrate and simvastatin on HDL-related biomarkers in low-HDL patients. *Atherosclerosis.* **2007**; 195(2); 385-91.

- ✓ Franceschini, G.; Sirtori, C.R.; Bosisio, E.; Gualandri, V.; Orsini, G.B.; Mogavero, A.M. et al. Relationship of the phenotypic expression of the A-IMilano apoprotein with plasma lipid and lipoprotein patterns. *Atherosclerosis*. **1985**; 58(1–3); 159–174.
- ✓ Francone, O.L., and Fielding, C.J. Effects of site-directed mutagenesis at residues cysteine-31 and cysteine-184 on lecithin-cholesterol acyltransferase activity. *PNAS* **1991;** 88(5); 1716-1720.
- ✓ Freeman, L. A.; Demosky, S. J. Jr; Konaklieva, M.; Kuskovsky, R.; Aponte, A.; Ossoli, A. F. et al. Lecithin:cholesterol acyltransferase activation by sulfhydryl-reactive small molecules: role of cysteine-31. *JPET* **2017**; 362(2); 306–318.
- ✓ Freeman, L. A.; Shamburek, R. D.; Sampson, M. L.; Neufeld, E. B.; Sato, M.; Karathanasis, S. K. & Remaley, A. T. Plasma lipoprotein-X quantification on filipin-stained gels: monitoring recombinant LCAT treatment ex vivo. *J. Lipid Res.* **2019**; 60(5); 1050–1057.
- ✓ Freeman, L.A.; Karathanasis, S.K.; Remaley, A.T. Novel lecithin: cholesterol acyltransferase-based therapeutic approaches. *Curr Opin Lipidol*. 2020; 31(2); 71-79.
- ✓ Frohlich, J. Role of lecithin: cholesterol acyltransferase and apolipoprotein AI in cholesterol esterification in lipoprotein-X in vitro. *J. Lipid Res* **1995**; 36(11); 2344-2354.
- ✓ Frohlich, J.; McLeod, R.; Pritchard, P.H.; Fesmire, J.; McConathy, W. Plasma lipoprotein abnormalities in heterozygotes for familial lecithin:cholesterol acyltransferase deficiency. *Metabolism.* **1988**; 37(1); 3-8.
- ✓ Fuchs B., Schiller J. Lysophospholipids: Their generation, physiological role and detection. Are they important disease markers? *Mini Rev. Med. Chem*. **2009**; 9; 368–378.
- ✓ Gai, Z.; Wang, T.; Visentin, M.; Kullak-Ublick, G.A.; Fu, X.; Wang, Z. Lipid accumulation and chronic kidney disease. *Nutrients*. **2019**; 11(4); 722.
- ✓ Gibson, M.C.; Korjian, S.; Tricoci, P.; Daaboul, Y.; Yee, M.; Jain, P. et al. Safety and tolerability of CSL112, a reconstituted, infusible, plasma-derived

apolipoprotein A-I, after acute myocardial infarction: the AEGIS-I trial (ApoA-I event reducing in ischemic syndromes I) *Circulation*. **2016**; 134(24); 1918–1930.

- ✓ Gillett, M.P.; Obineche, E.N.; Lakhani, M.S.; Abdulle, A.M; Amirlak, I.; Al Rukhaimi, M.; Suleiman, M.N. Levels of cholesteryl esters and other lipids in the plasma of patients with end-stage renal failure. *Ann Saudi Med*. **2001**; 21(5-6); 283-6.
- ✓ Glomset, J. A. The plasma lecithin: cholesterol acyltransferase reaction. *J. Lipid Res*. **1968**; 9(2); 155-167.
- ✓ Glukhova, A.; Hinkovska-Galcheva, V.; Kelly, R.; Abe, A.; Shayman, J.A.; Tesmer, J.J. Structure and function of lysosomal phospholipase A2 and lecithin:cholesterol acyltransferase. *Nat Commun* **2015**; 6; 6250.
- ✓ Gordon, T.; Castelli, W.P.; Hjortland, M.C.; Kannel, W.B.; Dawber, T.R. High density lipoprotein as a protective factor against coronary heart disease. The Framingham Study. *Am J Med.* **1977**; 62(5); 707–714.
- ✓ Goyal, J.; Wang, K.; Liu, M.; Subbaiah, P.V. Novel function of lecithin-cholesterol acyltransferase. Hydrolysis of oxidized polar phospholipids generated during lipoprotein oxidation. *J Biol Chem.* **1997**; 272(26); 16231-9.
- ✓ Graversen, J.H.; Castro, G.; Kandoussi, A.; Nielsen, H.; Christensen, E.I.; Norden, A.; Moestrup, S.K. A pivotal role of the human kidney in catabolism of HDL protein components apolipoprotein A-I and A-IV but not of A-II. *Lipids* **2008**; 43; 467–470.
- ✓ Guasch, A.; Deen, W. M.; Myers, B. D. Charge selectivity of the glomerular filtration barrier in healthy and nephrotic humans. *J. Clin. Invest.* **1993;** 92; 2274–2282.
- ✓ Guo, M.; Ma, S.; Xu, Y.; Huang, W.; Gao, M.; Wu, X. et al. Correction of Familial LCAT Deficiency by AAV-hLCAT prevents renal injury and atherosclerosis in hamsters. *Arterioscler Thromb Vasc Biol*. **2021;** ATVBAHA120315719. Epub ahead of print
- ✓ Hager, M.R.; Narla, D.A.; Tannock, L.R. Dyslipidemia in patients with chronic kidney disease. *Rev. Endocr. Metab. Disord*. **2017**; 18; 29–40.
- ✓ Hannun, Y.A.; Obeid, L.M. Sphingolipids and their metabolism in physiology and disease. *Nat Rev Mol Cell Biol*. **2018**; 19(3); 175-191

- ✓ Haraldsson, B.; Nyström, J. and Deen, W. M. Properties of the glomerular barrier and mechanisms of proteinuria. *Physiol. Rev* **2008;** 88(2); 451-487.
- ✓ Harayama, T.; Riezman, H. Understanding the diversity of membrane lipid composition. *Nat Rev Mol Cell Biol*. **2018**; 19(5); 281-296.
- ✓ Herman-Edelstein, M.; Scherzer, P.; Tobar, A.; Levi, M.; Gafter, U. Altered renal lipid metabolism and renal lipid accumulation in human diabetic nephropathy. *J Lipid Res.* **2014**; 55(3); 561–72.
- ✓ Hirata, A.; Okamura, T.; Sugiyama, D.; Kuwabara, K.; Kadota, A.; Fujiyoshi, A.; et al. NIPPON DATA90 Research Group. The relationship between very high levels of serum high-density lipoprotein cholesterol and cause-specific mortality in a 20-year follow-up study of Japanese general population. *J Atheroscler Thromb* **2016**; 23; 800–809.
- ✓ Hirsch-Reinshagen, V.; Donkin, J.; Stukas, S.; Chan, J.; Wilkinson, A.; Fan, J. et al. LCAT synthesized by primary astrocytes esterifies cholesterol on glia-derived lipoproteins. *J. Lipid Res.* **2009***;* 50(5); 885-893.
- ✓ Hoeg, J. M.; Santamarina-Fojo, S.; Berard, A. M.; Cornhill, J. F.; Herderick, E. E.; Feldman, S. H. C. C. et al.. Overexpression of lecithin:cholesterol acyltransferase in transgenic rabbits prevents diet-induced atherosclerosis. *Proc. Natl. Acad. Sci. USA*. **1996**; 93; 11448–453.
- ✓ Hovingh, G. K.; Smits, L. P.; Stefanutti, C.; Soran, H.; Kwok, S.; de Graaf J. et al. The effect of an apolipoprotein A-I-containing high-density lipoprotein-mimetic particle (CER-001) on carotid artery wall thickness in patients with homozygous familial hypercholesterolemia: the Modifying Orphan Disease Evaluation (MODE) study. *Am. Heart J*. **2015**; 169; 736–742 e731.
- ✓ Hua, W.; Huang, H.Z.; Tan, L.T.; Wan, J.M.; Gui, H.B.; Zhao, L. et al. CD36 mediated fatty acid-induced podocyte apoptosis via oxidative stress. *PLoS One*. **2015**; 10(5); e0127507.
- ✓ Ikewaki, K.; Rader, D.J.; Schaefer, J.R.; Fairwell, T.; Zech, L.A.; Brewer, H.B.Jr. Evaluation of apoA-I kinetics in humans using simultaneous endogenous stable isotope and exogenous radiotracer methods. *J Lipid Res* **1993**; 34; 2207-15.

- ✓ Imbasciati, E.; Paties, C.; Scarpioni, L.; Mihatsch, M.J. Renal lesions in familial lecithincholesterol acyltransferase deficiency. Ultrastructural heterogeneity of glomerular changes. *Am J Nephrol* **1986**; 6(1); 66–70.
- ✓ Itabe, H.; Hosoya, R.; Karasawa, K.; Jimi, S.; Saku, K.; Takebayashi S, et al. Metabolism of oxidized phosphatidylcholines formed in oxidized low density lipoprotein by lecithin-cholesterol acyltransferase. *J Biochem*. **1999**; 126(1); 153-61.
- ✓ Jessup, W.; Gelissen, I.C.; Gaus, K.; Kritharides, L. Roles of ATP binding cassette transporters A1 and G1, scavenger receptor BI and membrane lipid domains in cholesterol export from macrophages. *Curr Opin Lipidol* **2006**; 17; 247-57.
- ✓ Ji, Y.; Wang, N.; Ramakrishnan, R.; Sehayek, E.; Huszar, D.; Breslow, J.L.; Tall, A.R. Hepatic scavenger receptor BI promotes rapid clearance of high density lipoprotein free cholesterol and its transport into bile. *J Biol Chem* **1999**; 274; 33398-402.
- ✓ Jonas A. Lecithin cholesterol acyltransferase. *Biochim Biophys Acta* **2000**; 1529; 245-56.
- ✓ Karalis, I.; Jukema, J.W. HDL mimetics infusion and regression of atherosclerosis: is it still considered a valid therapeutic option?. *Curr Cardiol Rep*. **2018**; 20(8); 66.
- ✓ Karalis, I.; Rensen, P.C.N.; Jukema, J.W. Journey through cholesteryl ester transfer protein inhibition: from bench to bedside. *Circ Cardiovasc Qual Outcomes*. **2013**; 6(3); 360–366.
- ✓ Kataoka, Y.; Andrews, J.; Duong, M.; Nguyen, T.; Schwarz, N.; Fendler, J. et al. Regression of coronary atherosclerosis with infusions of the high-density lipoprotein mimetic CER-001 in patients with more extensive plaque burden. *Cardiovasc Diagn Ther*. **2017**; 7(3); 252–263.
- ✓ Kayser, F.; LaBelle, M.; Shan, B.; Zhang, J. and Zhou M; inventors, Amgen, Inc., assignee. Methods for treating atherosclerosis. U.S. patent 8426358. **2013**
- ✓ Kempen, H.J.; Gomaraschi, M.; Bellibas, S.E.; Plassmann, S.; Zerler, B.; Collins, H.L. et al. Effect of repeated apoA-IMilano/POPC infusion on lipids,

(apo)lipoproteins, and serum cholesterol efflux capacity in cynomolgus monkeys. *J Lipid Res*. **2013**; 54(9); 2341-53.

- ✓ Khera, A.V.; Cuchel, M.; de la Llera-Moya, M.; Rodrigues, A.; Burke, M.F.; Jafri, K. et al. Cholesterol efflux capacity, high-density lipoprotein function, and atherosclerosis. *N Engl J Med*. **2011**; 364(2); 127–135.
- ✓ Knuplez, E.; Marsche, G. An updated review of pro- and anti-inflammatory properties of plasma lysophosphatidylcholines in the vascular system. *Int J Mol Sci.* **2020**; 21(12); 4501.
- ✓ Ko, D.T.; Alter, D.A.; Guo, H.; Koh, M.; Lau, G.; Austin, P.C. et al. High-density lipoprotein cholesterol and cause-specific mortality in individuals without previous cardiovascular conditions: The CANHEART Study. *J Am Coll Cardiol* **2016**; 68: 2073–2083.
- ✓ Kontush A.; Chapman, M.J. Antiatherogenic function of HDL particle subpopulations: Focus on antioxidative activities. *Curr. Opin. Lipidol*. **2010**; 21; 312–318.
- ✓ Kontush, A. and Chapman, M. J. High-density lipoproteins. **2012**; Hoboken, NJ: John Wiley & Sons.
- ✓ Kontush, A. and Chapman, M.J. Functionally defective High-density lipoprotein: a new therapeutic target at the crossroads of dyslipidemia, inflammation, and atherosclerosis. *Pharmacol. Rev.* **2006**; 58; 342–374.
- ✓ Kontush, A. HDL and Reverse Remnant-Cholesterol Transport (RRT): Relevance to Cardiovascular Disease. *Trends Mol Med*. **2020**; 26; 1086-1100.
- ✓ Kontush, A.; Lhomme, M.; Chapman, M.J. Unraveling the complexities of the HDL lipidome. *J Lipid Res. 2013*; 54(11); 2950-2963.
- ✓ Kootte, R. S.; Smits, L. P.; van der Valk, F. M.; Dasseux, J. L.; Keyserling, C. H.; Barbaras, R. et al. Effect of open-label infusion of an apoA-I-containing particle (CER-001) on RCT and artery wall thickness in patients with FHA. *J. Lipid Res*. **2015**; 56; 703–712.
- ✓ Kozyraki, R.; Fyfe, J.; Kristiansen, M.; Gerdes, C.; Jacobsen, C.; Cui, S. et al. The intrinsic factor-vitamin B12 receptor, cubilin, is a high-affinity apolipoprotein A-I

receptor facilitating endocytosis of high-density lipoprotein. *Nat Med* **1999**; 5; 656-61.

- ✓ Krikken, J.A.; Gansevoort, R.T.; Dullaart, R.P.F.; on behalf of the PSG. Lower HDL-C and apolipoprotein A-I are related to higher glomerular filtration rate in subjects without kidney disease. *J Lipid Res* **2010**; 51; 1982–1990.
- ✓ Kuang, Y.L.; Paulson, K.E.; Lichtenstein, A.H. and Lamon-Fava, S. Regulation of the expression of key genes involved in HDL metabolism by unsaturated fatty acids. *Br. J. Nutr.* **2012;** 108(8); 1351-1359.
- ✓ Kuchta, A.; Cwiklinska, A.; Czaplinska, M.; Wieczorek, E.; Kortas-Stempak, B.; Gliwinska A. et al. Plasma levels of prebeta1-HDL are significantly elevated in non-dialyzed patients with advanced stages of chronic kidney disease. *Int. J. Mol. Sci.* **2019**; 20; 1202.
- ✓ Kuivenhoven, J.A.; Pritchard, H.; Hill, J.; Frohlich, J.; Assmann, G.; Kastelein; J. The molecular pathology of lecithin:cholesterol acyltransferase (LCAT) deficiency syndromes. *J Lipid Res*. **1997**; 38(2); 191-205.
- ✓ Kuroda, M.; Bujo, H.; Aso, M.; Saito, Y. Adipocytes as a vehicle for ex vivo gene therapy: novel replacement therapy for diabetes and other metabolic diseases.
- ✓ Kwiterovich, P.O. The John Hopkins Textbook of Dyslipidemia chapter 1. Philadelphia, USA: Lippincott Willams and Wilkins, **2010**
- ✓ Lacquaniti, A.; Bolignano, D.; Donato, V.; Bono, C.; Fazio, M.R.; Buemi, M. Alterations of lipid metabolism in chronic nephropathies: Mechanisms, diagnosis and treatment. *Kidney Blood Press. Res*. **2010**; 33; 100–110.
- ✓ Lager, D.J.; Rosenberg, B.F.; Shapiro, H.; Bernstein, J. Lecithin cholesterol acyltransferase deficiency: ultrastructural examination of sequential renal biopsies. *Mod Pathol* **1991**; 4(3); 331–5.
- ✓ Lagor, W.R.; Johnston, J.C.; Lock, M.; et al. Adeno-associated viruses as liver-directed gene delivery vehicles: focus on lipoprotein metabolism. *Methods Mol Biol* 2013; 1027; 273–307.
- ✓ Lambert, G.; Sakai, N.; Vaisman, B.L.; Neufeld, E.B.; Marteyn, B.; Chan, C.C. Analysis of glomerulosclerosis and atherosclerosis in lecithin cholesterol acyltransferase-deficient mice. *J Biol Chem*. **2001**; 276(18);15090-8.

- ✓ Lavallée, B., Provost, P. R. and Bélanger, A. Formation of pregnenolone-and dehydroepiandrosterone-fatty acid esters by lecithin-cholesterol acyltransferase in human plasma high density lipoproteins. *Biochim Biophys Acta* **1996**; 1299(3); 306-312.
- ✓ Lee, J.Y.; Timmins, J.M.; Mulya, A.; Smith, T.L.; Zhu, Y.; Rubin, E.M. et al. HDLs in apoA-I transgenic Abca1 knockout mice are remodeled normally in plasma but are hypercatabolized by the kidney. *J Lipid Res* **2005**; 46; 2233–2245.
- ✓ Levey, A.S.; de Jong, P.E.; Coresh, J.; El Nahas, M.; Astor, B.C.; Matsushita K. et al. The definition, classification, and prognosis of chronic kidney disease: A KDIGO Controversies Conference report. *Kidney Int*. **2011**; 80; 17–28.
- ✓ Li, X.; Chuang, P.Y.; D'Agati, V.D.; Dai, Y.; Yacoub, R.; Fu, J. et al. Nephrin preserves podocyte viability and glomerular structure and function in adult kidneys. *J Am Soc Nephrol.* **2015**; 26(10); 2361–77.
- ✓ Lin, T.A.; Wu, V.C.; Wang, C.Y. Autophagy in chronic kidney diseases. *Cells*. **2019**; 8(1); 61.
- ✓ Liu, M.; Subbaiah, P.V . Activation of plasma lysolecithin acyltransferase reaction by apolipoproteins A-I, C-I and E. *Biochim Biophys Acta*. **1993**;1168(2); 144-52.
- ✓ Madsen, C.M. and Nordestgaard, B.G. Is it time for new thinking about high-density lipoprotein? *Arterioscler. Thromb. Vasc. Biol*. **2018**; 38; 484–486.
- ✓ Madsen, C.M.; Varbo, A. and Nordestgaard, B.G. Extreme high high-density lipoprotein cholesterol is paradoxically associated with high mortality in men and women: Two prospective cohort studies. *Eur Heart J* **2017**; 38; 2478–2486.
- ✓ Maeba, R.; Kojima, K.I.; Nagura, M.; Komori, A.; Nishimukai, M.; Okazaki, T.; Uchida, S. Association of cholesterol efflux capacity with plasmalogen levels of high-density lipoprotein: A cross-sectional study in chronic kidney disease patients. *Atherosclerosis*. **2018**; 270; 102–109.
- ✓ Maeba, R.; Ueta, N.. Ethanolamine plasmalogens prevent the oxidation of cholesterol by reducing the oxidizability of cholesterol in phospholipid bilayers. *J. Lipid Res*. *2003*; 44; 164–171.
- ✓ Magill, P.; Rao, S.N.; Miller, N.E.; Nicoll, A.; Brunzell, J.; Hilaire, S.S; Lewis, B. Relationships between the metabolism of high-density and very-low density

lipoproteins in man: Studies of apolipoprotein kinetics and adipose tissue lipoprotein lipase activity. *Eur J Clin Invest* **1982**; 12; 113–120.

- ✓ Malle, E.; De Beer, F.C. Human serum amyloid A (SAA) protein: a prominent acute-phase reactant for clinical practice. *Eur. J. Clin. Investig*. **1996**; 26; 427–435.
- ✓ Manthei, K.A.; Yang, S.M.; Baljinnyam, B.; Chang, L.; Glukhova, A.; Yuan, W. et al. Molecular basis for activation of lecithin:cholesterol acyltransferase by a compound that increases HDL cholesterol. *Elife*. **2018**; 7; e41604.
- ✓ Marsche, G.; Heine, G.H.; Stadler, J.T.; Holzer, M. Current understanding of the relationship of HDL composition, structure and function to their cardioprotective properties in chronic kidney disease. *Biomolecules*. **2020**; 10; 1348.
- ✓ Martin, C.E.; Jones, N. Nephrin signaling in the podocyte: an updated view of signal regulation at the slit diaphragm and beyond. *Front Endocrinol*. **2018**; 9; 302.
- ✓ Martinez, L.O.; Jacquet, S.; Esteve, J.P.; Rolland, C.; Cabezon, E.; Champagne, E. et al. Ectopic beta-chain of ATP synthase is an apolipoprotein A-I receptor in hepatic HDL endocytosis. *Nature* **2003**; 421; 75–79.
- ✓ Matsuura, F.; Wang, N.; Chen, W.; Jiang, X.C.; Tal,l A.R. HDL from CETP-deficient subjects shows enhanced ability to promote cholesterol efflux from macrophages in an apoE- and ABCG1-dependent pathway. *J Clin Invest* **2006**; 116;1435–42.
- ✓ Mattjus, P.; Slotte, J. P. Does cholesterol discriminate between sphingomyelin and phosphatidylcholine in mixed monolayers containing both phospholipids? *Chem. Phys. Lipids* **1996**; 81; 69–80.
- ✓ McLean, J.; Fielding, C.; Drayna, D.; Dieplinger, H.; Baer, B.; Kohr, W. et al. Cloning and expression of human lecithin-cholesterol acyltransferase cDNA. *Proc Natl Acad Sci U S A*. **1986**; 83; 2335–9.
- ✓ McPherson, P.A.; Young, I.S.; McEneny, J. A dual role for lecithin:cholesterol acyltransferase in lipoprotein oxidation. *Free Radic Biol Med*. **2007**;43(11); 1484-93.

- ✓ Merscher-Gomez,S.; Guzman, J.; Pedigo, C.E.; Lehto, M.; Aguillon-Prada, R.; Mendez, A, et al. Cyclodextrin protects podocytes in diabetic kidney disease. *Diabetes*. **2013**; 62(11); 3817–27.
- ✓ Miarka, P.; Idzior-Waluś, B.; Kuźniewski, M.; Waluś-Miarka, M.; Klupa, T.; Sułowicz W. Corticosteroid treatment of kidney disease in a patient with familial lecithin-cholesterol acyltransferase deficiency. *Clin Exp Nephrol*. **2011**; 15(3); 424-9.
- ✓ Michalczyk, K.; Ziman, M. Nestin structure and predicted function in cellular cytoskeletal organisation. *Histol Histopathol* **2005**; 2; 665.
- ✓ Miida T.; Miyazaki, O.; Hanyu, O.; Nakamura, Y.; Hirayama, S.; Narita, I. et al. LCAT-dependent conversion of prebeta1-HDL into alpha-migrating HDL is severely delayed in hemodialysis patients. *J. Am. Soc. Nephrol*. **2003**; 14; 732–738.
- ✓ Moestrup, S.K.; Kozyraki, R. Cubilin, a high-density lipoprotein receptor. *Curr Opin Lipidol* **2000**; 11; 133-40.
- ✓ Moestrup, S.K.; Nielsen, L.B. The role of the kidney in lipid metabolism. *Curr Opin Lipidol* **2005**; 16; 301–306.
- ✓ Moradi, H.; Pahl M.V.; Elahimehr, R.; Vaziri, N.D. Impaired antioxidant activity of high-density lipoprotein in chronic kidney disease. *Transl. Res*. **2009**; 153; 77–85.
- ✓ Mundel, P.; Shankland, S.J. Podocyte biology and response to injury. *J Am Soc Nephrol*. **2002**; 13(12); 3005–15.
- ✓ Narayanan, S. Biochemistry and clinical relevance of lipoproteinX. *Ann. Clin. Lab. Sci.* **1984**;14(5); 371-4.
- ✓ Ng, D.S.; Xie, C.; Maguire, G.F.; Zhu, X.; Ugwu, F.; Lam, E.; Connelly, P.W. Hypertriglyceridemia in lecithin-cholesterol acyltransferase-deficient mice is associated with hepatic overproduction of triglycerides, increased lipogenesis, and improved glucose tolerance. *J Biol Chem*. **2004**; 279(9); 7636-42.
- ✓ Nicholls, S.J.; Andrews, J.; Kastelein, J.J.P.; Merkely, B.; Nissen, S.E.; Ray, K.K. et al. Effect of serial infusions of CER-001, a pre-β high-density lipoprotein mimetic, on coronary atherosclerosis in patients following acute coronary

syndromes in the CER-001 atherosclerosis regression acute coronary syndrome trial: a randomized clinical trial. *JAMA Cardiol*. **2018**; 3(9); 815-822.

- ✓ Nichols, A.V.; Krauss, R.M.; Musliner, T.A. Non-denaturing polyacrylamide gradient gel electrophoresis. *Methods Enzymol.* **1986;** 128; 417-31.
- ✓ Nikkila, E.A.; Taskinen, M.R. and Sane, T. Plasma high-density lipoprotein concentration and subfraction distribution in relation to triglyceride metabolism. *Am Heart J* **1987**; 113; 543–548.
- ✓ Nissen, S.E.; Tsunoda, T.; Tuzcu, E.M.; Schoenhagen, P.; Cooper, C.J.; Yasin, M. et al. Effect of recombinant ApoA-I Milano on coronary atherosclerosis in patients with acute coronary syndromes: a randomized controlled trial.
- ✓ Nordestgaard, B.G. and Varbo, A. Triglycerides and cardiovascular disease. *Lancet* **2014**; 384; 626–635
- ✓ Norum, K. R., and E. Gjone. The effect of plasma transfusion on the plasma cholesterol esters in patients with familial plasma lecithin:cholesterol acyltransferase deficiency. *Scand.J Clin. Lab. Invest.* **1984**; 22; 339-342.
- ✓ Norum, K.R.; Gjone, E. Familial serum-cholesterol esterification failure. A new inborn error of metabolism. *Biochim Biophys Acta* **1967**; 144; 698–700.
- ✓ Norum, K.R.; Remaley, A.T.; Miettinen, H.E.; Strøm, E.H.; Balbo, B.E.P.; Sampaio, C.A.T.L. et al. Lecithin:cholesterol acyltransferase: symposium on 50 years of biomedical research from its discovery to latest findings. *J Lipid Res*. **2020**; 61(8); 1142-1149.
- ✓ O, K.; Hill, J.S.; Pritchard, P.H. Role of N-linked glycosylation of lecithin:cholesterol acyltransferase in lipoprotein substrate specificity. *Biochim Biophys Acta*. **1995**; 1254(2); 193-7.
- ✓ Ossoli, A.; Neufeld, E.B.; Thacker, S.G.; Vaisman, B.; Pryor, M.; Freeman, L.A. et al. Lipoprotein X Causes Renal Disease in LCAT Deficiency. *PLoS One* **2016**; 11(2); e0150083.
- ✓ Ossoli, A.; Simonelli, S.; Varrenti, M.; Morici, N.; Oliva, F.; Stucchi, M. et al. Recombinant LCAT (lecithin:cholesterol acyltransferase) rescues defective HDL (high-density lipoprotein)-mediated endothelial protection in acute coronary syndrome. *Arterioscler Thromb Vasc Biol*. **2019**; 39(5); 915-924.

- ✓ Ossoli, A.; Simonelli, S.; Vitali, C.; Franceschini, G.; Calabresi, L. Role of LCAT in atherosclerosis. *J Atheroscler Thromb*. **2016**; 23(2); 119-27
- ✓ Ossoli, A.; Strazzella, A.; Rottoli, D.; Zanchi, C.; Locatelli, M.; Zoja, C. et al. CER-001 ameliorates lipid profile and kidney disease in a mouse model of familial LCAT deficiency. *Metabolism.* **2021**; 116; 154464.
- ✓ Parks, J.S.; Gebre, A.K. Long-chain polyunsaturated fatty acids in the sn-2 position of phosphatidylcholine decrease the stability of recombinant high density lipoprotein apolipoprotein A-I and the activation energy of the lecithin:cholesterol acyltransferase reaction. *J Lipid Res*. **1997**; 38(2); 266-75.
- ✓ Patsch, J.R.; Gotto, A.R. Jr; Olivercrona, T.; Eisenberg, S. Formation of high density lipoprotein2-like particles during lipolysis of very low density lipoproteins in vitro*. Proc. Natl. Acad. Sci. U. S. A*. **1978**; 75; 4519–4523.
- ✓ Pavanello, C.; Calabresi, L. Genetic, biochemical, and clinical features of LCAT deficiency: update for 2020. *Curr Opin Lipidol*. **2020**; 31(4); 232-237.
- ✓ Pavanello, C.; Ossoli, A.; Turri, M.; Strazzella, A.; Simonelli, S.; Laurenzi, T. et al. Activation of naturally occurring lecithin:cholesterol acyltransferase mutants by a novel activator compound. *J Pharmacol Exp Ther*. **2020**; 375(3); 463-468.
- ✓ Pedrelli, M.; Davoodpour, P.; Degirolamo, C.; Gomaraschi, M.; Graham, M.; Ossoli, A. et al. Hepatic ACAT2 knock down increases ABCA1 and modifies HDL metabolism in mice. *PLoS One*. **2014**; 9(4); e93552.
- ✓ Piper, D.E.; Romanow, W.G.; Gunawardane, R.N.; Fordstrom, P.; Masterman, S.; Pan, O. et al. The high-resolution crystal structure of human LCAT. *J Lipid Res*. **2015**; 56(9); 1711-9.
- ✓ Pownall, H.J.; Pao, Q.; Massey, J.B. Acyl chain and headgroup specificity of human plasma lecithin:cholesterol acyltransferase. Separation of matrix and molecular specificities. *J Biol Chem*. **1985**; 260(4); 2146-52.
- ✓ Proctor, G.; Jiang, T.; Iwahashi, M.; Wang, Z.; Li, J.; Levi, M. Regulation of renal fatty acid and cholesterol metabolism, inflammation, and fibrosisin Akita and OVE26 micewith type1diabetes. *Diabetes* **2006**; 55(9);2502–9.
- ✓ Rader, D.J. and Tall, A.R. The not-so-simple HDL story: Is it time to revise the HDL cholesterol hypothesis? *Nat Med* **2012**; 18; 1344–1346.

- ✓ Rader, D.J.; Ikewaki, K.; Duverger, N.; Schmidt, H.; Pritchard, H.; Frohlich J. et al. Markedly accelerated catabolism of apolipoprotein A-II (ApoA-II) and high density lipoproteins containing ApoA-II in classic lecithin: Cholesterol acyltransferase deficiency and fish-eye disease. *J. Clin. Investig*. **1994**; 93; 321–330.
- ✓ Rajaram, O.V.; Barter P.J. Reactivity of human lipoproteins with purified lecithin: cholesterol acyltransferase during incubations in vitro. *Biochim Biophys Acta.* **1985;** 835; 41-49.
- ✓ Rigotti, A.; Trigatti, B.; Babitt, J.; Penman, M.; Xu, S.; Krieger, M. Scavenger receptor BI--a cell surface receptor for high density lipoprotein. *Curr Opin Lipidol* **1997**; 8; 181-8.
- ✓ Rohatgi, A.; Khera, A.; Berry, J.D.; Givens, E.G.; Ayers, C.R.; Wedin, K.E., et al. HDL cholesterol efflux capacity and incident cardiovascular events. *N Engl J Med*. **2014**; 371(25); 2383–2393.
- ✓ Rohrl, C.; Pagler, T.A.; Strobl, W.; Ellinger, A.; Neumuller, J.; Pavelka, M. et al. Characterization of endocytic compartments after holo-high density lipoprotein particle uptake in HepG2 cells. *Histochem Cell Biol* **2010**;133; 261–272.
- ✓ Rosenson, R.S. The high-density lipoprotein puzzle: why classic epidemiology, genetic epidemiology, and clinical trials conflict? *Arterioscler Thromb Vasc Biol.* **2016**; 36(5); 777–782.
- ✓ Rosenson, R.S.; Davidson, M.H.; Hirsh, B.H.; Kathiresan, S.; Gaudet, D. Genetics and causality of triglyceride-rich lipoproteins in atherosclerotic cardiovascular disease. *J. Am. Coll. Cardiol.* **2014**; 64; 2525–2540.
- ✓ Rousset, X.; Vaisman, B.; Amar, M.; Sethi, A.A. and Remaley A.T. Lecithin:cholesterol acyltransferase: from biochemistry to role in cardiovascular disease. *Curr Opin Endocrinol Diabetes Obes* **2009**; 16(2); 163.
- ✓ Saito, A.; Pietromonaco, S.; Loo, A.K.; Farquhar, M.G. Complete cloning and sequencing of rat gp330/“megalin,” a distinctive member of the low density lipoprotein receptor gene family. *Proc Natl Acad Sci USA* **1994**; 91; 9725–9729.
- ✓ Saito, A.; Sato, H.; Iino, N.; Takeda, T. Molecular mechanisms of receptor-mediated endocytosis in the renal proximal tubular epithelium. *J Biomed Biotechnol* **2010**; 2010; 403272.

- ✓ Santamarina-Fojo, S.; Hoeg, J.M.; Assmann, G.; Brewer, Jr H.B. Lecithin cholesterol acyltransferase deficiency and fish eye disease. In: Scriver CR, Beaudet AL, Sly WS, Valle D, editors. The metabolic and molecular bases of inherited diseases. New York: McGraw-Hill; 2001. p. 2817–33
- ✓ Schaefer, E.J.; Wetzel, M.G.; Bengtsson, G.; Scow, R.O.; Brewer, H.B. Jr, Olivecrona, T. Transfer of human lymph chylomicron constituents to other lipoprotein density fractions during in vitro lipolysis. *J. Lipid Res.* **1982**; 23; 1259–1273.
- ✓ Schiffer, M.; Bitzer, M.; Roberts, I.S.; Kopp, J.B.; ten Dijke, P.; Mundel, P. et al. Apoptosis in podocytes induced by TGF-beta and Smad7. *J Clin Invest*. **2001**; 108(6); 807-16.
- ✓ Sessa, A.; Battini, G.; Meroni, M.; Daidone, G.; Carnera, I.; Brambilla, P.L., et al. Hypocomplementemic type II membranoproliferative glomerulonephritis in a male patient with familial lecithin-cholesterol acyltransferase deficiency due to two different allelic mutations. *Nephron.* **2001**; 88; 268–72.
- ✓ Shamburek, R. D.; Bakker-Arkema, R.; Auerbach, B. J.; Krause, B. R.; Homan, R.; Amar, M. J. et al. Familial lecithin:cholesterol acyltransferase deficiency: First-in-human treatment with enzyme replacement. *J Clin Lipidol*. **2016**; 10(2); 356-67.
- ✓ Shamburek, R.D.; Bakker-Arkema, R.; Shamburek, A.M.; Freeman, L.A.; Amar, M.J.; Auerbach, B. et al. Safety and tolerability of ACP-501, a recombinant human lecithin:cholesterol acyltransferase, in a phase 1 single-dose escalation study. *Circ Res*. **2016**; 118(1); 73-82.
- ✓ Sheng, J.; Li, H.; Dai, Q.; Lu, C.; Xu, M.; Zhang, J.; Feng, J. NR4A1 Promotes diabetic nephropathy by activating MFF-mediated mitochondrial fission and suppressing parkin-mediated mitophagy. *Cell Physiol Biochem*. **2018**; 48(4); 1675-1693.
- ✓ Simonelli, S.; Gianazza, E.; Mombelli, G. et al. Severe high-density lipoprotein deficiency associated with autoantibodies against lecithin:cholesterol acyltransferase in non-Hodgkin lymphoma. *Arch Intern Med.* **2012**; 172(2); 179–181.

- ✓ Simonelli, S.; Tinti, C.; Salvini, L.; Tinti, L.; Ossoli, A.; Vitali, C. et al. Recombinant human LCAT normalizes plasma lipoprotein profile in LCAT deficiency. *Biologicals*. **2013**; 41; 446–449.
- ✓ Sirtori, C.R.; Calabresi, L.; Franceschini, G.; Baldassarre, D.; Amato, M.; Johansson, J. et al. Cardiovascular status of carriers of the apolipoprotein A-I(Milano) mutant: the Limone sul Garda study. *Circulation*. **2001**; 103(15); 1949–1954
- ✓ Skretting, G.; Gjernes, E.; Prydz, H. Regulation of lecithin: cholesterol acyltransferase by TGF-β and interleukin-6. *Biochim Biophys Acta* **1995**; 1255(3); 267-272.
- ✓ Sorci-Thomas, M.G.; Curtiss, L.; Parks, J.S.; Thomas, M.J.; Kearns, M.W. Alteration in apolipoprotein A-I 22-mer repeat order results in a decrease in lecithin:cholesterol acyltransferase reactivity. *J Biol Chem*. **1997**; 272(11); 7278-84.
- ✓ Soutar, A.K.; Garner, C.W.; Baker, H.N.; Sparrow, J.T.; Jackson, R.L.; Gotto, A.M.; Smith, L.C. Effect of the human plasma apolipoproteins and phosphatidylcholine acyl donor on the activity of lecithin: cholesterol acyltransferase. *Biochemistry*. **1975**; 14(14); 3057-64.
- ✓ Speer T.; Rohrer, L.; Blyszczuk, P.; Shroff, R.; Kuschnerus, K.; Kränkel N. et al. Abnormal high-density lipoprotein induces endothelial dysfunction via activation of Toll-like Receptor-2. *Immunity*. **2013**; 38; 754–768.
- ✓ Sriram, R.; Lagerstedt, J.O.; Petrlova, J.; Samardzic, H.; Kreutzer, U.; Xie, H. et al. Imaging apolipoprotein AI in vivo. *NMR Biomed* **2011**; 24; 916–924.
- ✓ Stoekenbroek, R.M.; van den Bergh Weerman, M.A.; Hovingh, G.K.; Potter van Loon, B.J.; Siegert, C.E.; Holleboom, A.G. Familial LCAT deficiency: from renal replacement to enzyme replacement. *Neth J Med*. **2013**; 71(1); 29-31.
- ✓ Strazzella, A.; Ossoli, A.; Calabresi, L. High-Density Lipoproteins and the Kidney. *Cells*. **2021**; 10(4); 764.
- ✓ Su, W.; Chen, J.; Yang, H.; You, L.; Xu, L.; Wang, X. et al. Expression of nestin in the podocytes of normal and diseased human kidneys. *Am J Physiol Regul Integr Comp Physiol*. **2007**; 292(5); R1761–7.

- ✓ Subbaiah, P.V.; Albers, J.J.; Chen, C.H.; Bagdade, J.D. Low density lipoprotein-activated lysolecithin acylation by human plasma lecithin-cholesterol acyltransferase. Identity of lysolecithin acyltransferase and lecithin-cholesterol acyltransferase. *J Biol Chem*. **1980**; 255(19); 9275-80.
- ✓ Subbaiah, P.V.; Jiang, X.C.; Belikova, N.A.; Aizezi, B.; Huang, Z.H.; Reardon, C.A. Regulation of plasma cholesterol esterification by sphingomyelin: effect of physiological variations of plasma sphingomyelin on lecithin-cholesterol acyltransferase activity. *Biochim Biophys Acta* **2012**; 1821(6); 908–13.
- ✓ Subbaiah, P.V.; Liu, M. Disparate effects of oxidation on plasma acyltransferase activities: inhibition of cholesterol esterification but stimulation of transesterification of oxidized phospholipids. *Biochim Biophys Acta* **1996**; 1301(1-2); 115–26.
- ✓ Subbaiah, P.V.; Liu, M. Role of sphingomyelin in the regulation of cholesterol esterificationin the plasma lipoproteins. Inhibition of lecithin-cholesterol acyltransferase reaction. *J Biol Chem* **1993**; 268(27); 20156–63.
- ✓ Subbaiah, P.V.; Subramanian, V.S.; Liu, M. Trans unsaturated fatty acids inhibit lecithin:cholesterol acyltransferase and alter its positional specificity. *J Lipid Res* **1998**; 39(7); 1438–47.
- ✓ Suda, T.; Akamatsu, A.; Nakaya, Y.; Masuda, Y.; Desaki, J. Alterations in erythrocyte membrane lipid and its fragility in a patient with familial lecithin:cholesterol acyltrasferase (LCAT) deficiency. *J Med Invest*. **2002**; 49(3-4); 147-55.
- ✓ Suematsu, Y.; Goto, M.; Park, C.; Nunes, A.C.F.; Jing, W.; Streja E. et al. Association of serum paraoxonase/arylesterase activity with all-cause mortality in maintenance hemodialysis patients. *J. Clin. Endocrinol. Metab*. **2019**; 104; 4848–4856.
- ✓ Sun, Y.; Ge, X.; Li, X.; He, J.; Wei, X.; Du, J. et al. High-fat diet promotes renal injury by inducing oxidative stress and mitochondrial dysfunction. *Cell Death Dis.* **2020**; 11(10); 1-14.
- ✓ Sun, Z.; Welty, F.K.; Dolnikowski, G.G.; Lichtenstein, A.H.; Schaefer, E.J. Effects of a national cholesterol education program step II diet on apolipoprotein A-IV

metabolism within triacylglycerol-rich lipoproteins and plasma. *Am J Clin Nutr* **2001**; 74; 308–314.

- ✓ Tait, S.W.; Green, D.R. Mitochondrial regulation of cell death. *Cold Spring Harb Perspect Biol*. **2013**; 5(9); a008706.
- ✓ Takabatake, Y.; Kimura, T.; Takahashi, A.; Isaka, Y. Autophagy and the kidney: health and disease. *Nephrol Dial Transplant*. **2014**; 29(9); 1639-47.
- ✓ Tanigawa, H.; Billheimer, J.T.; Tohyama, J.; Fuki, I.V.; Ng, D.S.; Rothblat, G.H.; Rader, D.J. Lecithin: cholesterol acyltransferase expression has minimal effects on macrophage reverse cholesterol transport in vivo. *Circulation* **2009**; 120; 160-9.
- ✓ Tardif, J.C. Effects of reconstituted high-density lipoprotein infusions on coronary atherosclerosis: a randomized controlled trial. *JAMA*. **2007**; 297(15); 1675–1682.
- ✓ Tardif, J.C.; Ballantyne, C.M.; Barter, P.; Dasseux, J.L.; Fayad, Z.A.; Guertin, M.C. et al. Effects of the high-density lipoprotein mimetic agent CER-001 on coronary atherosclerosis in patients with acute coronary syndromes: a randomized trial. *Eur Heart J*. **2014**; 35(46); 3277–3286.
- ✓ Tardy, C.; Goffinet, M.; Boubekeur, N.; Ackermann, R.; Sy, G.; Bluteau, A. et al. CER-001, a HDL-mimetic, stimulates the reverse lipid transport and atherosclerosis regression in high cholesterol diet-fed LDL-receptor deficient mice. *Atherosclerosis* **2014**; 232; 110–118.
- ✓ Tardy, C.; Goffinet, M.; Boubekeur, N.; Cholez, G.; Ackermann, R.; Sy, G. et al. HDL and CER-001 inverse-dose dependent inhibition of atherosclerotic plaque formation in *apoE*$^{-/-}$ mice: evidence of ABCA1 down-regulation. *PLoS One*. **2015**;10(9); e0137584.
- ✓ Temel, R.E.; Brown, J.M. A new framework for reverse cholesterol transport: Non biliary contributions to reverse cholesterol transport. *World J Gastroenterol* **2010**; 16; 5946–5952.
- ✓ Torsvik, H.; Gjone, E.; Norum, K.R. Familial plasma cholesterol ester deficiency. Clinical studies of a family. *Acta Med Scand* **1968**; 183; 387–91.

- ✓ Toyama, E.Q.; Herzig, S.; Courchet, J.; Lewis, T.L. Jr, Losón, O.C.; Hellberg, K. et al. AMP-activated protein kinase mediates mitochondrial fission in response to energy stress. *Science* **2016**; 351(6270); 275-281.
- ✓ Turner, S.; Voogt, j.; Davidson, M.; Glass, A.; Killion, S.; Decaris, J. et al. Measurement of reverse cholesterol transport pathways in humans: in vivo rates of free cholesterol efflux, esterification, and excretion. *J. Am. Heart Assoc*. **2012**; 1; e001826
- ✓ Vaisman, B.L.; Neufeld, E.B.; Freeman, L.A.; Gordon, S.M.; Sampson, M.L.; Pryor, M. et al. LCAT enzyme replacement therapy reduces LpX and improves kidney function in a mouse model of familial LCAT deficiency. *J Pharmacol Exp Ther.* **2019**; 368(3); 423-434.
- ✓ Vakifahmetoglu-Norberg, H.; Ouchida, A.T.; Norberg, E. The role of mitochondria in metabolism and cell death. *Biochem. Biophys. Res. Commun*. **2017**; 482; 426–431.
- ✓ Valkova, N.; Yunis, R.; Mak, S.K.; Kang, K. and Kültz, D. Nek8 mutation causes overexpression of galectin1, sorcin, and vimentin and accumulation of the major urinary protein in renal cysts of jck mice. *Mol. Cell Proteomics*. **2005;** 4; 1009-1018.
- ✓ Vantourout, P.; Radojkovic, C.; Lichtenstein, L.; Pons, V.; Champagne, E.; Martinez, L.O. Ecto-F(1)-ATPase: A moonlighting protein complex and an unexpected apoA-I receptor. *World J Gastroenterol* **2010**; 16; 5925–5935.
- ✓ Viestenz, A.; Schlötzer-Schrehardt, U.; Hofmann-Rummelt, C.; Seitz, B.; Küchle, M. Histopathology of corneal changes in lecithin-cholesterol acyltransferase deficiency. *Cornea*. **2002**; 21(8); 834-7.
- ✓ Vohl, M.C.; Neville, T.A.M.; Kumarathasan, R.; Braschi, S. and Sparks, D.L. A novel lecithin-cholesterol acyltransferase antioxidant activity prevents the formation of oxidized lipids during lipoprotein oxidation. *Biochemistry*, **1999**; 38(19); 5976-5981.
- ✓ Wang, N.; Arai, T.; Ji, Y.; Rinninger, F.; Tall, A.R. Liver-specific overexpression of scavenger receptor BI decreases levels of very low density lipoprotein ApoB, low

density lipoprotein ApoB, and high density lipoprotein in transgenic mice. *J Biol Chem* **1998**; 273; 32920-6.

- ✓ Wang, X.; Collins, H.L.; Ranalletta, M.; Fuki, I.V.; Billheimer, J.T.; Rothblat, G.H. et al. Macrophage ABCA1 and ABCG1, but not SRBI, promote macrophage reverse cholesterol transport in vivo. *J Clin Invest* **2007**; 117; 2216-24.
- ✓ Warden, C.H.; Langner, C.A.; Gordon, J.I.; Taylor, B.A.; McLean, J.W. and Lusis, A.J. Tissue-specific expression, developmental regulation, and chromosomal mapping of the lecithin: cholesterol acyltransferase gene. Evidence for expression in brain and testes as well as liver. *J. Biol. Chem.* **1989**; 264(36); 21573-81.
- ✓ Webb, N.R.; De Beer, M.C.; Asztalos, B.F.; Whitaker, N.; Van der Westhuyzen, D.R.; De Beer, F.C. Remodeling of HDL remnants generated by scavenger receptor class B type I. *J Lipid Res* **2004**; 45; 1666-73.
- ✓ Wiersma, H.; Gatti, A.; Nijstad, N.; Elferink, R.P.; Kuipers, F.; Tietge, U.J. Scavenger receptor class B type I mediates biliary cholesterol secretion independent of ATP-binding cassette transporter g5/g8 in mice. *Hepatology* **2009**; 50; 1263–1272.
- ✓ Winder, A. F.; Garner, A.; Sheraidah, G. A., and Barry, P. Familial lecithin: cholesterol acyltransferase deficiency. Biochemistry of the cornea. *J. Lipid Res*. **1985;** 26(3); 283-287.
- ✓ Wyler von Ballmoos, M.C.; Haring, B.; Sacks, F.M. The risk of cardiovascular events with increased apolipoprotein CIII: A systematic review and meta-analysis. *J. Clin. Lipidol*. **2015**; 9; 498–510.
- ✓ Yancey, P.G.; Bortnick, A.E.; Kellner-Weibel, G.; de la Llera-Moya, M.; Phillips, M.C. and. Rothblat, G.H. Importance of differ-ent pathways of cellular cholesterol efflux. *Arterioscler Thromb VascBiol* **2003**; 23; 712–9.
- ✓ Yang, C.Y.; Manoogian, D.; Pao, Q.U.E.I.N.; Lee, F.S.; Knapp, R.D.; Gotto Jr, A.M., & Pownall, H.J. Lecithin: cholesterol acyltransferase. Functional regions and a structural model of the enzyme. *J. Biol. Chem.* **1987**; 262(7); 3086-3091.
- ✓ Yawata, Y.; Miyashima, K.; Sugihara, T.; Murayama, N.; Hosoda, S.; Nakashima, S. et al. Self-adaptive modification of red-cell membrane lipids in

lecithin:cholesterol acyltransferase deficiency. Lipid analysis and spin labeling. *Biochim Biophys Acta Biomembr* **1984**; 769(2); 440-448.

- ✓ Yee, M.S.; Pavitt, D.V.; Richmond, W.; Cook, H.T.; McLean, A.G.; Valabhji, J.; Elkeles, R.S. Changes in lipoprotein profile and urinary albumin excretion in familial LCAT deficiency with lipid lowering therapy. *Atherosclerosis*. **2009**; 205(2); 528-32.
- ✓ Yokota, R.; Bhunu, B.; Toba, H. and Intapad, S. Sphingolipids and kidney disease: Possible role of preeclampsia and intrauterine growth restriction (IUGR). *Kidney360* **2021**; 2(3); 534-541.
- ✓ Yu, H.; Kistler, A.; Faridi, M.H.; Meyer, J.O.; Tryniszewska, B.; Mehta; D. et al. Synaptopodin limits TRPC6 podocyte surface expression and attenuates proteinuria. *J Am Soc Nephrol*. **2016**; 27(11); 3308-3319.
- ✓ Zechner, R.; Dieplinger, H.; Steyer, H.; Groener, J.E.; Calvert, G.D.; Kostner, G.M. In vitro formation of HDL-2 from HDL-3 and triacylglycerol-rich lipoproteins by the action of lecithin:cholesterol acyltransferase and cholesterol ester transfer lipoprotein. *Biochim Biophys Acta* **1987**; 918: 27-36.
- ✓ Zewinger, S.; Reiser, J.; Jankowski, V.; Alansary, D.; Hahm, E.; Triem S. et al. Apolipoprotein C3 induces inflammation and organ damage by alternative inflammasome activation. *Nat. Immunol*. **2020**; 21; 30–41.
- ✓ Zhao, Y.; Thorngate, F.E.; Weisgraber, K.H.; Williams, D.L.; Parks, J.S. Apolipoprotein E is the major physiological activator of lecithin-cholesterol acyltransferase (LCAT) on apolipoprotein B lipoproteins. *Biochemistry*. **2005**; 44(3);1013-25.
- ✓ Zheng, K.H.; Kaiser, Y.; van Olden, C.C.; Santos, R.D.; Dasseux, J.L.; Genest, J. et al. No benefit of HDL mimetic CER-001 on carotid atherosclerosis in patients with genetically determined very low HDL levels. *Atherosclerosis.* **2020**; 311; 13-19.
- ✓ Zoja, C.; Abbate, M.; Remuzzi, G. Progression of chronic kidney disease: insights from animal models. *Curr Opin Nephrol Hypertens*. **2006**; 15(3); 250–7.
- ✓ Zoja, C.; Garcia, P.B.; Rota, C.; Conti, S.; Gagliardini, E. Corna, D. et al. Mesenchymal stem cell therapy promotes renal repair by limiting glomerular

podocyte and progenitor cell dysfunction in adriamycin-induced nephropathy. *Am J Physiol Renal Physiol*. **2012**; 303(9); F1370–8.